

UNCLASSIFIED

AD

405 974

DEFENSE DOCUMENTATION CENTER

FOR

SCIENTIFIC AND TECHNICAL INFORMATION

CAMERON STATION, ALEXANDRIA, VIRGINIA



UNCLASSIFIED

NOTICE: When government or other drawings, specifications or other data are used for any purpose other than in connection with a definitely related government procurement operation, the U. S. Government thereby incurs no responsibility, nor any obligation whatsoever; and the fact that the Government may have formulated, furnished, or in any way supplied the said drawings, specifications, or other data is not to be regarded by implication or otherwise as in any manner licensing the holder or any other person or corporation, or conveying any rights or permission to manufacture, use or sell any patented invention that may in any way be related thereto.

63-3-6

405974

RADC-TDR-63-67



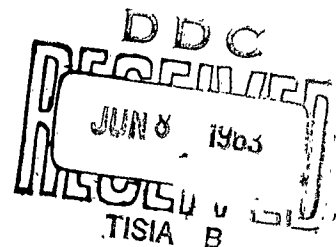
TRANSIT TIME EFFECTS IN PHASED ARRAYS

405 974

TECHNICAL DOCUMENTARY REPORT NO. RADC-TDR-63-67

May 1963

Techniques Laboratory
Rome Air Development Center
Research and Technology Division
Air Force Systems Command
Griffiss Air Force Base, New York



Project No. 4506, Task No. 450604

(Prepared under Contract No. AF30(602)2646 by Electrical Engineering
Department, Syracuse University Research Institute, Syracuse, New York)

FOREWORD

The work covered by this report was done under the sponsorship of the Rome Air Development Center under Contract Number AF30(602)-2646. The author, Dr. Richard E. Gildersleeve, wishes to acknowledge the assistance of the Syracuse University Computing Center personnel who aided in programming the operation of the IBM 650 computer, and to acknowledge the assistance of Mr. Erdogan Bolgan and Mr. Rajanikant Patel for their assistance in converting the large volume of data into the many graphs which were required to present the data in useable form.

This task was performed under the direction of Dr. David K. Cheng, Project Director.

Task Report No. 4

SURI Report No. EE957-6302T4

ABSTRACT

Large linear arrays, when excited by pulses of very short duration, in the order of a few cycles, with all elements excited simultaneously, give rise to radiation patterns which have a very non-uniform side lobe structure, and result in degradation of the main lobe if the pulses are too short.

This report presents a set of pulses produced at given points in space as a result of exciting an array of 49 elements, with half-wave spacing, by pulses of five cycles and less, the phase of the excitation was varied to cause the main lobe to scan through 20 degrees off boresight. The techniques for applying the results to excitations of more than five cycles were given.

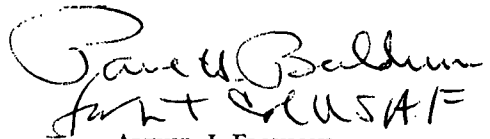
A family of radiation patterns are given, to show the variations in the patterns as a function of time, for the several pulse durations studied. The curves clearly show the build-up and decay of the patterns; the fluctuations in the side lobe structure, and the growth and decay of the main lobe both in width and amplitude.

It was concluded that this method of excitation and lobe switching is feasible provided the minimum pulse duration is determined for the given array size and desired scan angle, based upon specified limits in main lobe degradation. Side lobe suppression could be provided by appropriate selection of amplitude distribution.

PUBLICATION REVIEW

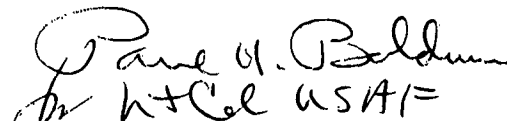
This report has been reviewed and is approved.

Approved:



ARTHUR J. FROHLICH
Chief, Techniques Laboratory
Directorate of Aerospace Surveillance and Control

Approved:



WILLIAM T. POPE
Acting Director of Aerospace Surveillance and Control

TABLE OF CONTENTS

	<i>Page</i>
I Introduction	1
II Pulse Shape Computations.....	3
III Analysis of Incident Pulses.....	7
IV Instantaneous Radiation Patterns.....	39
V Analysis of Radiation Patterns.....	106
VI Summary and Conclusions.....	109
VII References	112

I. INTRODUCTION

1.1 Statement of the Problem

The far field radiation patterns for arrays of dipoles has been discussed in the literature in much detail but in general little or no consideration is given to the time variations of the field. The majority of the references recognize that the field is a function of ωt and due recognition of the relative phasing is made. The standard patterns as generally presented show field intensity or power as a function of polar or azimuthal angle of constant range. For most applications the information presented in these patterns is ample. For pulsed transmissions the pulse duration is frequently large compared to the build-up and decay times so that these times are of minor importance. For many radar systems the received signal is not influenced appreciably by the time variations in the antenna patterns.

With the advent of extremely large arrays and very short pulses, the time variations in field intensity become a matter of concern. It is the object of this report to study the resultant antenna patterns when pulses are extremely short and the arrays are very large. The analysis is made for a specific array with assigned excitation pulse durations, and attempts are made to generalize the data obtained to show how the results will vary with changes in parameters.

1.2 Approach to the Problem

The problem was studied for the particular case of simultaneous excitation to all elements of the array, but with both amplitude and phase distributions as variable parameters.

In treating the problem the customary assumptions were made with regard to far-zone patterns and ideal siting. In addition, point sources were assumed for the array elements. To permit reasonable computations a linear broadside array of 49 elements was selected, with half-wave spacing between elements, resulting in an array 24 wavelengths long. Only the case of uniform amplitude distribution was considered, but several cases of progressive relative phase were examined to show the variations in the resulting pattern as a function of beam location off boresight.

The analysis was made using very short pulses and the results were extended to cover the full range of pulse durations from one cycle to c.w. A study of pulse shapes incident upon the radar target as a function of angle off boresight was an inherent part of this analysis.

When the array elements are excited by relatively long duration pulses the resultant pulse at the distant target is a composite whose duration is increased over that of the excitation pulses by an amount equal to the build-up (or decay) time. This time interval is a function of target angle off boresight and array length (number of elements for a given element spacing). For large pulses the transient buildup of the resultant pulse is followed by an interval characterized by a steady-state sinusoidal wave whose duration is dependent upon the excitation pulse duration. The steady-state condition is then followed by a transient decay interval equal in duration to the build-up time.

Transmitted pulses were obtained, for fixed range, as a function of azimuth angle, for the several values of relative phase, from data computed on an IBM 650 computer. Conventional radiation patterns are readily obtainable from this data by the simple process of plotting the peak of the steady-state sinusoid for pulses of long duration as a function of their respective azimuth angles. In this instance the time factor is not considered. It is only necessary that the duration of the excitation pulses be sufficiently long so that the steady-state condition is reached throughout the range of azimuth angle under consideration. Symmetry considerations in many cases will eliminate the necessity for computing pulse shapes for corresponding angles to the right and left of boresight.

As the excitation pulse duration is reduced a situation will be reached wherein the composite pulse does not contain a steady-state portion. Instead, the transient decay will begin before the transient buildup ends. This situation occurs first at large angles off boresight, where the difference in path length for the end elements of the array is maximum. As the pulse duration is decreased this situation occurs for progressively smaller angles off boresight. The radiation pattern can no longer

be determined in the manner described above. Instead, it must be considered as a time-dependent phenomenon and can be determined from the computed pulse shapes by selecting appropriate instances of time and comparing the values of all pulses at the same instant. A family of radiation patterns plotted at selected intervals of time show the variations during the interval from initial buildup to final decay, as a function of azimuth angle.

Since the resulting radiation patterns bear little resemblance to the conventional steady-state patterns, a family of patterns was obtained to show the variations as a function of time for patterns resulting from excitation pulses of long duration, examined during the steady-state interval. These were then used as the reference patterns when the excitation pulses were reduced in duration below the point where the transient decay began before the end of the build-up interval.

In the specification for the study of this problem the range of excitation pulse durations to be considered was given by

$$\frac{0.1L}{C} \leq \frac{\tau}{\sin \theta_0} \leq \frac{10L}{C} \text{ seconds} \quad (1-1)$$

where

L = array length

C = velocity of light

τ = excitation pulse duration

θ_0 = scan angle measured from broadside with beam scan angles ranging from 0 to $\pm 45^\circ$.

In terms of N array elements with equal separation, d , $L = (N - 1)d$

$$\tau = \frac{p(N-1)d}{C} \sin \theta_0 \text{ sec.} \quad (1-2)$$

where

$$0.1 \leq p \leq 10$$

For

$$d = \frac{\lambda}{2}$$

$$\tau = \frac{p(N-1)\lambda}{2C} \sin \theta_0 \text{ sec.} \quad (1-3)$$

Since one cycle of r-f has a duration of T seconds

$$\tau = \frac{p(N-1)\lambda}{2TC} \sin \theta_0 \text{ cycles} \quad (1-4)$$

Substitution of $C = \lambda f$ and $f = \frac{1}{T}$ into Eq. (1-4)

results in

$$\tau = \frac{p(N-1)}{2} \sin \theta_0 \text{ cycles} \quad (1-5)$$

as the expression for the excitation pulse duration.

Future reference to the excitation pulse duration, τ , will be in terms of cycles of excitation, rather than time, to eliminate frequency dependence.

II. PULSE SHAPE COMPUTATION

2.1 Composition of Pulses

A pulse incident upon a distant target is a composite of the sinusoidal radiations from each of the array elements. Since in general the path length from the several elements to the target differs, the sinusoids will arrive with essentially the same amplitude but differing in phase. The difference in path length is too small to produce a measurable amplitude difference.

The phase difference, Ψ , in degrees, between sinusoids from adjacent elements, can be expressed as

$$\Psi = d_r \sin \theta + \Psi_0 \quad (2-1)$$

where d_r is the distance in electrical degrees between sources, ($\lambda/2$ separation corresponds to 180 degrees), θ is the azimuth angle of the target off boresight, and Ψ_0 is the phase difference in degrees between the excitations to adjacent elements. The term $d_r \sin \theta$ is the contribution to the phase difference due to the difference in path lengths.

We may arbitrarily choose any element of the array of N elements as our reference, and the selection of the reference element can be made a matter of convenience in programming a computer. It should be understood that Ψ_0 is a controllable phase angle, which determines the location of the main lobe of the array pattern, and carries an appropriate sign to provide phase lead or lag. We

will assume that the excitation pulse durations are integral multiples of the period of a sine wave and the reference pulse has zero phase.

Assume that the right hand element of the array, as shown in Figure 2.1, is the reference element, and that a progressive phase difference, Ψ_0 , is established relative to that element. The radiation fields from each of the N elements arriving at a distant target located at an angle, θ , will be delayed by an amount equal to $(n-1)d_r \sin \theta$, where n is the element number, ranging from 1 to N . The phase difference, Ψ_n , of the excitation of the n th element relative to that of the first will be:

$$\Psi_n = (n-1) (d_r \sin \theta + \Psi_0) \quad (2-2)$$

The resultant pulse arriving at the target can be determined by summing the waveforms from all elements. Figure 2.2 illustrates the form of the individual waves as they arrive at the target, using time $t = 0$ as that time at which the wave from the nearest element arrives at the target. In this illustration a leading constant phase, Ψ_0 , was chosen.

If all elements were simultaneously excited in phase the curves in Figure 2.2 would all be sinusoids given by

$$\begin{cases} \sin \omega t & , & t > 0 \\ 0 & , & t < 0 \end{cases} \quad (2-3)$$

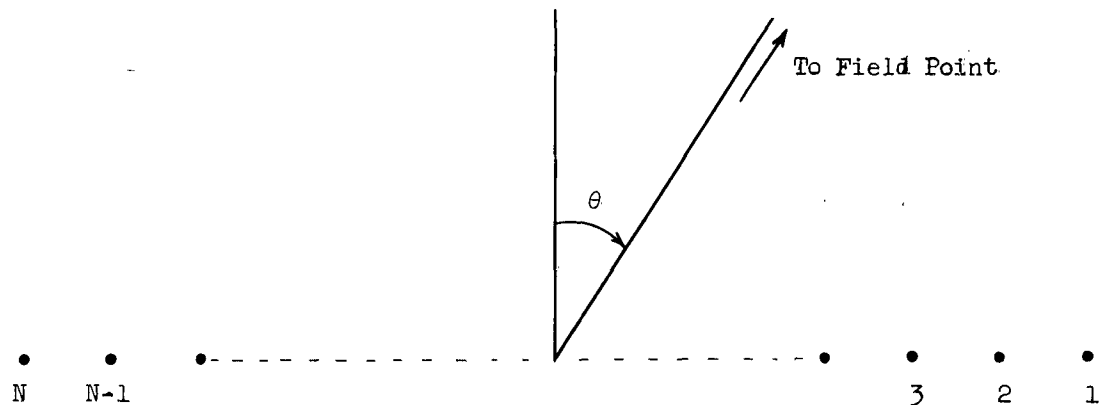


FIGURE 2.1 Array Orientation

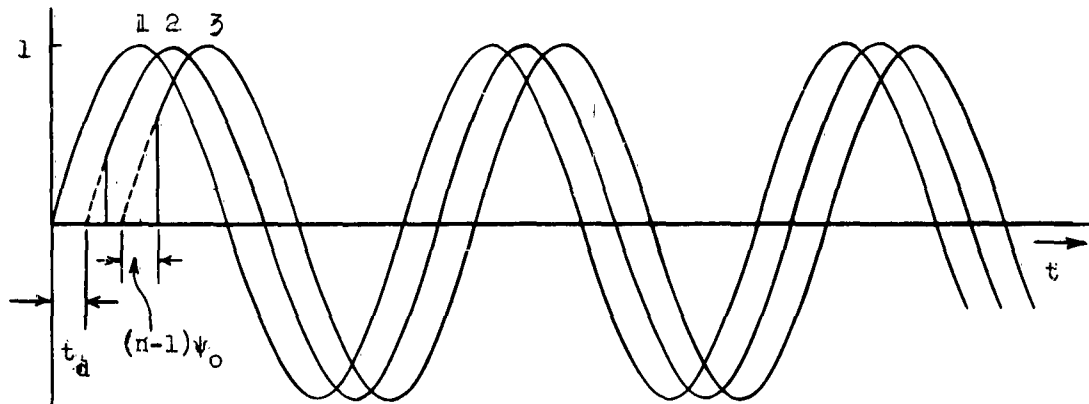


FIGURE 2.2 Individual Waves Arriving at Point in Space from Successive Radiators

with amplitudes normalized, separated by time t_d which is then a function of element spacing and angle θ , given by $(N - 1)d, \sin \theta$, for each successive element. This is illustrated by the dotted portions of the curves. When Ψ_0 is changed from zero, again with simultaneous excitation, the relative phase difference is changed, and for negative Ψ_0 this becomes an increase in phase difference. In addition, since all elements are excited simultaneously, all waves have their leading portions clipped by an amount which is a function of Ψ_0 and element number. The time delay, t_d , for the arrival of successive waves at the target, is not only a function of Ψ_n , but also the clipped portion of the waveform must be considered. This latter consideration radically alters the shape of the leading and trailing edges of the resultant waveform and is particularly important, when very short duration pulses are used. In Figure 2.2 no particular excitation pulse duration is assumed, hence the sinusoids are broken off before actual termination. The resultant pulse shape, obtained by a summation of clipped sinusoids, each displaced in time by the delay time t_d , is characterized by a build-up interval consisting of a succession of step changes in amplitude until such time as the last signal arrives at the target. In the normalized pulse diagrams, in which the summation is divided by the number of elements to produce a maximum amplitude of unity for the zero phase case, the relative amplitudes of the in-

dividual step discontinuities are negligible insofar as reproducing them on the pulse diagrams is concerned. The diagrams are smooth-curve approximations of the steps illustrated in Figure 2.3 which is a magnified segment, not normalized, to show the way the leading portion is formed. In this figure Ψ_n is arbitrary.

To obtain the representative pulse shapes as a function of azimuth angles and as a function of progressive phase angle, Ψ_0 , an IBM 650 computer was programmed to produce data which could be plotted against time, with the time scale converted to equivalent electrical degrees.

2.2 Method of Computation

The details of the computer program will not be presented here since they are a function of the particular computer used. With more extensive facilities than was available for this task the computation time could be reduced and it could be possible to plot the results directly, a technique which also was not available for this work. Some general comments could prove useful, however.

The technique used to compute the resultant pulse at a specified range for a given phase angle and given azimuth angle was essentially one of sampling data. The amplitude of the individual sinusoids from each of the 49 elements was computed at selected intervals of time. Obviously the shorter this interval the closer will be the approximation to the true pulse shape. However, shorten-

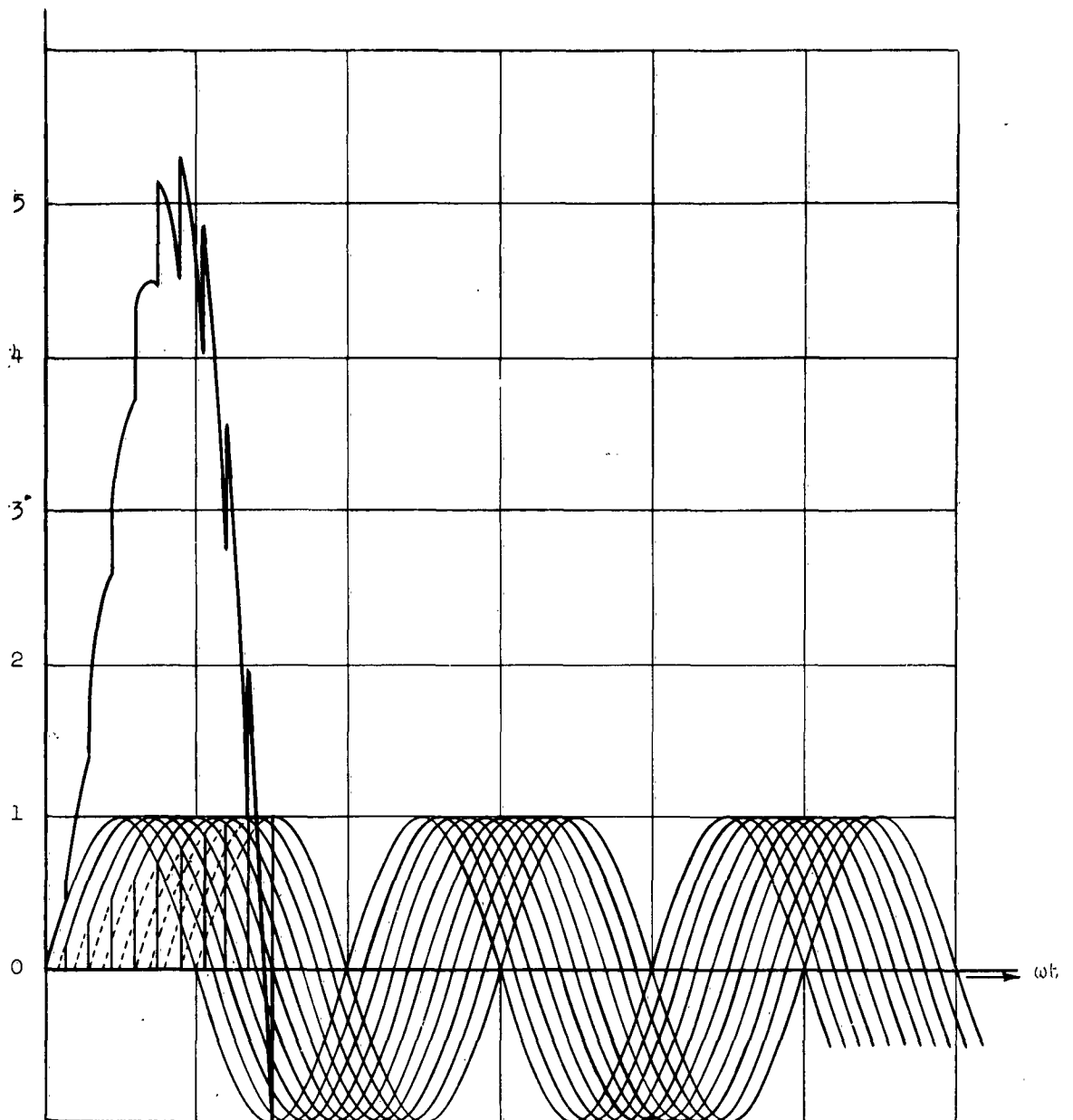


FIGURE 2.3 Pulse Formation Magnified

ing the sampling time interval increases the number of computations necessary for determination of a given pulse, and hence increases the computer time. A compromise must be made. The interval between sample points was chosen equal to 30 electrical degrees, after comparison with computations made with much smaller intervals between sample points. A negligible loss in detail

is experienced by the choice of interval duration that was selected. Although this interval may appear to be large when excitations of a very few cycles are considered, it results in a large number of sample points due to the large incident pulse duration which occurs at moderately large azimuth angles. On the other hand, an appreciable increase in interval duration to reduce the number

of sample points and thereby reduce computation time results in too much loss of detail in the computed pulses and hence in the antenna patterns.

Computation of pulse waveforms incident upon a target was accomplished by programming the computer to sum N sinusoidal waveforms having progressive phase differences as given by equation 2-2 with d_r fixed at $\lambda/2 = 180^\circ$ and with assigned values of Ψ_0 . For a given value of azimuth angle θ the program provided a set of values of instantaneous normalized field intensity at 30 electrical degree intervals (in lieu of time intervals) from $\omega t = 0$ to the value of ωt corresponding to the termination of the particular pulse. The program involved summation of N sinusoids, with the clipped leading portion of each sinusoid removed in accordance with the equation $(n-1)\Psi_0$. Since the wave train from element 1 could terminate before the wave train from element n , where $1 < n \leq N$, arrives at the target, which is the case when $(n-1)t_d > \tau$ (the excitation pulse duration),

the computer program was written to handle this situation. For many of the computed pulses the instantaneous field intensity consisted of the summation of less than N sinusoids throughout the entire duration of the incident pulse. The program provided for the summation of a maximum of N sinusoids. For these pulses the steady-state condition was reached prior to the termination of the first sinusoid. This condition is a function of both the time τ and the angle θ . Considerable computer time was saved by programming the computer to recognize the steady-state, since this portion of the incident pulse is a sinusoid.

For each value of Ψ_0 , and each selected value of θ , computations were made for several values of τ . The values of θ selected for these computations were initially chosen with equal increments, but subsequent intermediate values of θ were later chosen for points where more detail in the antenna pattern was needed. Predetermination of critical points was not possible.

III. ANALYSIS OF INCIDENT PULSES

Pulse shapes and radiation patterns were obtained for progressive phase differences of 0° , 30° , 45° , and 60° with a spread of the azimuth angle in each case selected to cover at least the first side lobe of the conventional radiation pattern, each side of the main lobe. Selected pulse shapes and radiation patterns are shown in this report to illustrate representative trends, rather than including all the computed pulses and patterns, since the volume of data is very large. It has been concluded that inclusion of every pattern would serve no useful purpose, since these curves apply to a particular array of 49 elements. Corresponding patterns for arrays of other than 49 elements would differ in detail, and must be computed for the array in question if such detail should be desired. Sufficient patterns have been included to provide support for the analysis.

3.1 Uniform Amplitude Constant Phase

This is the conventional broadside array with the main beam normal to the line of elements. Since $\sin \theta = 0$ for $\theta = 0^\circ$ and since $\Psi_0 = 0$ the radiation from all elements will arrive at the target simultaneously in phase when the target is on boresight ($\theta = 0^\circ$). Hence for this position the resultant pulse will be a sinusoid with a normalized amplitude of one, (normalization being accomplished by dividing the amplitude by N , the total number of elements in the array, with unit amplitude distribution assumed) and a duration τ , the excitation pulse duration. The resultant pulse in no way differs from the conventional pulse, therefore this diagram is not shown.

As the angle off boresight, θ , increases, two effects are noted. The leading edge of the resultant pulse begins to deviate from the sinusoidal form, the amplitude of the steady-state portion of the pulse (if such exists) is reduced, and the trailing edge of the pulse also deviates from the sinusoidal form. The pulse duration increases with increasing angle, but since this increase, $\Delta\tau$, is not a function of the excitation pulse duration, τ , the excitation pulse duration for a given angle θ is increased by the constant amount $\Delta\tau$ upon arrival at the target, independent of the number of cycles

present in the excitation pulse.

Figures 3.2 and 3.3 illustrate the changes just described.

Figure 3.1 is a conventional normalized pattern for this array. On this diagram the values of normalized $|E|$ have been indicated by an X corresponding to each value of θ for which pulses were computed. It will be seen that in each case the $|E|$ is the maximum of the steady-state portion of the pulse. This pattern will be compared later with the time dependent patterns.

Computations of pulses were made at intervals of $\Delta\theta$ equal to 0.5° , starting with $\theta = 0$, and some additional computations at intermediate values of θ were made at critical pattern points. Each figure has a continuous steady state sinusoid, following a transient build-up interval, shown as a solid line. For any excitation of M cycles the incident pulse can be constructed for any angle θ by locating the point on the appropriate steady-state sinusoid at the time corresponding to $360 M$ degrees and superimposing the standard trailing edge for that θ , provided M is sufficiently large so that steady-state is attained.

In general the transient build-up of the pulses attains a higher positive peak than the subsequent steady-state peaks. The transient decay has a corresponding large negative peak. The initial peaks are the result of addition of positive going sine waves, delayed in time because of the separation between elements and a non-zero θ , and because of the simultaneous excitations of all the elements. For $t < 0$ the excitation is zero. After $t = \tau/2$, half-period, the negative portion of the sine waves reduces the total amplitude as shown in the steady-state regions.

Three excitation pulse durations, 1 cycle, 3 cycles, and 5 cycles were studied to show the growth of the transmitted pulses as a function of angle off boresight. Comparison of the three pulses for any given angle θ is sufficient to determine the shape of any pulse of larger duration provided the excitation has an integral number of cycles (see Figure 3.4 for example). Fractional cycles will produce some differences. Trailing portions of the three pulses are shown as dotted lines

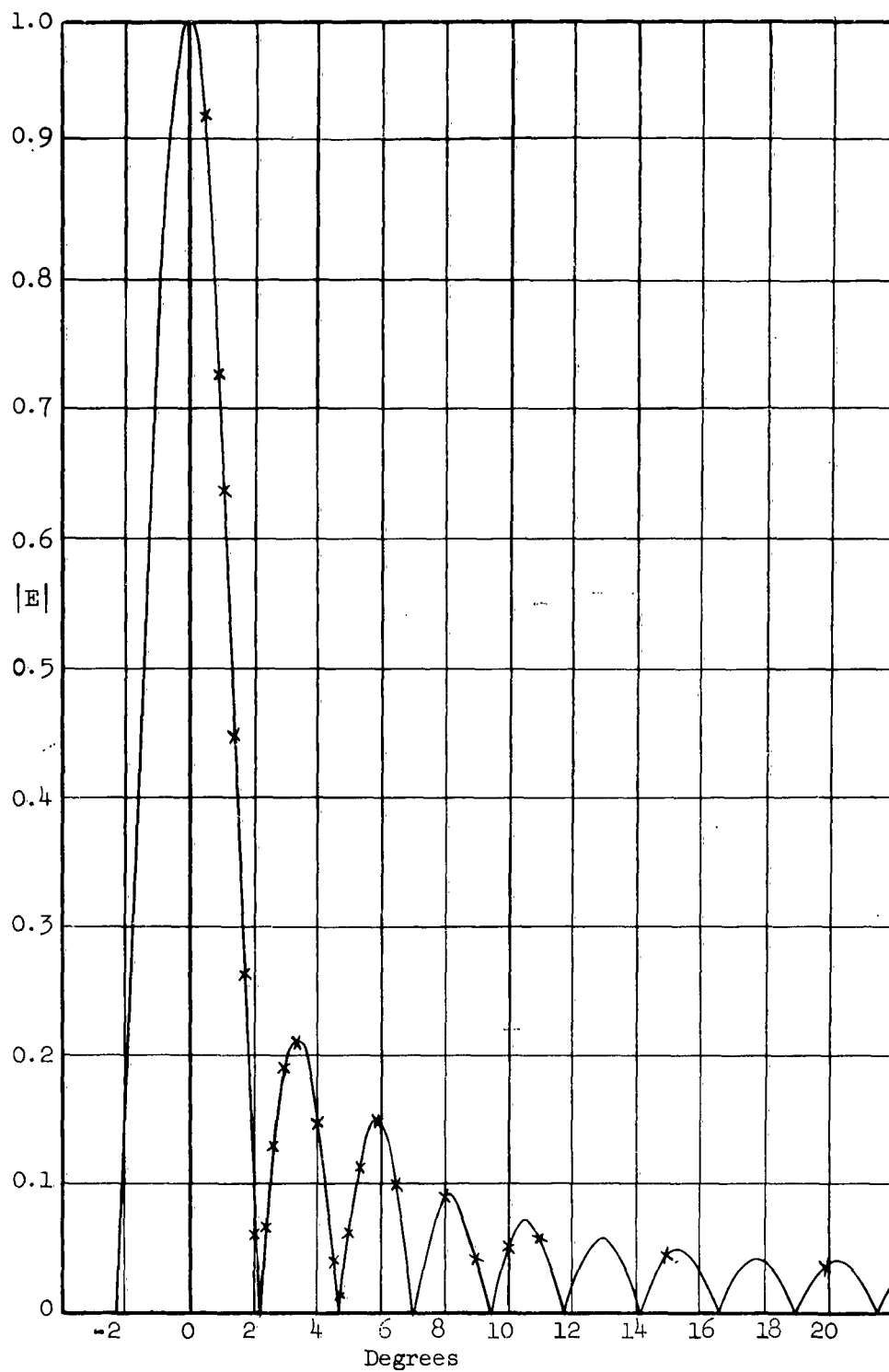


FIGURE 3.1 Conventional Normalized Radiation Pattern

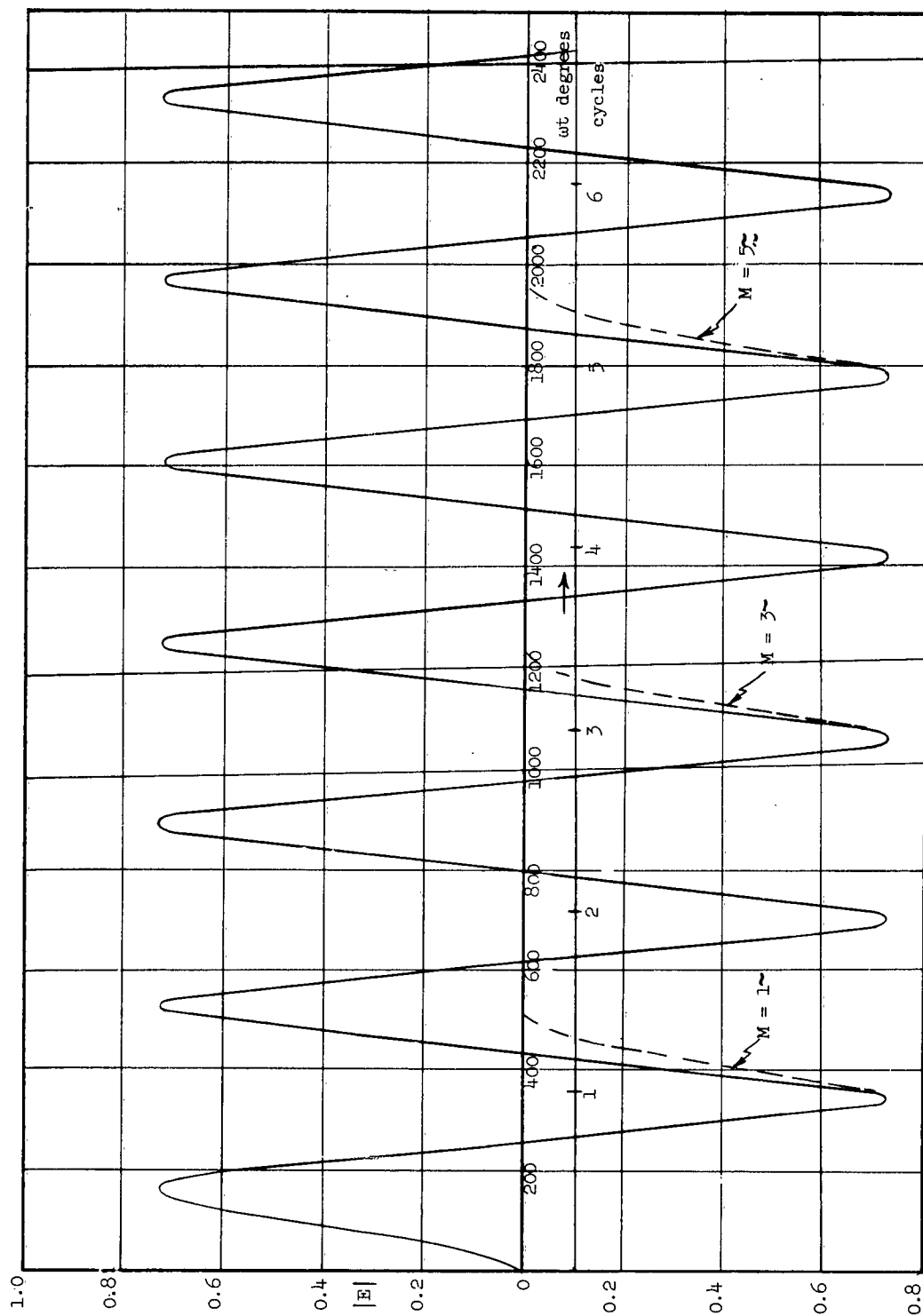


FIGURE 3.2 Transmitted Pulse Shapes $\psi_0 = 0^\circ$ $\theta = 1.0^\circ$

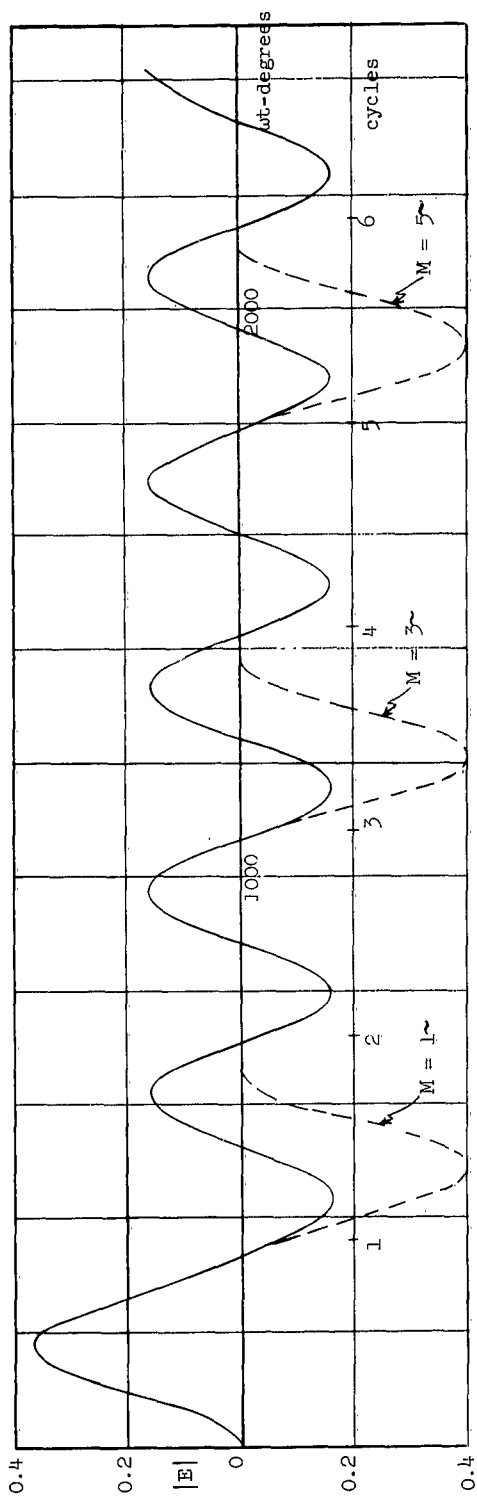


FIGURE 3.3 Transmitted Pulse Shapes $\psi_0 = 0^\circ$ $\theta = 2.0^\circ$

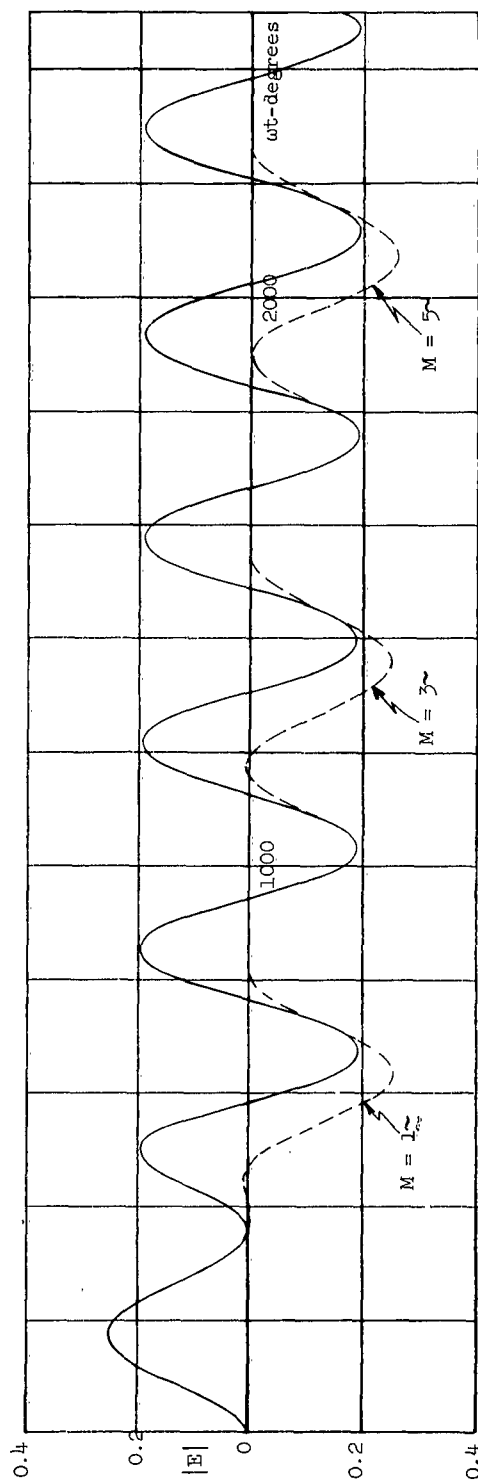


FIGURE 3.4 Transmitted Pulse Shapes $\psi_0 = 0^\circ$ $\theta = 3.0^\circ$

in Figures 3.2 through 3.5, since there is no overlapping of trailing ends of pulses in this range of θ . Beginning with Figure 3.6 the resultant pulse duration exceeds $(M + 2)360^\circ$, therefore the trailing end of pulse M will overlap the trailing end of pulse $M + 2$. To avoid confusion the one cycle and five cycle pulses have been omitted. The trailing end of the five cycle pulse is the same as the three cycle pulse up to Figure 3.7 where the three cycle pulse no longer has a steady state portion. The trailing portion of the one cycle pulse continues moving out as θ increases.

Starting with about Figure 3.4 an interval appears between the leading portion and the trailing portion, for 1 cycle excitation, which is essentially zero amplitude. This interval starts at $t = \tau$, the excitation pulse duration and ends at $t = \tau_t$, where τ_t is the transmitted pulse duration. When $\tau_t > 2\tau$ we see this condition.

Beginning with about Figure 3.5 a second positive pulse appears in the leading portion, for excitations of more than one cycle. Subsequent illustrations give these leading pulses the appearance of a sine wave superimposed on a positive d-c component. The d-c component is equal to E_{\max} of the sine wave, and is called E_D .

Examination of the waveforms presented will show that the resultant pulse is characterized by three distinct portions for $\theta > \theta_c$. In the interval $0 < \omega t \leq \omega t_1 = M \times 360^\circ$, for M cycles excitation, the waveform can be represented by the expression

$$|E| = E_D - E_D \cos \omega t \quad (3-1)$$

In the interval $\omega t_1 < \omega t \leq \omega t_2$ the composite pulse is of zero amplitude, where ωt_2 is a function of θ as follows

$$\omega t_2 = (N - 1) \times 180 \sin \theta \quad (3-2)$$

It corresponds to that instant of time when the radiation from the last element arrives at the field point at the angle θ . The third portion of the pulse can be represented by the equation

$$|E| = -E_D + E_D \cos \omega t \quad (3-3)$$

during the interval $\omega t_2 < \omega t \leq \omega t_3 = M \times 360 + (N - 1) 180 \sin \theta$. The zero amplitude portion of the waveform in the interval $\omega t_1 < \omega t \leq \omega t_2$ comes

about for the following reason. At the time t_1 the sum of the waves (from q elements) which have arrived up to this time is zero. The wave from the $q + 1$ element arrives at $t_1 + \Delta t$ but the wave from element 1 terminates, the sum remaining zero. Slight variations from zero do occur during the brief interval of time between the termination of wave 1 and the start of wave $q + 1$ but the variations are negligible.

The angle θ_c introduced above, is the critical angle off boresight, where, for a given excitation pulse duration, the condition described occurs. It can be computed from Eq. 2-2 by letting $\Psi_n = M \times 360^\circ$ with $\Psi_0 = 0$. For the angle θ_c , $\omega t_1 = \omega t_2 = \Psi_n$, $d_r = \lambda/2 = 180^\circ$, and $(n - 1) = 48$ for a 49-element array. From Eq. 2-2

$$\sin \theta_c = \frac{M \times 360}{(n - 1) 180} \quad (3-4)$$

or

$$\sin \theta_c = \frac{2M}{48} = \frac{M}{24} \quad (3-5)$$

where M is the number of cycles of excitation. The values of θ_c are:

M	$\sin \theta_c$	θ_c	
1	0.0417	2.39°	Compare Figures 3.3 and 3.4
3	0.1250	7.18°	Compare Figures 3.6 and 3.8
5	0.2083	12.02°	

3.2 Uniform Amplitude, 30° Leading Phase

A 30° progressive phasing of the array elements produced several effects which differ from the uniform phase case. The main beam now appears at approximately 9.6° off axis as shown in Figure 3.9 which is the normal pattern for the array. The crosses indicate angles for which pulse computations were made. Not all pulses are illustrated herein. Figure 3.10 is the pulse diagram for this value of θ , showing the steady-state waveform reaching a normalized value of one but only after a build-up time equivalent to about four cycles of excitation. Obviously, only pulses of more than four cycles duration will build up to the steady-

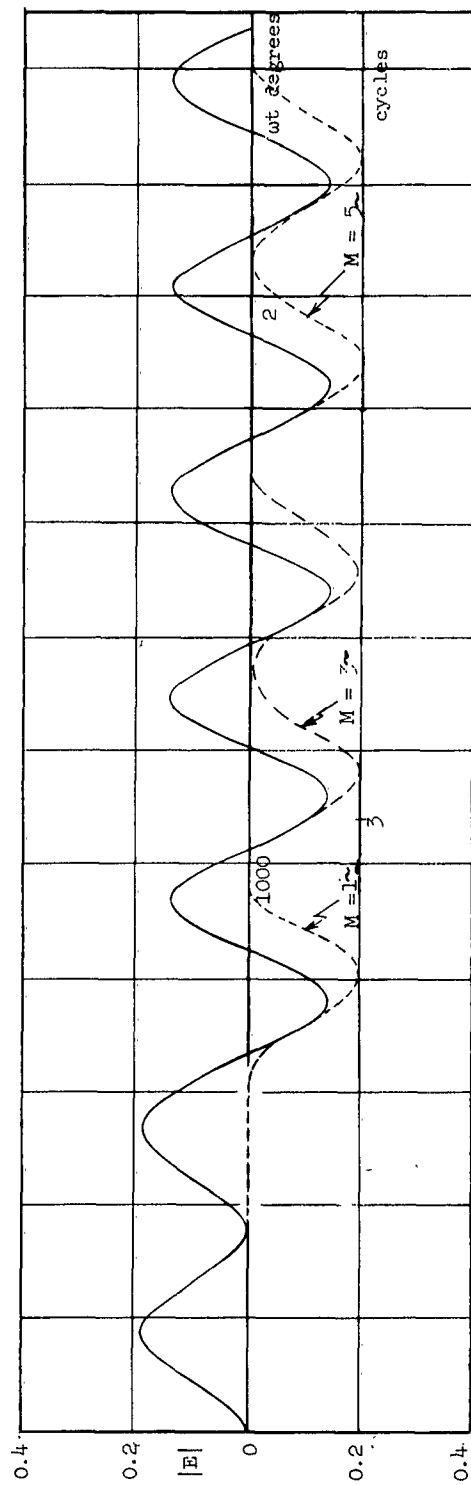


FIGURE 3.5 Transmitted Pulse Shapes $\psi_0 = 0^\circ$ $\theta = 4.0^\circ$

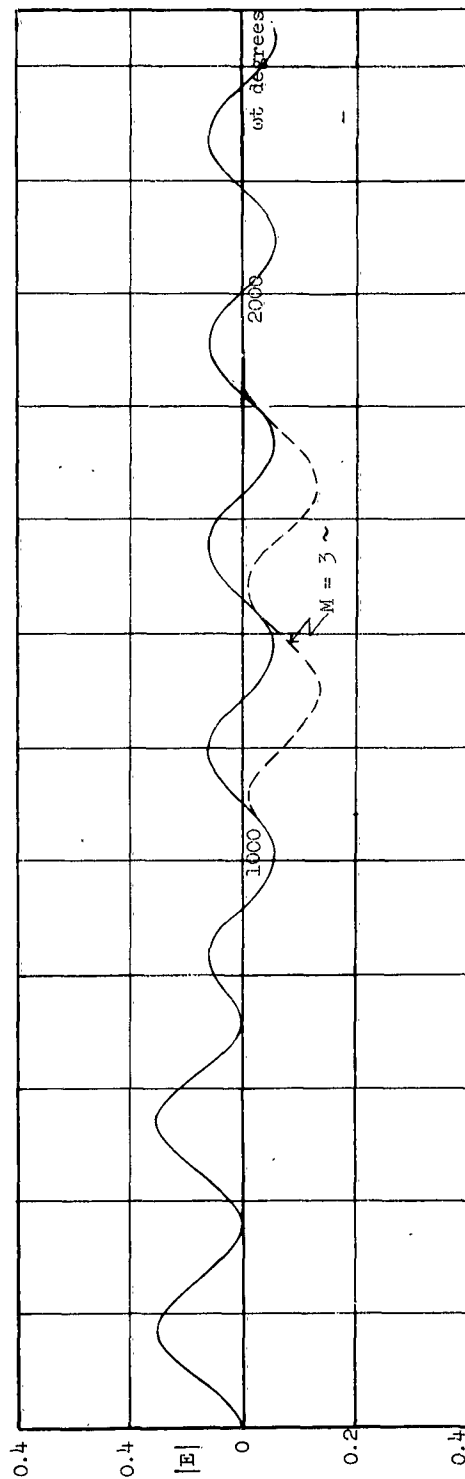


FIGURE 3.6 Transmitted Pulse Shapes $\psi_0 = 0^\circ$ $\theta = 5.0^\circ$

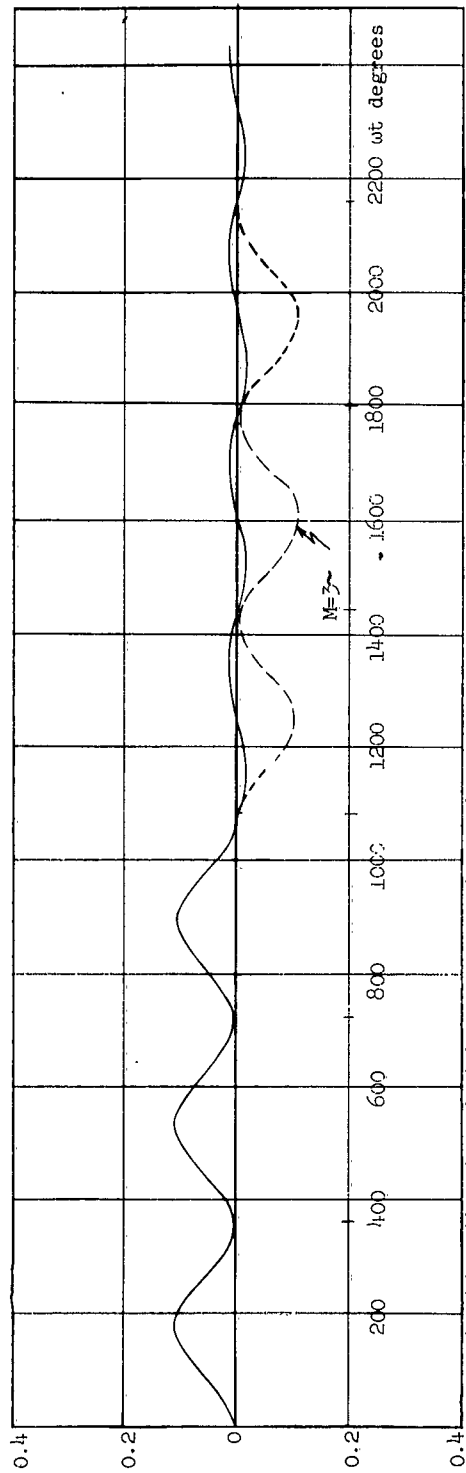


FIGURE 3.7 Transmitted Pulse Shapes $\psi_0 = 0^\circ$ $\theta = 7^\circ$

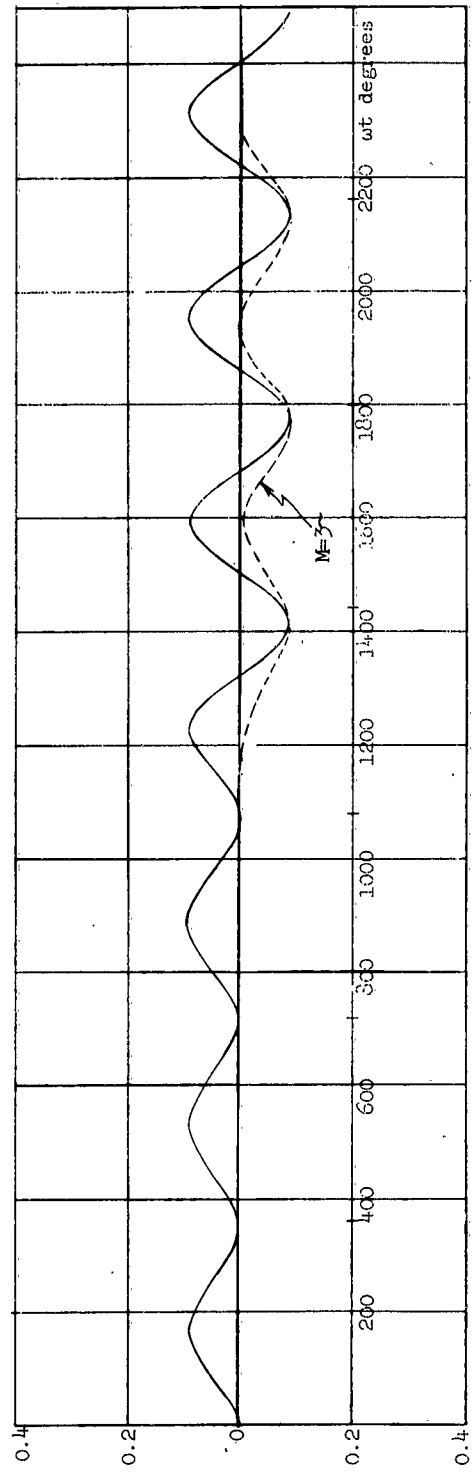


FIGURE 3.8 Transmitted Pulse Shapes $\psi_0 = 0^\circ$ $\theta = 8^\circ$

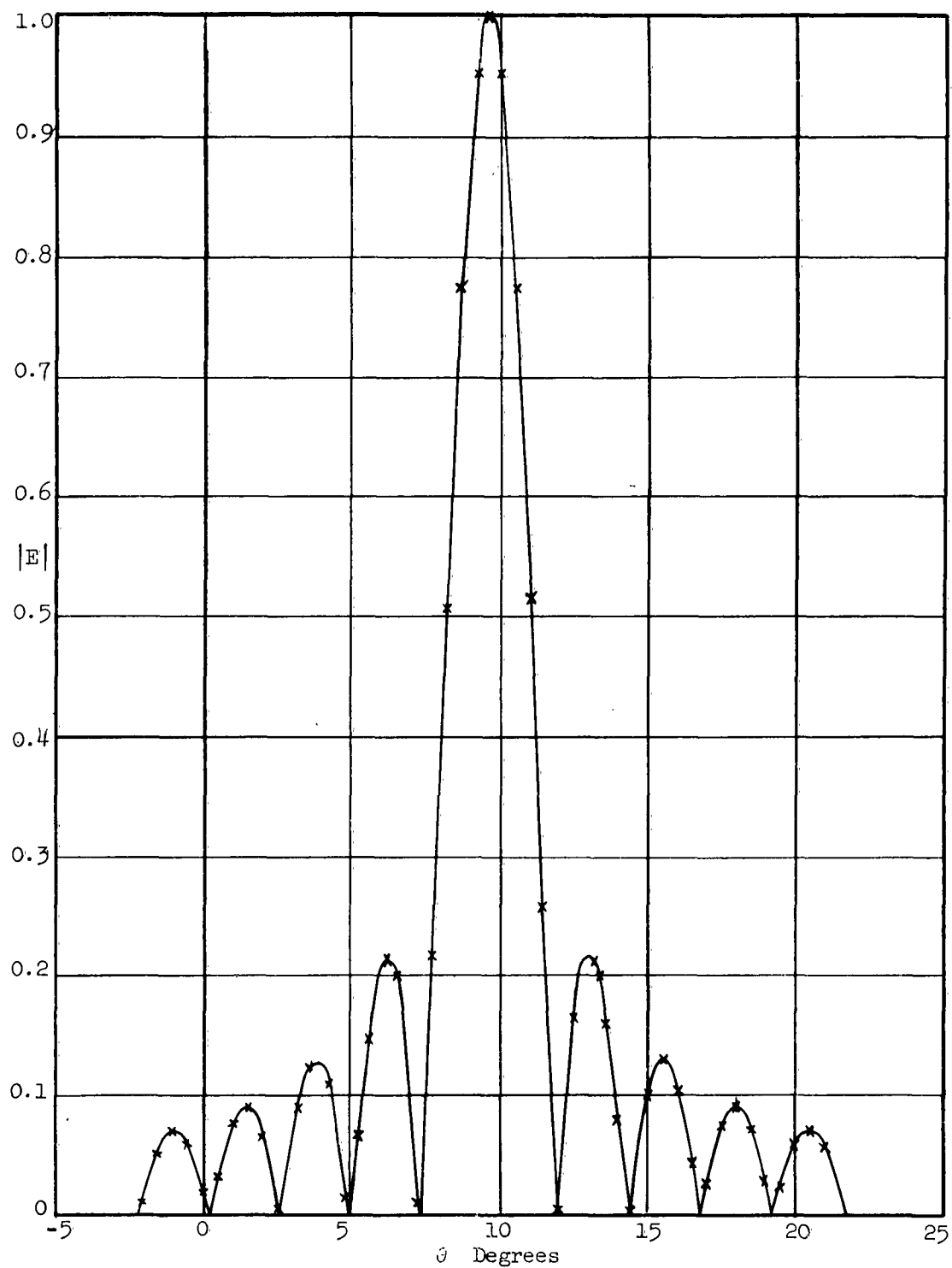


FIGURE 3.9 Conventional Radiation Pattern $\psi_0 = 30^\circ$

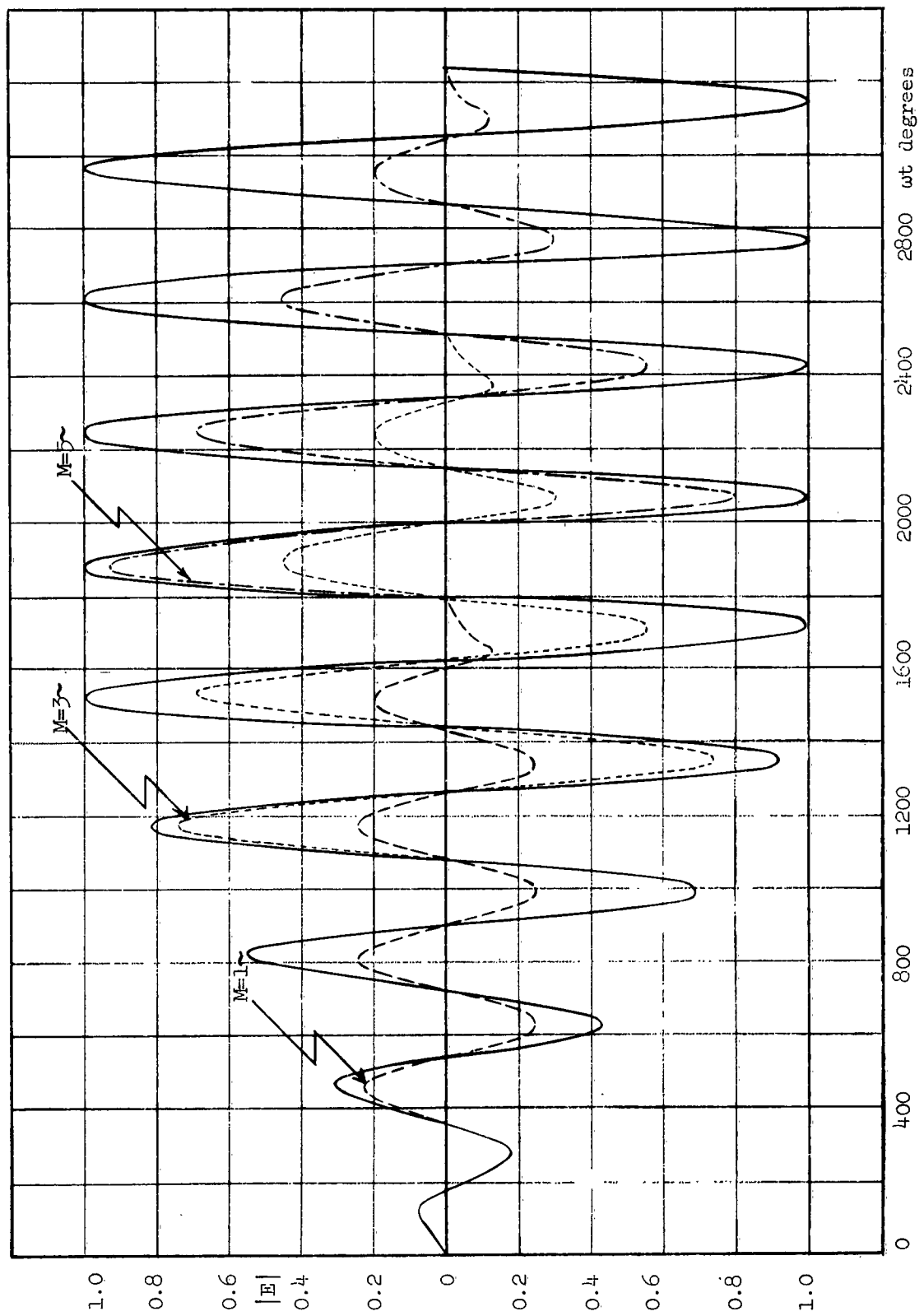


FIGURE 3.10 Transmitted Pulse Shapes $\psi_0 = 30^\circ$ $\theta = 9.594$

state normalized value of one before the trailing end begins. We will see that an increase in progressive phase angle will result in an increase in this build-up time.

Figures 3.11 through 3.14 are representative patterns for progressively larger values of θ . They serve to illustrate trends in pulse variations for increasing θ and increasing excitation pulse duration. At this point a clarifying statement regarding interpretation of the pulse diagram is in order. Each diagram represents a composite of the signal arriving at a target point in space under conditions of (a) very long pulses, shown as the solid curve, (b) pulses resulting from array excitations of one cycle, three cycles, and five cycles, shown in part as solid lines, in part as broken lines. In some diagrams all three excitations are illustrated. In others, where overlapping occurs, one or two examples may be omitted for clarity, with the selection of those to be illustrated being based upon the information that they show. To see a full pulse one should start at $\omega t = 0$ and trace along the solid curve to $\omega t = 360$, 1080, or 1800, depending upon whether the excitation was one, three or five cycles. From these points a broken curve will be followed to its end to trace out the remainder of the pulse.

Peculiarities begin to appear in Figure 3.12 for $\theta = 12.0^\circ$, which is very close to the first null in the normal radiation pattern. For long duration pulses (M is greater than five cycles) there is a build-up in signal strength which is considerably greater than the peak steady-state value (0.32 compared with 0.015). The one-cycle and three-cycle pulses reach a maximum value and maintain this value through several oscillations, but the five-cycle pulse decays toward the value attained in the steady state by the cw case, and then builds back up to the maximum before finally falling off to zero. Pulses of more than five cycles duration of the excitation would all behave in the manner of the five cycle pulse for this angle, θ , the only difference being the number of cycles of steady-state appearing between the two transient portions.

In figure 3.13 a different type of variation from the sinusoid is represented, in the region 1000 degrees $< \omega t < 1600^\circ$. This variation appears again in the 5 cycle pulse in the range $2100^\circ < \omega t < 2700^\circ$ but has little effect upon the one cycle and

three cycle pulses. Pulses of more than 5 cycles would show the effect in a similar manner to the 5 cycles pulse. For larger values of θ the variation changes in character and location and, as observed in Figure 3.14, a second region of deviation from the sinusoid appears. This results in a region of essentially zero amplitude in the range $1800^\circ < \omega t < 2400^\circ$ for the 5 cycle pulse. In this diagram the one cycle and three cycle pulses have been omitted for clarity, since they overlap the five cycle pulse in the region of interest. They do not have a zero amplitude region but the three cycle pulse now shows the variation which occurs in the region $600^\circ < \omega t < 1200^\circ$, repeated but inverted in the region $2300^\circ < \omega t < 2900^\circ$.

Figures 3.15 through 3.19 are representative pulse patterns for the angular range $9^\circ > \theta > 3^\circ$. In this range similar effects are noted but with variations which result in a lack of symmetry in the instantaneous radiation patterns for the antenna, although the steady-state patterns are essentially symmetrical. This will be discussed in more detail in the chapter devoted to radiation patterns. The differences in the two sides are primarily due to the instantaneous excitation effects.

3.4 Uniform Amplitude, 45° Leading Phase

Figure 3.20 shows the conventional radiation pattern obtained with a 45° progressive phase, and uniform amplitude excitation to the 49-element array. The main lobe is centered at 14.48° off boresight. Figures 3.21 through 3.26 show some representative pulse shapes for this case. Similarities can be observed in comparison with the 30° case but in general the anomalies are emphasized. Portions of the instantaneous radiation patterns were obtained for this case by plotting pulses for the points marked by crosses in Figure 3.20. Not as many points were computed for this value of θ as for the other three. After some computations were made it was decided that additional computations would not furnish enough new information to justify the time required to make them.

3.5 Uniform Amplitude, 60° Leading Phase

For this phase angle the conventional pattern is shown in Figure 3.27 with points marked by

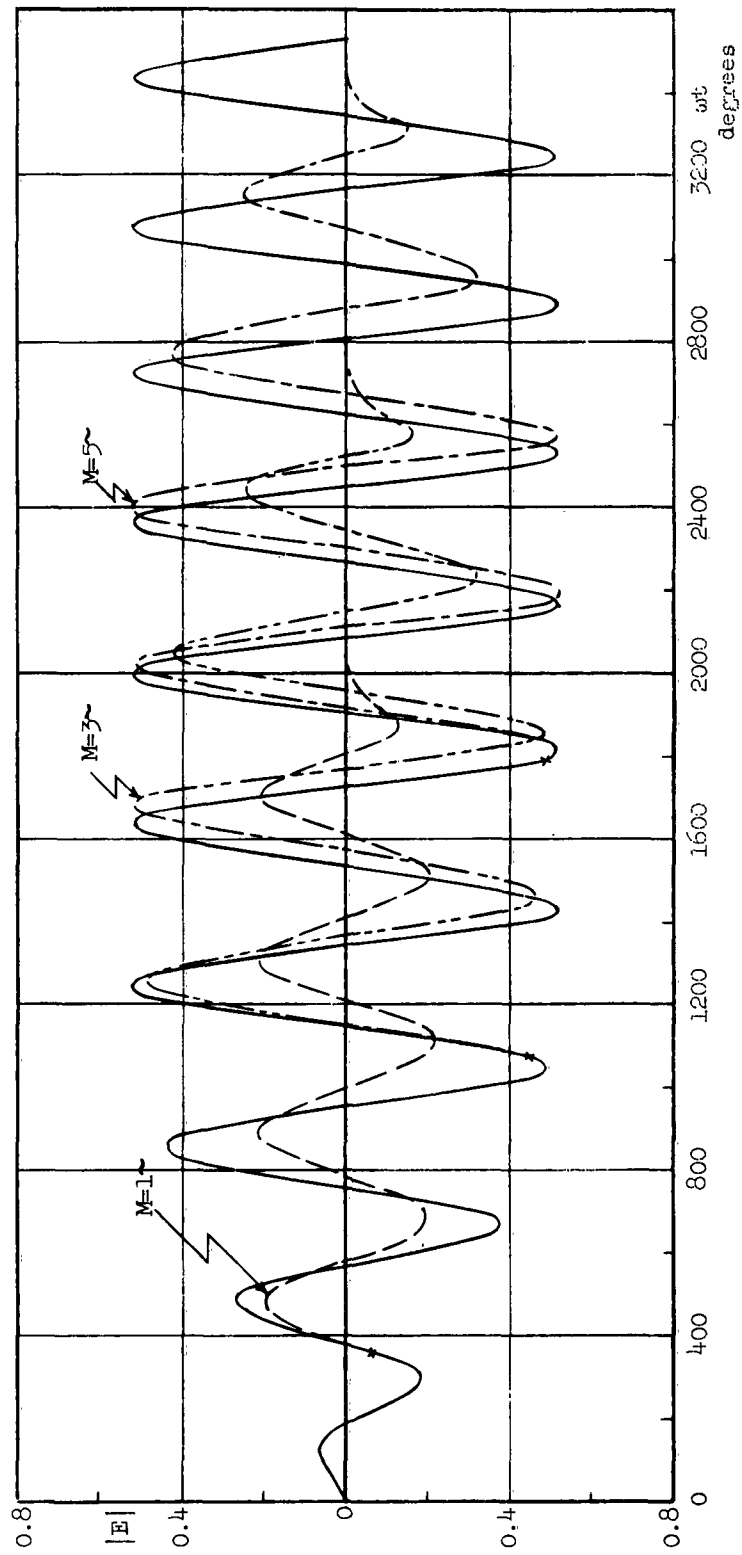


FIGURE 3.11 Transmitted Pulse Shapes $\psi_0 = 30^\circ$ $\theta = 11^\circ$

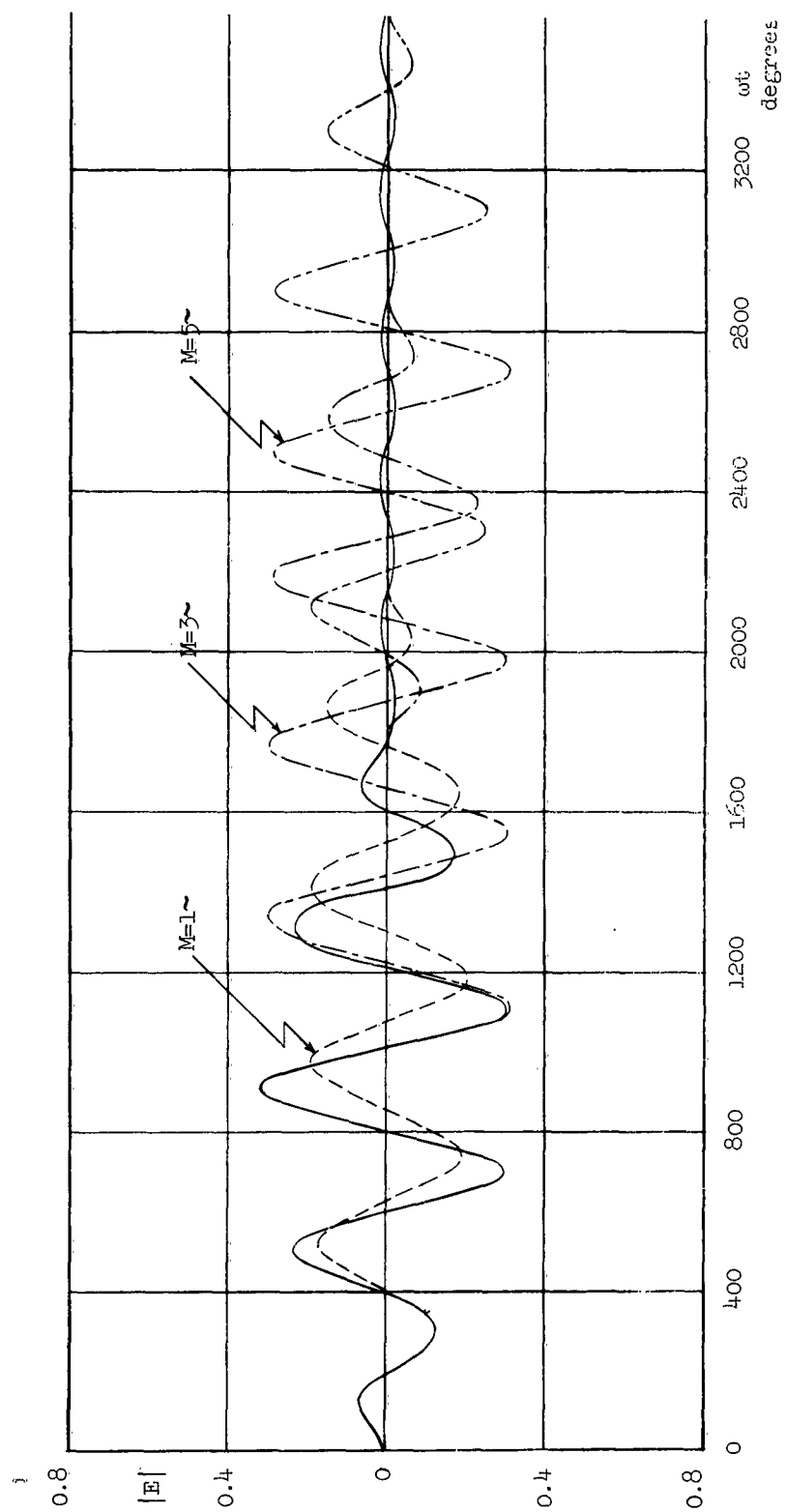


FIGURE 3.12 Transmitted Pulse Shapes $\psi_0 = 30^\circ$ $\theta = 12^\circ$

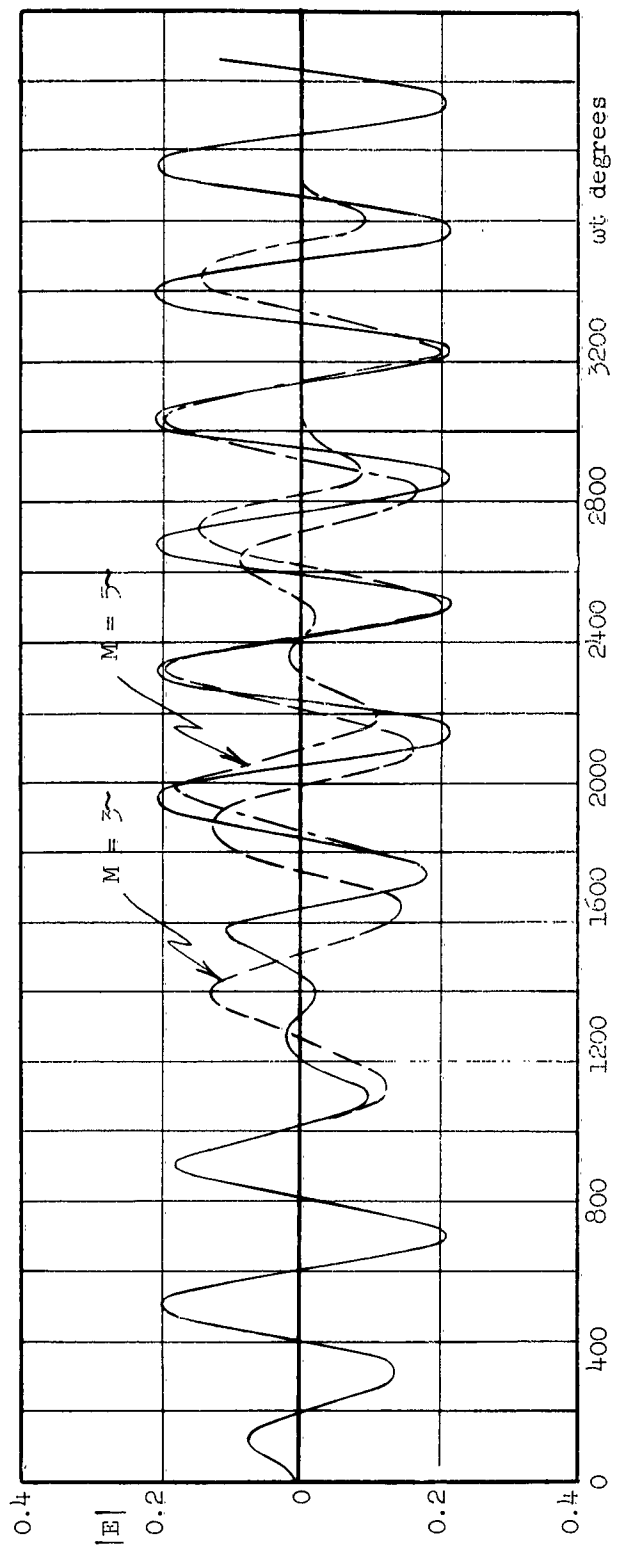


FIGURE 3.13 Transmitted Pulse Shapes $\psi_0 = 30^\circ$ $\theta = 13.0^\circ$

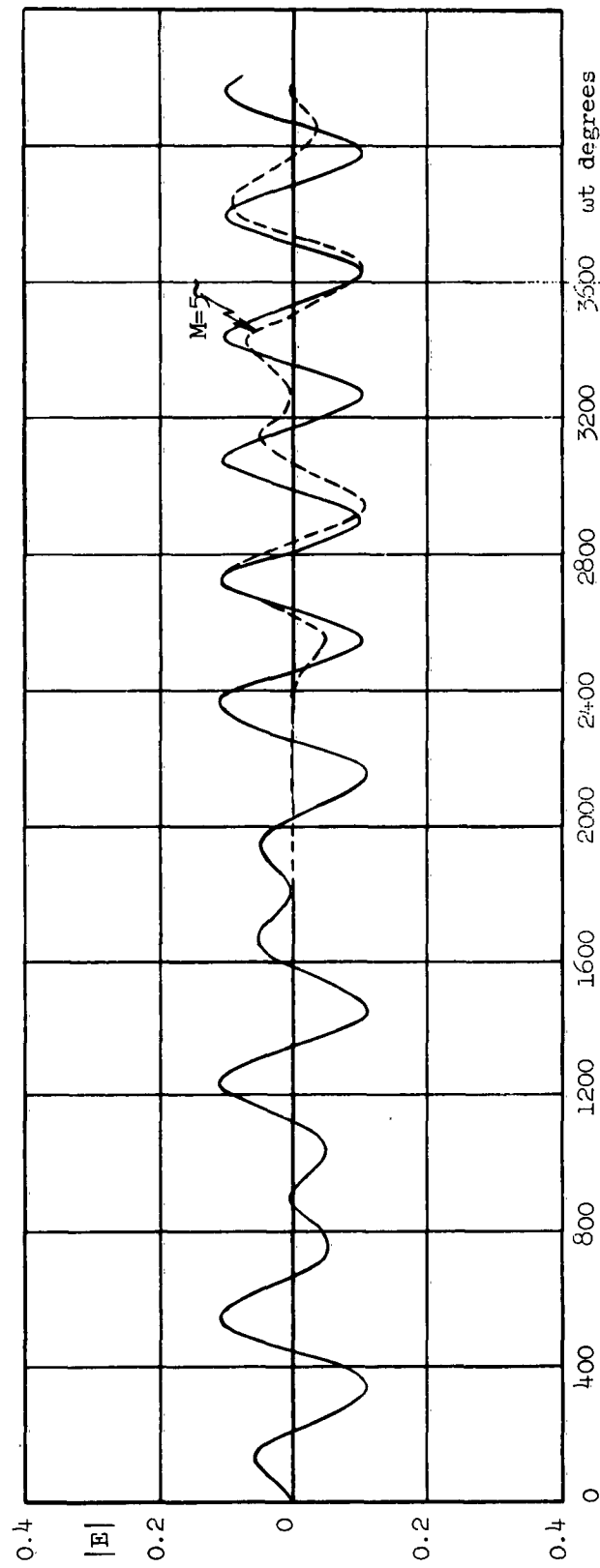


FIGURE 3.14 Transmitted Pulse Shapes $\psi_0 = 30^\circ$ $\theta = 16^\circ$

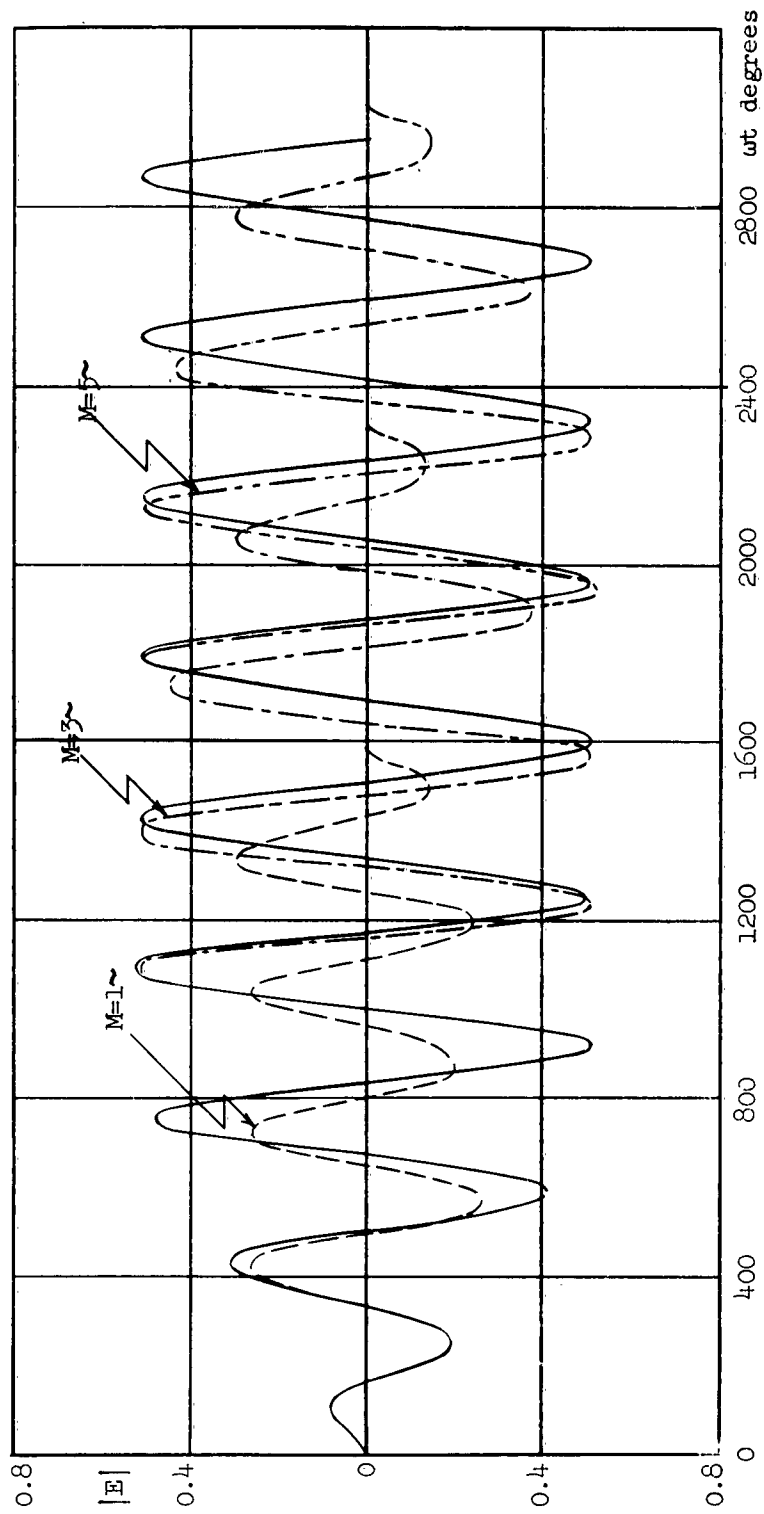


FIGURE 3.15 Transmitted Pulse Shapes $\psi_0 = 30^\circ$ $\theta = 8.2^\circ$

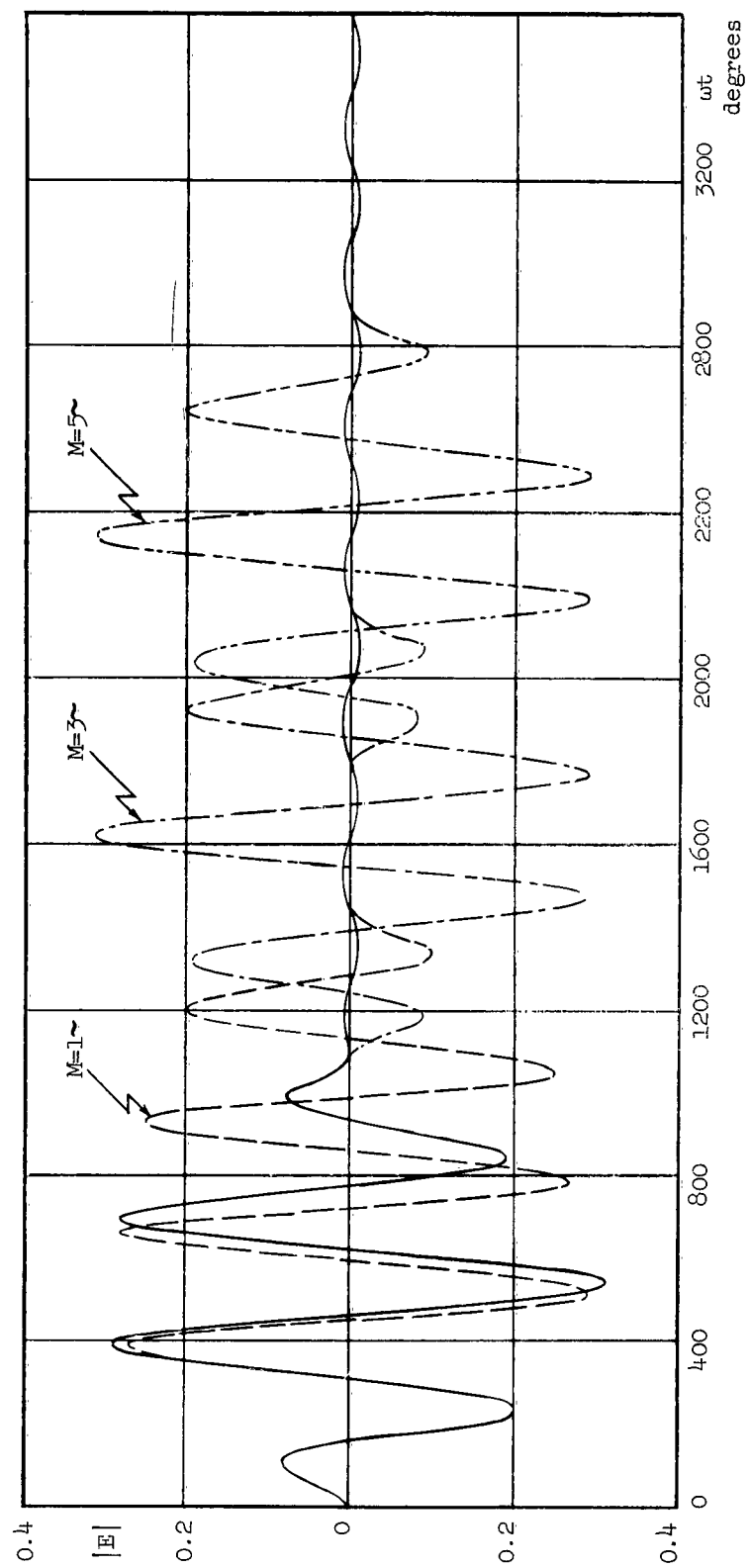


FIGURE 3.16 Transmitted Pulse Shapes $\psi_0 = 30^\circ$ $\theta = 7.2^\circ$

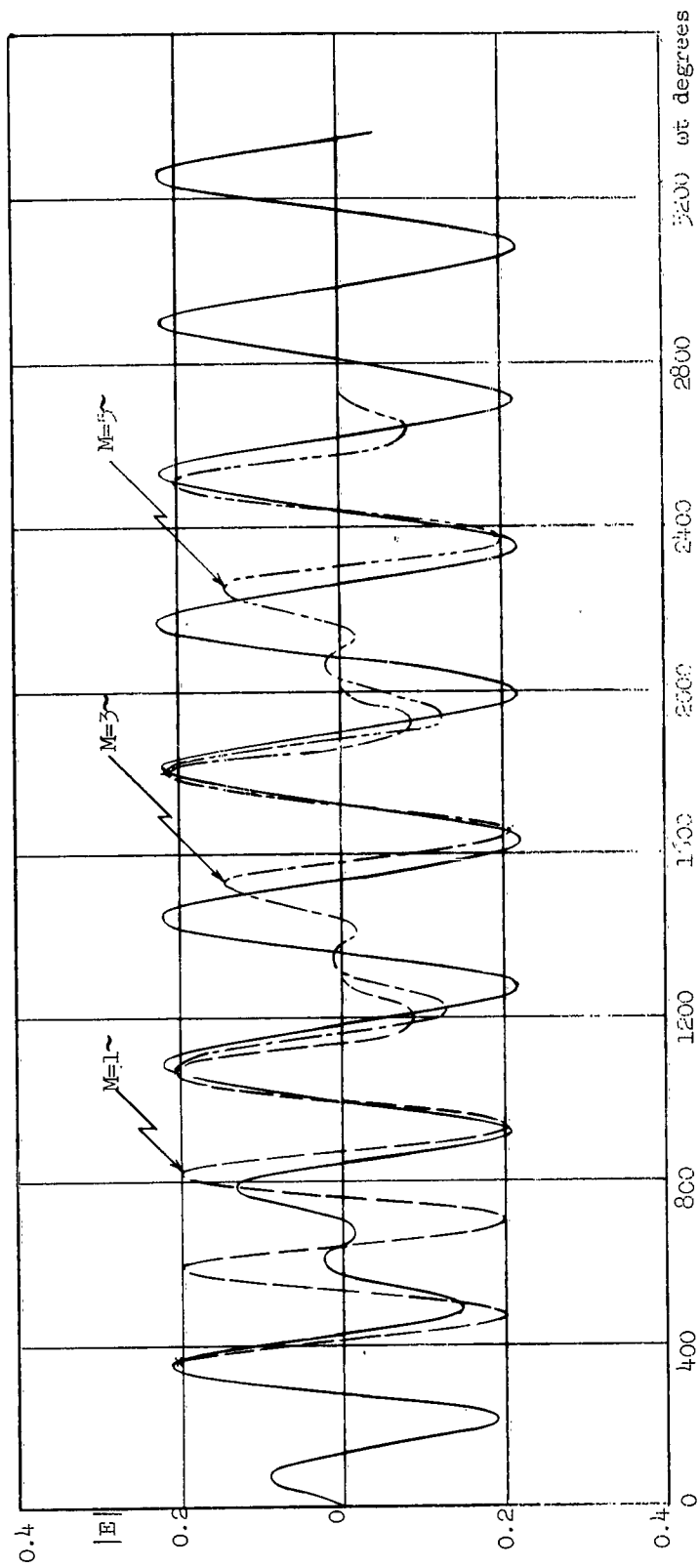


FIGURE 3.17 Transmitted Pulse Shapes $\psi_0 = 30^\circ$ $\theta = 6.2^\circ$

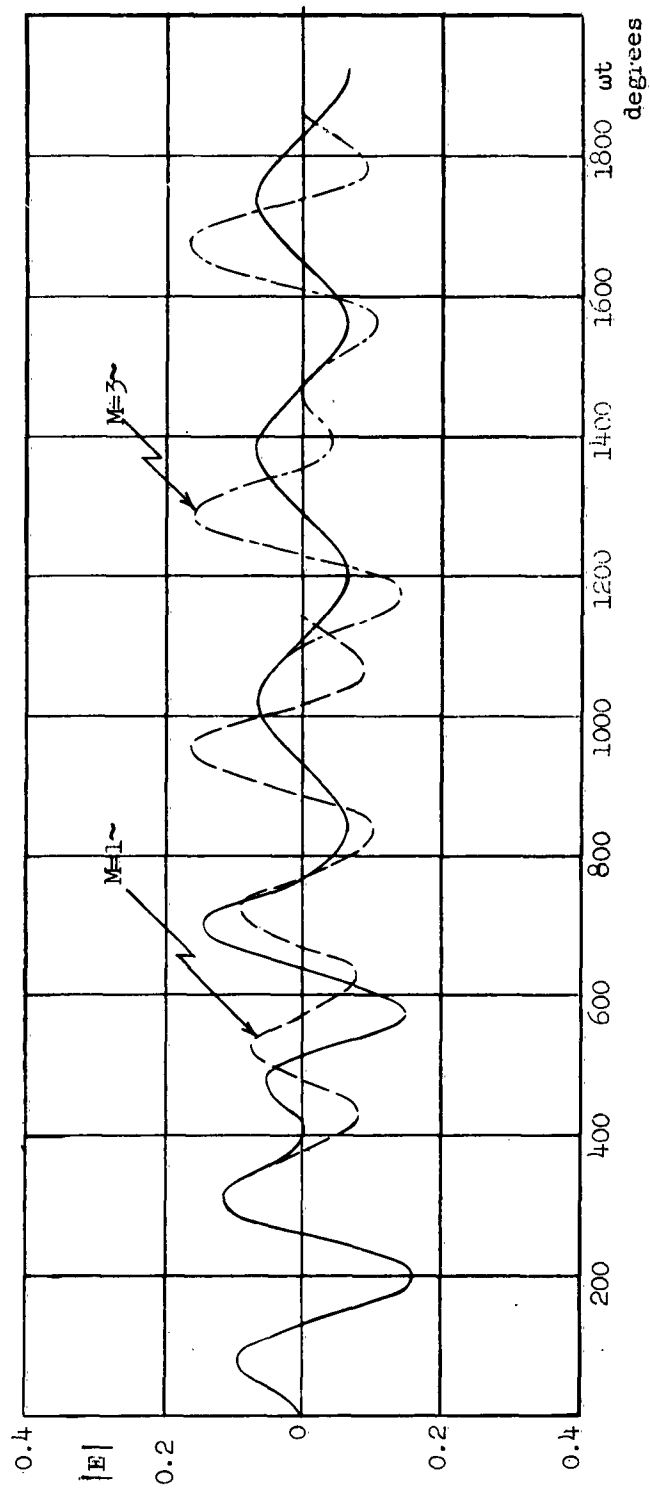


FIGURE 3.18 Transmitted Pulse Shapes $\psi_0 = 30^\circ$ $\theta = 5.2^\circ$

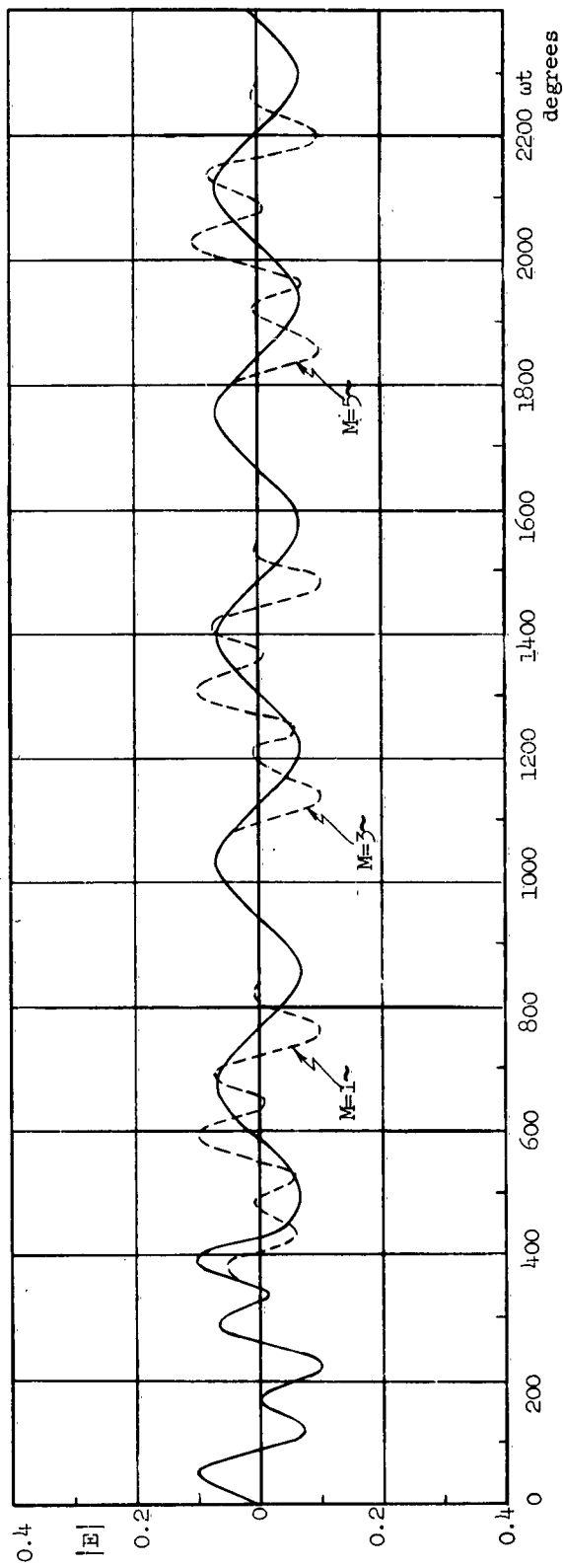


FIGURE 3.19 Transmitted Pulse Shapes $\psi_0 = 30^\circ$ $\theta = 3^\circ$

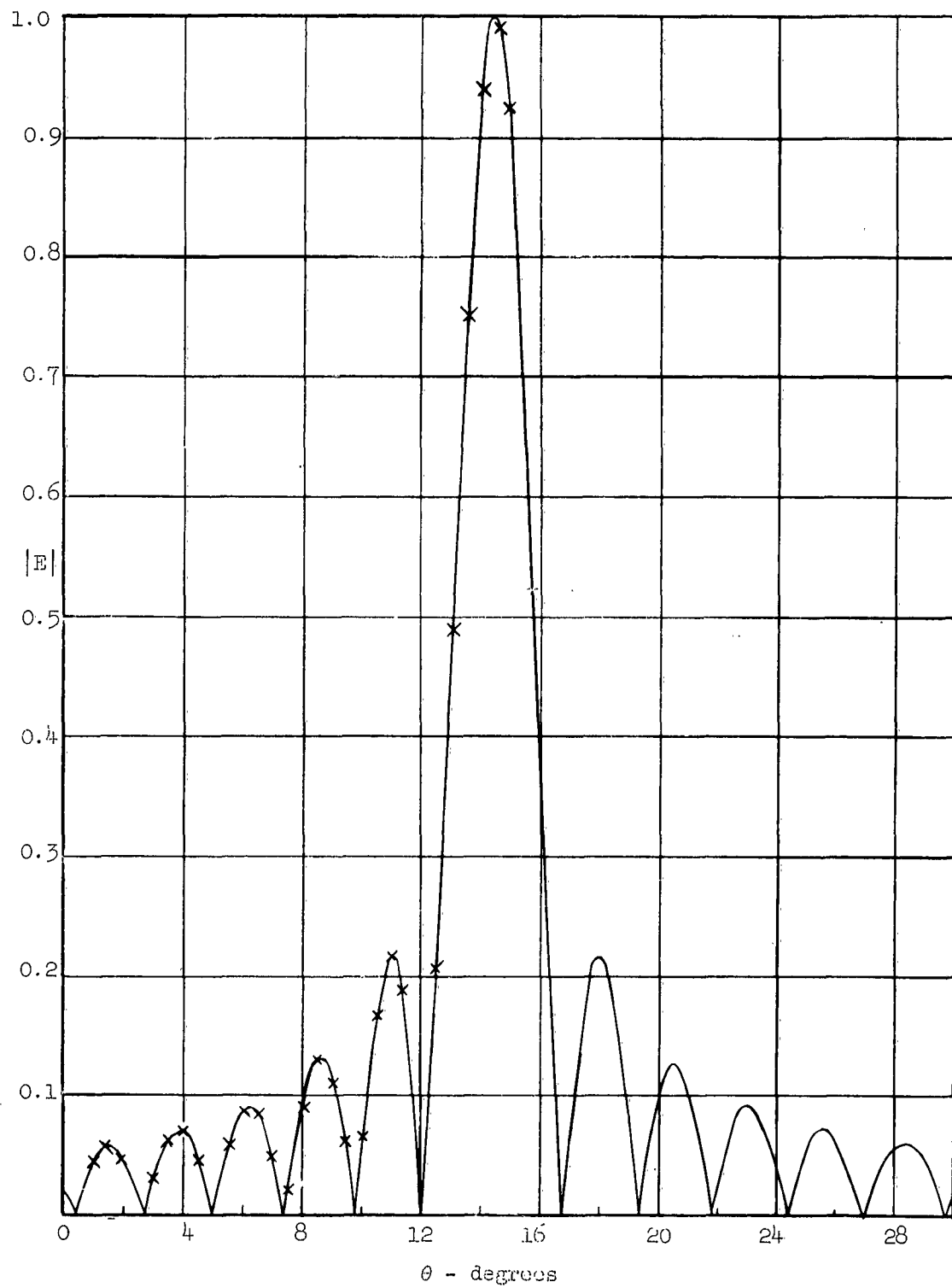


FIGURE 3.20 Conventional Radiation Pattern $\psi_0 = 45^\circ$

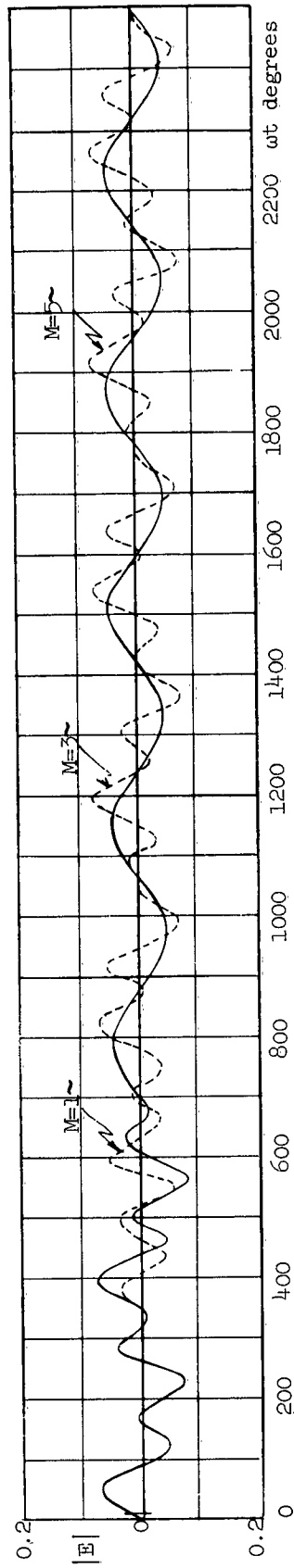


FIGURE 3.21 Transmitted Pulse Shapes $\psi_0 = 45^\circ$ $\theta = 4.5^\circ$

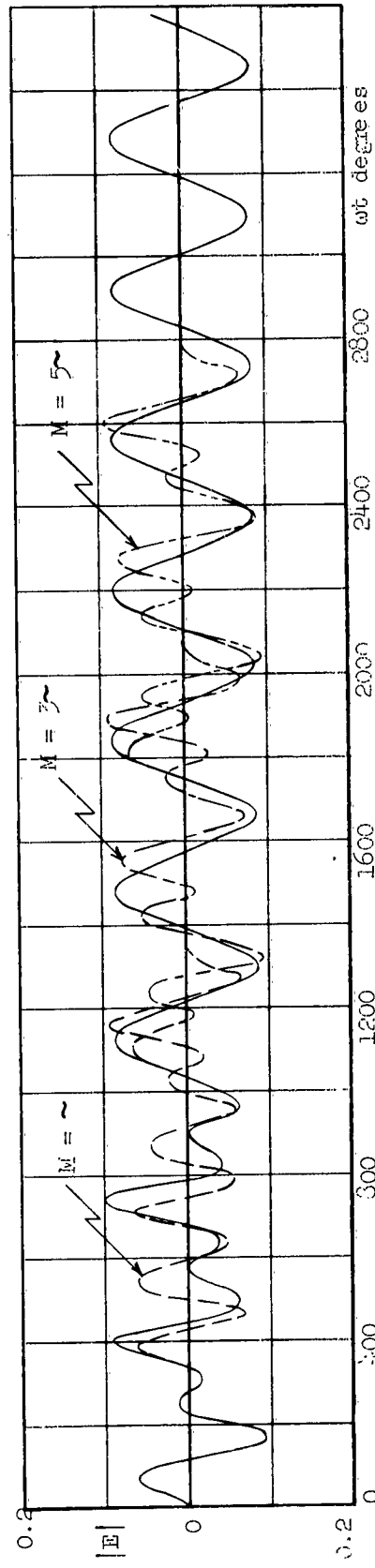


FIGURE 3.22 Transmitted Pulse Shapes $\psi_0 = 45^\circ$ $\theta = 6.5^\circ$

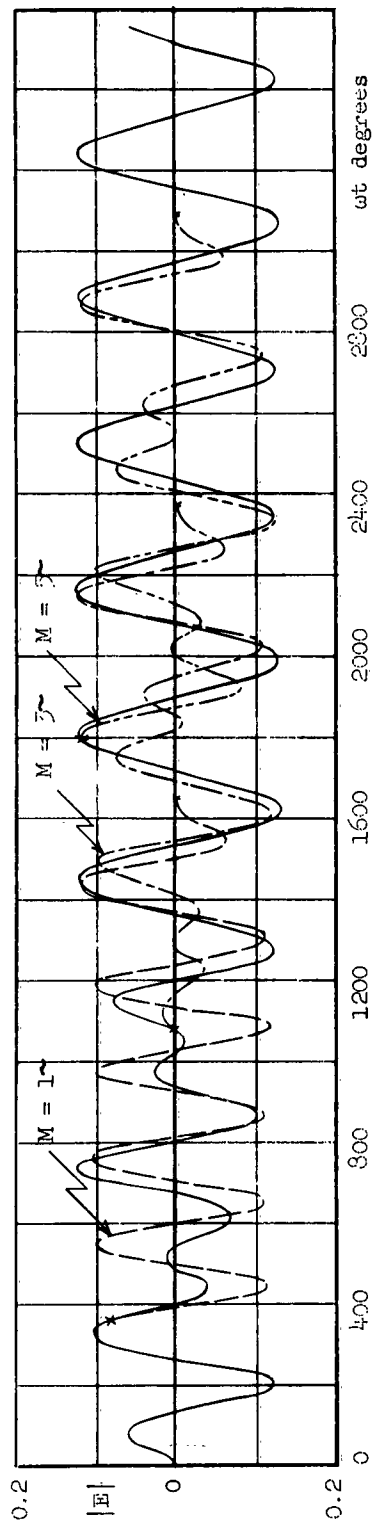


FIGURE 3.23 Transmitted Pulse Shapes $\psi_0 = 45^\circ$ $\theta = 8.5^\circ$

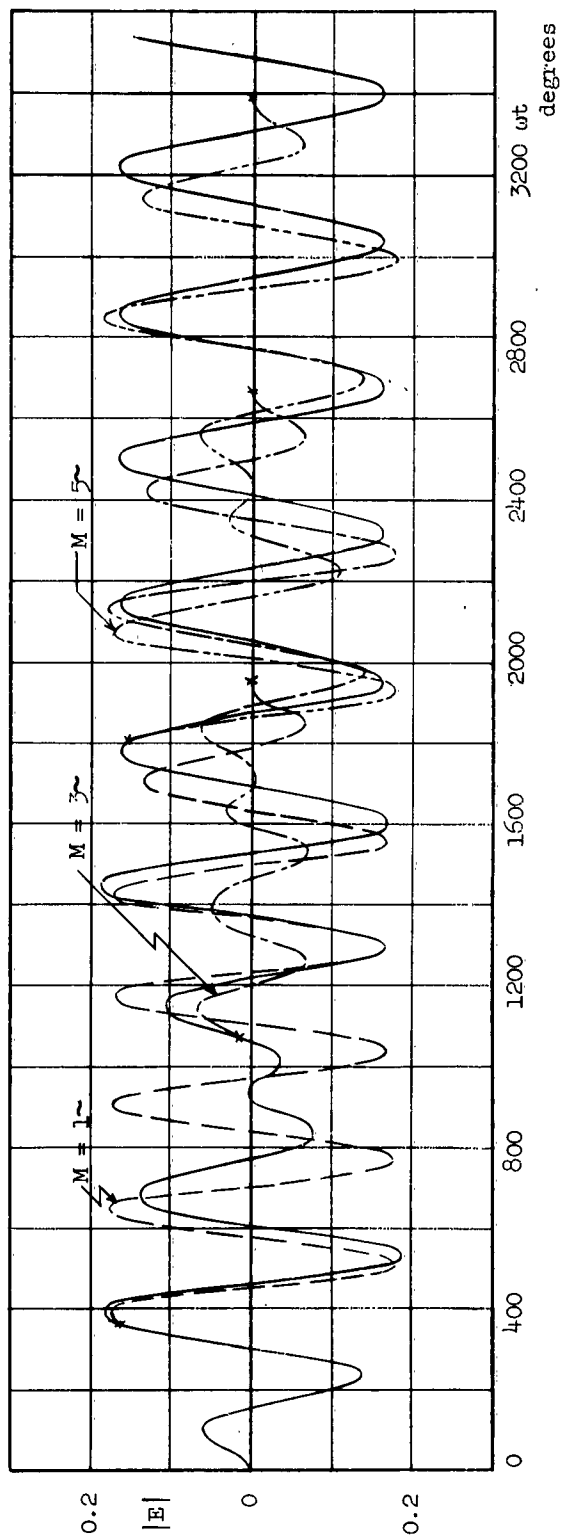


FIGURE 3.24 Transmitted Pulse Shapes $\psi_0 = 45^\circ$ $\theta = 10.5^\circ$

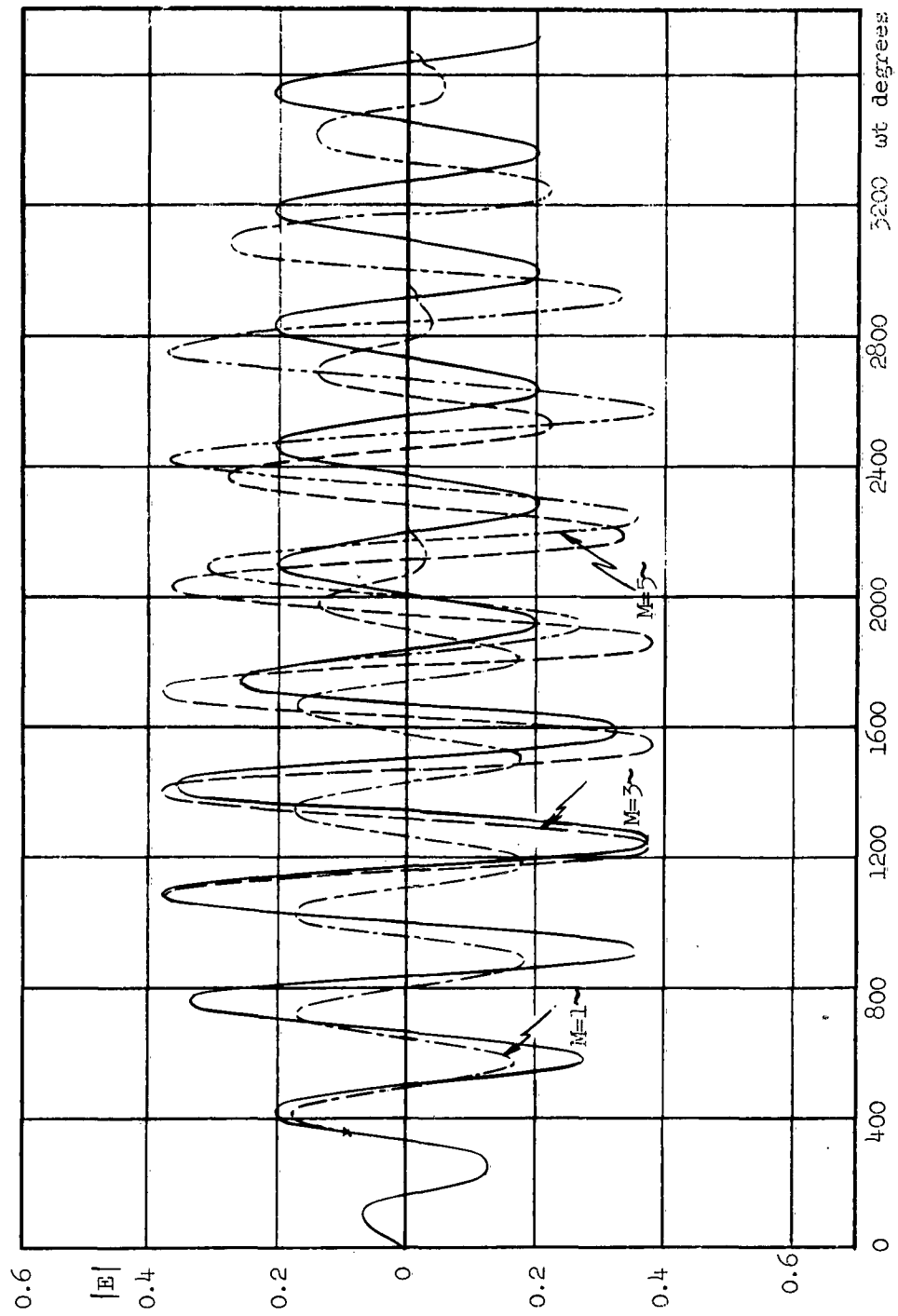


FIGURE 3.25 Transmitted Pulse Shapes $\psi_0 = 45^\circ$ $\theta = 12.5^\circ$

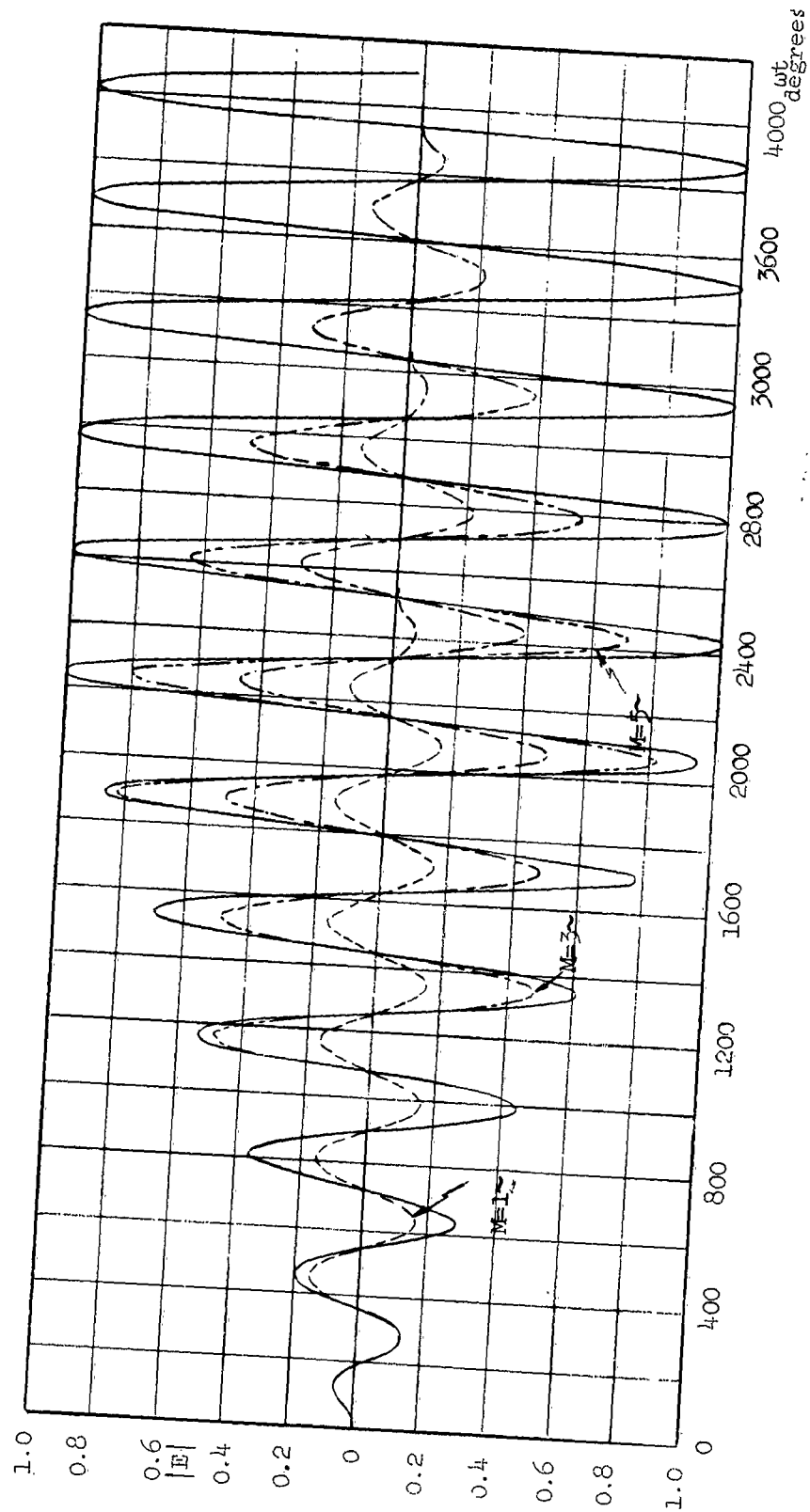


FIGURE 3.26 Transmitted Pulse Shapes $\psi_0 = 45^\circ$ $\theta = 14.5^\circ$

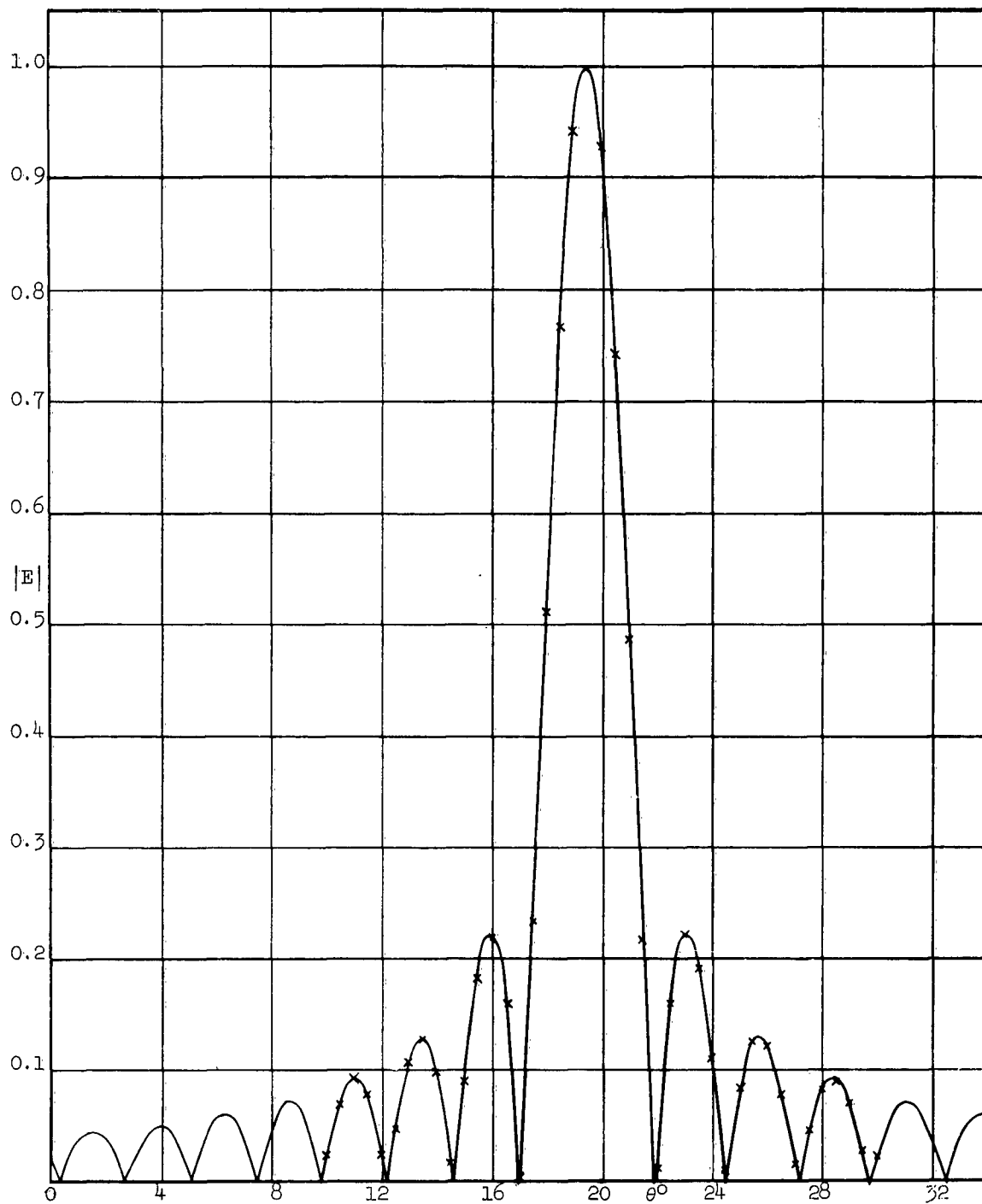


FIGURE 3.27 Conventional Radiation Pattern $\psi_0 = 60^\circ$

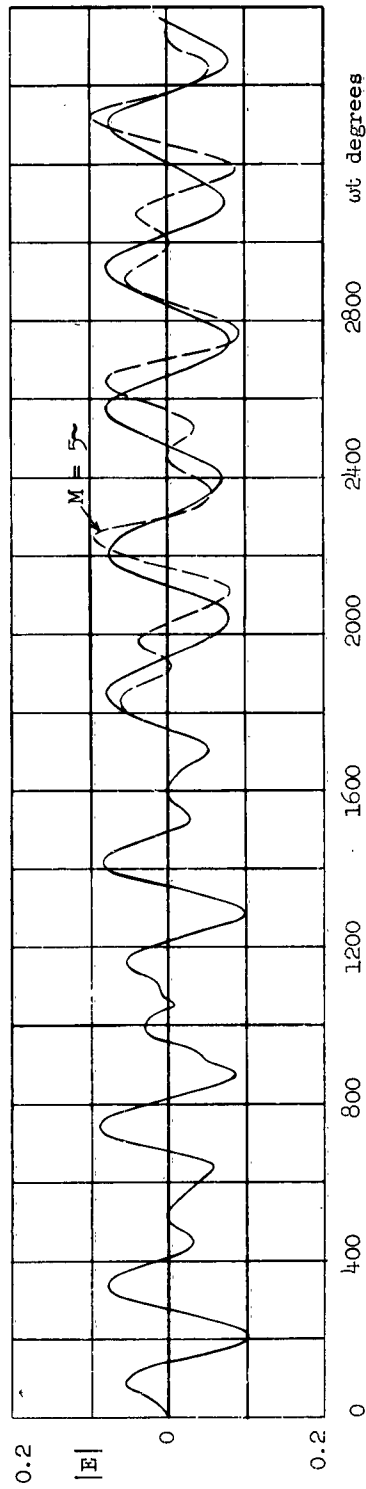


FIGURE 3.28 Transmitted Pulse Shapes $\psi_0 = 60^\circ$ $\theta = 11.5^\circ$

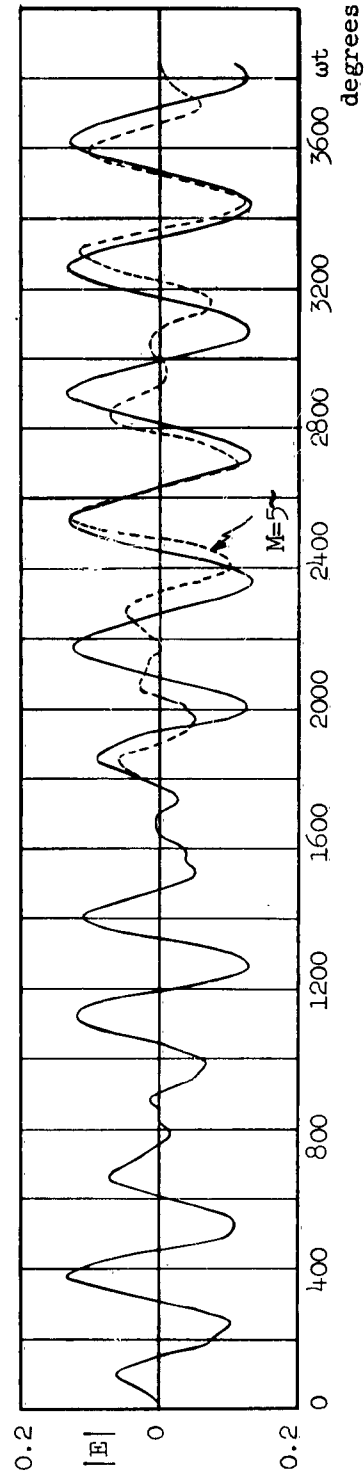


FIGURE 3.29 Transmitted Pulse Shapes $\psi_0 = 60^\circ$ $\theta = 13.5^\circ$

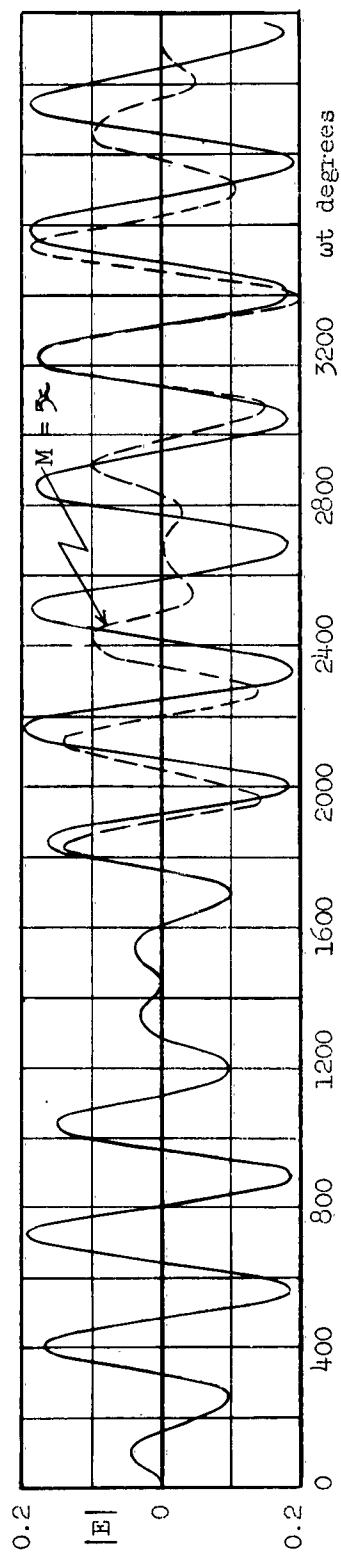


FIGURE 3.30 Transmitted Pulse Shapes $\psi_0 = 60^\circ$ $\theta = 15.5^\circ$

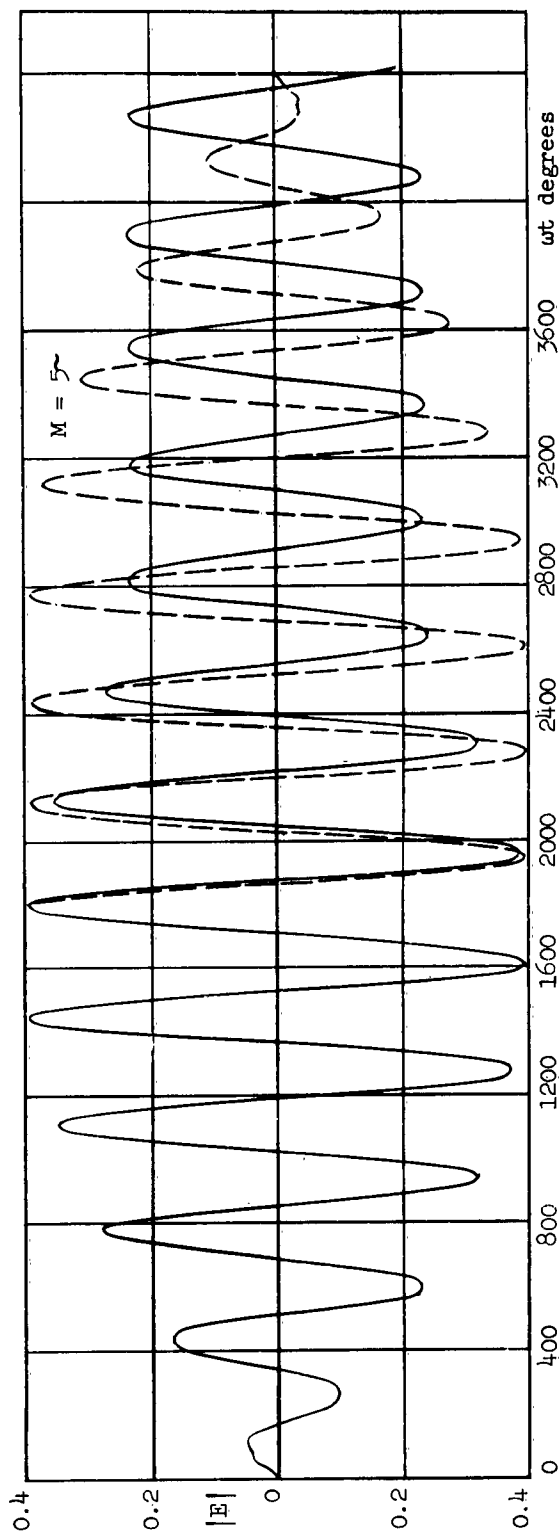


FIGURE 3.31 Transmitted Pulse Shape $\psi_0 = 60^\circ$ $\theta = 17.5^\circ$

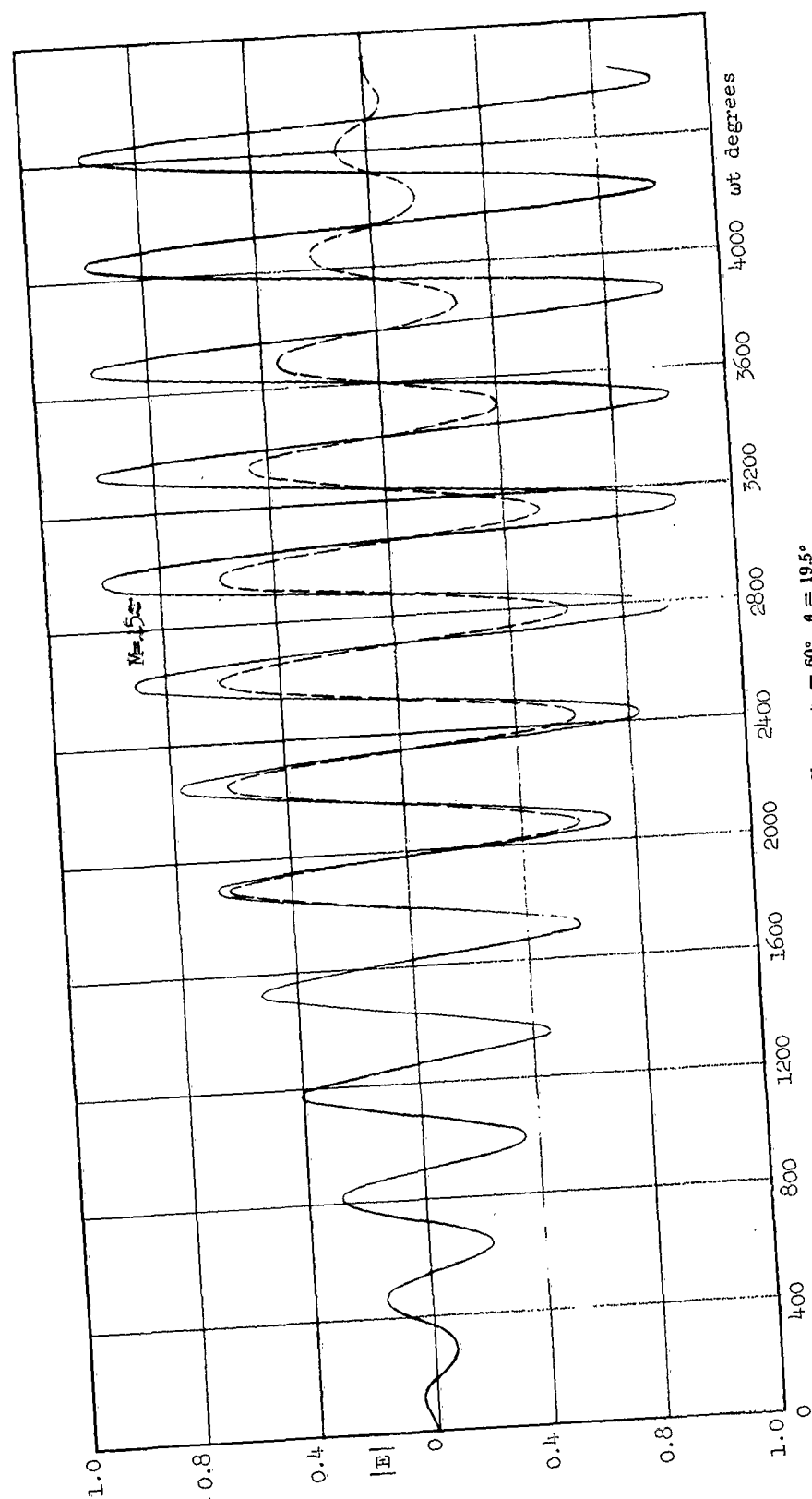


FIGURE 3.32 Transmitted Pulse Shape $\psi_0 = 60^\circ$ $\theta = 19.5^\circ$

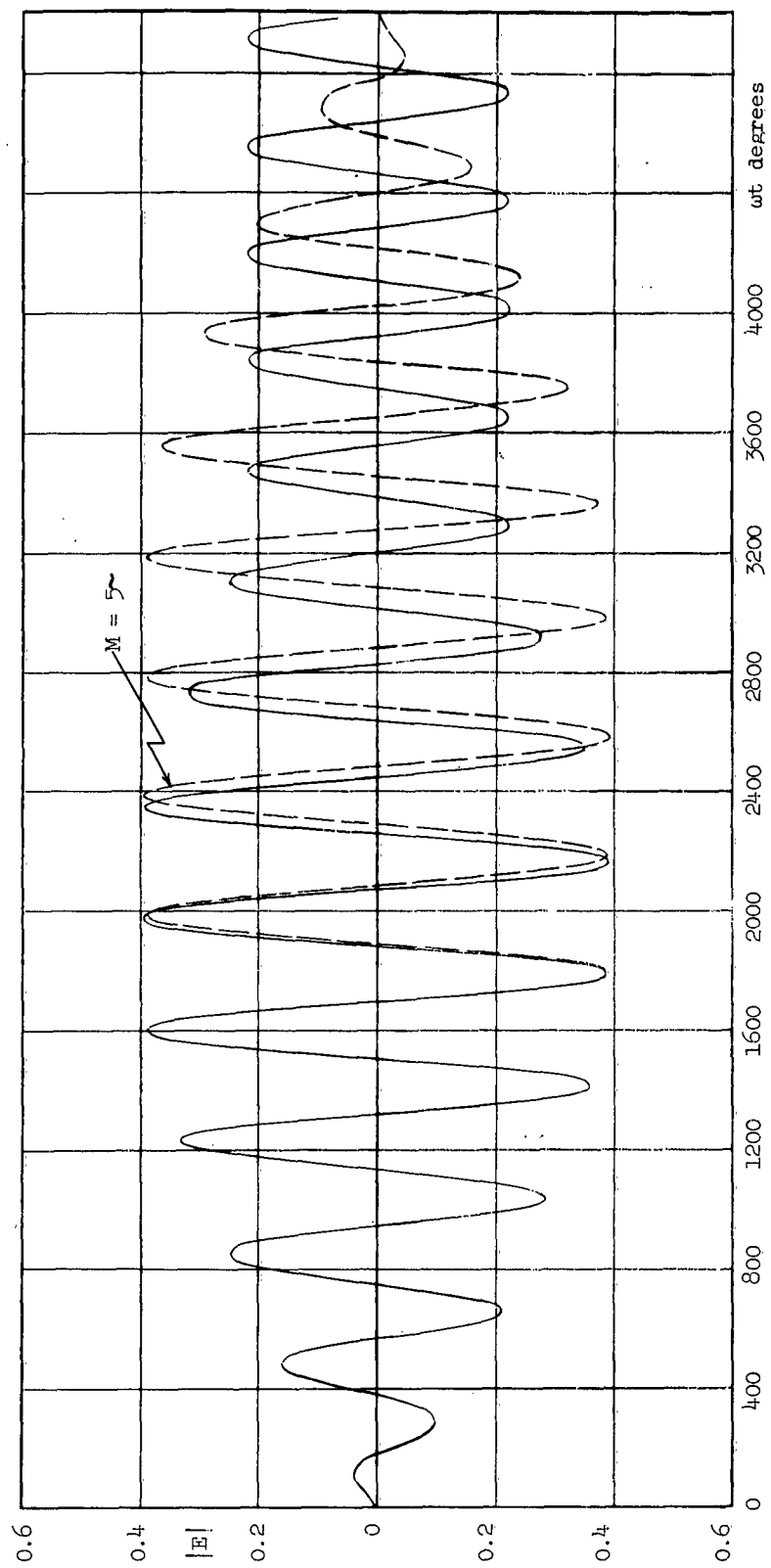


FIGURE 3.33 Transmitted Pulse Shapes $\psi_0 = 60^\circ$ $\theta = 21.5^\circ$

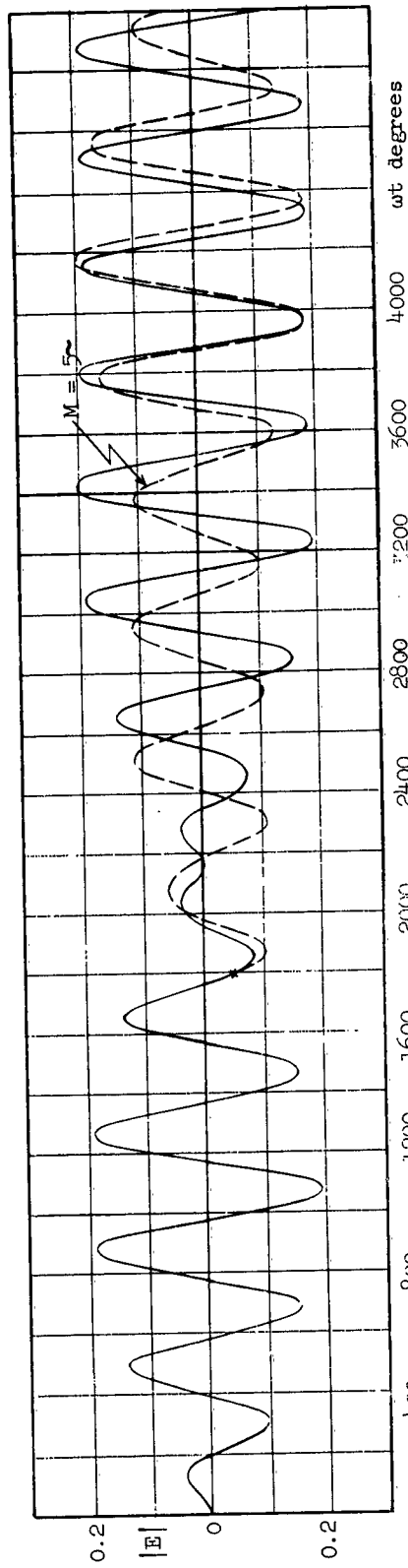


FIGURE 3.34 Transmitted Pulse Shapes $\psi_0 = 60^\circ$ $\theta = 23.5^\circ$

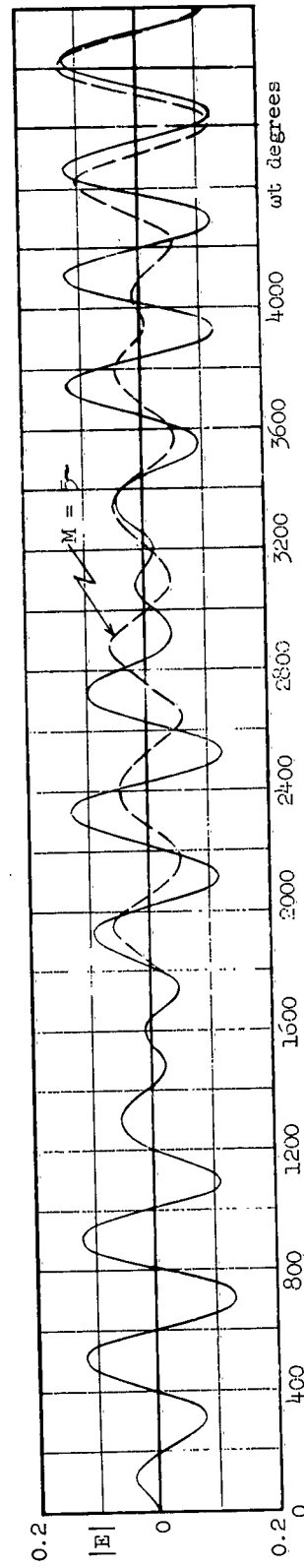


FIGURE 3.35 Transmitted Pulse Shapes $\psi_0 = 60^\circ$ $\theta = 25.5^\circ$

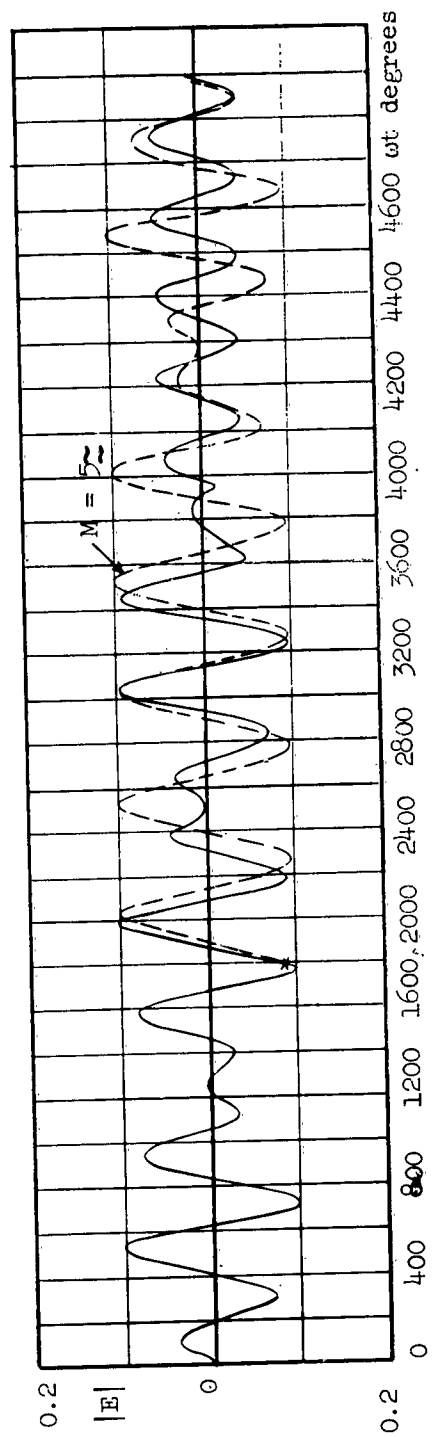


FIGURE 3.36 Transmitted Pulse Shapes $\psi_0 = 60^\circ$ $\theta = 27.5^\circ$

crosses to show the angles for which pulses were computed. Representative pulse shapes are shown in Figures 3.28 through 3.36, with only the five-cycle excitation case illustrated because the pulses

for the other two cases overlap. As with the smaller phase angle cases, anomalies appear, but moved further out along the base line as would be expected.

IV. INSTANTANEOUS RADIATION PATTERNS

Determination of the radiation patterns as a function of time for each of the several phase angles considered was accomplished through the use of the large number of pulse diagrams. This method was chosen rather than programming a computer to give the final result directly, because the latter method would have required a very complex computer program; and would involve an excessive amount of time on the IBM 650. A computer with a larger memory capacity and with a plotter connected to the output could conceivably do the job at an efficient speed to justify obtaining complete solutions from the computer.

The technique used required the selection of values of $|E|$ at the same value of ωt corresponding to a particular instant of time for all values of θ computed for a given excitation pulse duration. The data obtained in this manner constituted a single radiation pattern for the instant of time selected. A large family of these curves is required to show in detail how the radiation pattern fluctuates as a function of time and as a function of pulse duration. However, a certain amount of work is saved by recognizing that some of the radiation patterns can be applied to pulses of different excitation durations. The time intervals ranging from $0^\circ < \omega t < M_k 360^\circ$ apply for all excitation pulses of durations $\tau \geq M_k 360^\circ$, since that portion of the resultant pulses is the same for all. M_k is the number of cycles in a particular pulse. For every new $M_j (M_j > M_k)$ it is only necessary to plot additional patterns for values of ωt in the range for which the resultant pulses are not alike.

The amount of information that is obtained from the plots of the instantaneous radiation patterns becomes a function of the increments of θ that are selected when plotting pulses, and the intervals of time selected for computing the pulses and also in plotting patterns. The two time intervals for these two operations are not necessarily the same. For this work the pulse shapes were computed using $\omega t = 30^\circ$ for the time intervals, whereas $\omega t = 90^\circ$ was chosen for obtaining radiation patterns.

Patterns were plotted as $|E|$ vs. θ with relative

phasing shown by plus and minus signs under the appropriate portions of the curves. This was found helpful in comparing the curves, as an aid in observing changes in specific side lobes.

Presentation of the patterns in a manner which clearly illustrates how the radiation patterns fluctuate with time is extremely difficult. A single diagram presentation was attempted for the one-cycle case but even with colored pencils the diagram became very difficult to read with only the first five curves plotted, in the range $0 < \omega t < 450^\circ$. In a black-and-white presentation, as a technical report is generally printed, one must resort to a variety of broken lines, all different. The diagram then becomes even more difficult to read. Hence, selected patterns have been shown as separate diagrams, grouped initially by phase angle and secondarily by excitation pulse duration. The patterns could be studied either by examining successive patterns or by observing variations among all patterns which are separated in ωt by intervals of 360° .

4.1 Uniform Amplitude, Zero Phase Radiation Patterns

Patterns for the uniform amplitude, zero phase case are presented first. Figures 4.1 through 4.7 show pattern variations for the one-cycle case. Figures 4.8 through 4.21 show the variations for the three-cycle case. Figures 4.1 through 4.4 apply to this case also, for values of ωt through 360° . Figures 4.22 through 4.33 show the variations in the pattern for the 5-cycle case.

4.2 Uniform Amplitude, 30° Progressive Phase Radiation Patterns

For the 30° phase angle case, with one cycle excitation pulse, the variations in the radiation patterns are illustrated in Figures 4.34 through 4.37. These four diagrams are shown primarily because they apply to the 3 and 5 cycle cases as well. Figures 4.38 and 4.39, when compared with Figures 4.34 and 4.35, show how the patterns have

changed after a lapse of time equivalent to $\omega t = 720^\circ$. No additional patterns are shown for this case because the trends are well illustrated by the other two cases although to a much greater degree. In fact, the five cycle case can serve to illustrate the shorter pulse behavior, but representative patterns for the other cases are shown to present the deviations from the five cycle case.

Figures 4.40 through 4.51 represent the three cycle case, including those of the 1 cycle case which apply; namely, Figures 4.34 through 4.37. Some intermediate values of ωt have been omitted.

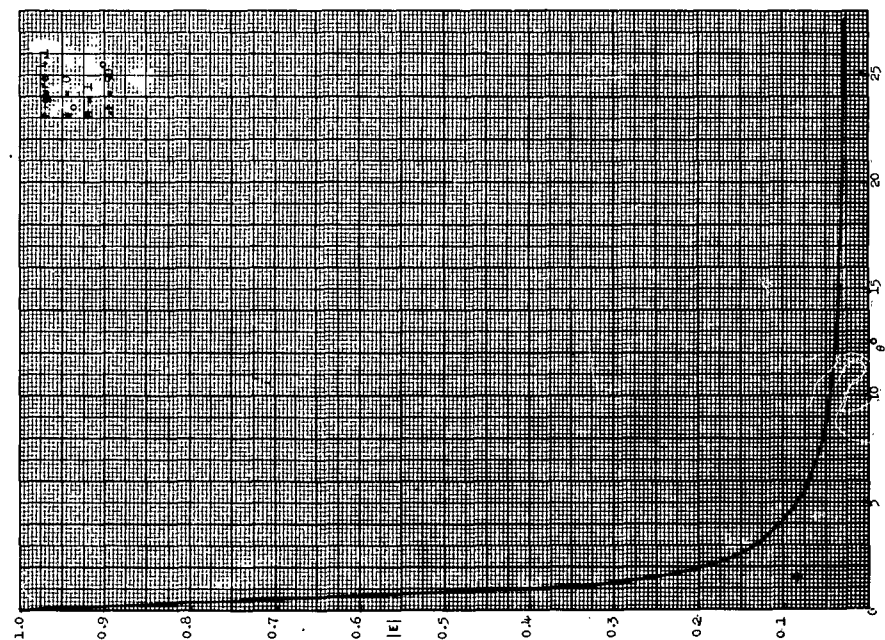
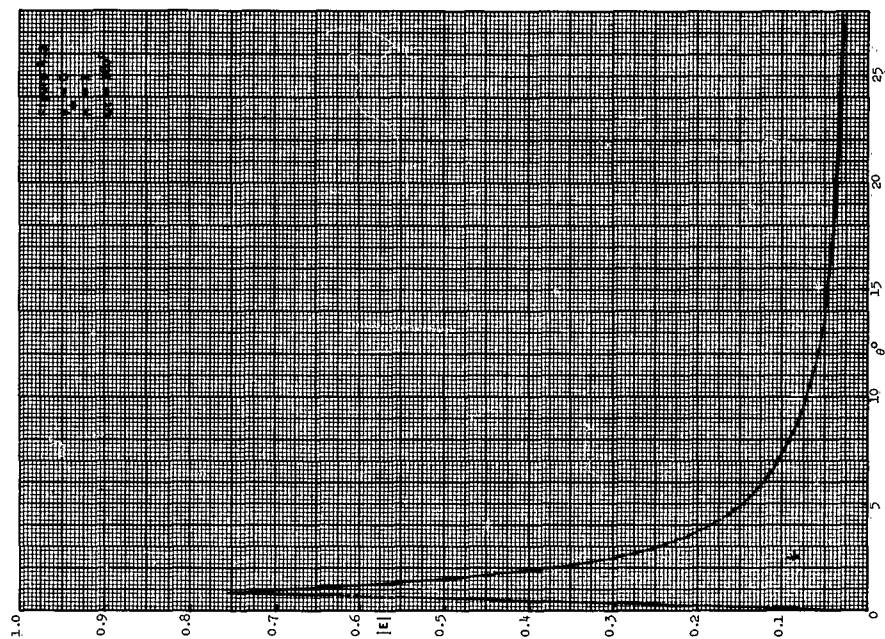
Figures 4.52 through 4.64 represent the five cycle case, including those of the one cycle case (Figures 4.34 through 4.37) and the three cycle case (Figures 4.40 through 4.44) which apply. Again, some intermediate values of ωt have been omitted.

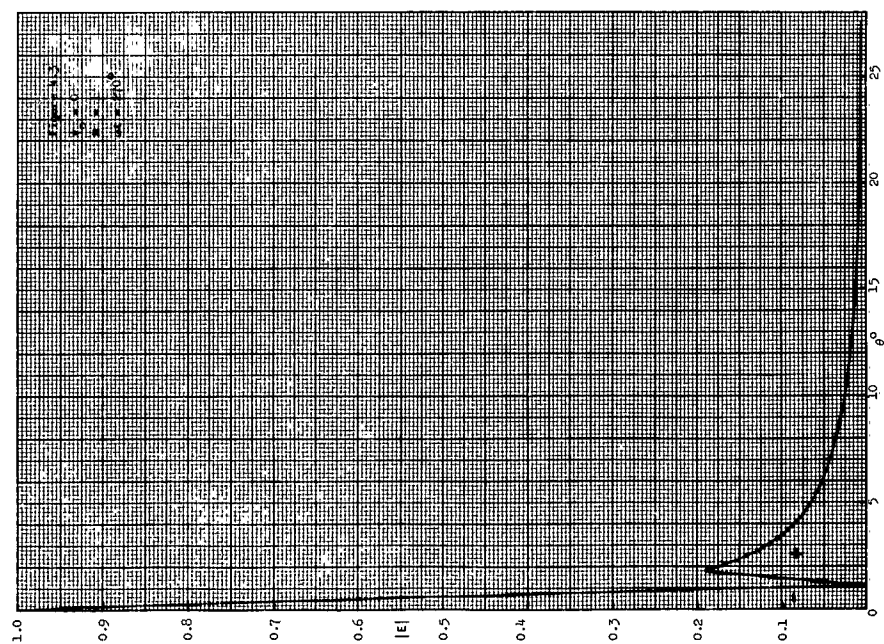
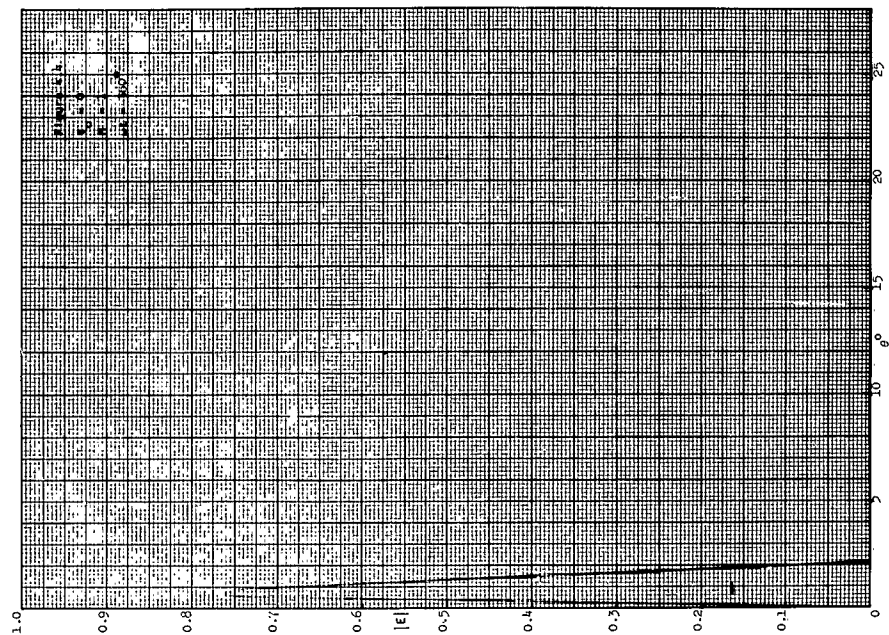
4.3 Uniform Amplitude, 45° Progressive Phase Radiation Patterns

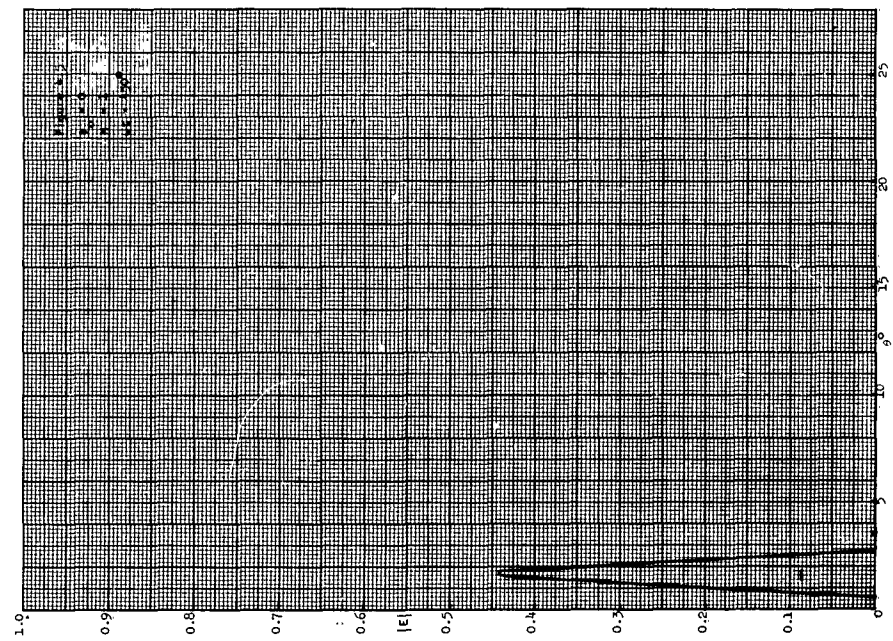
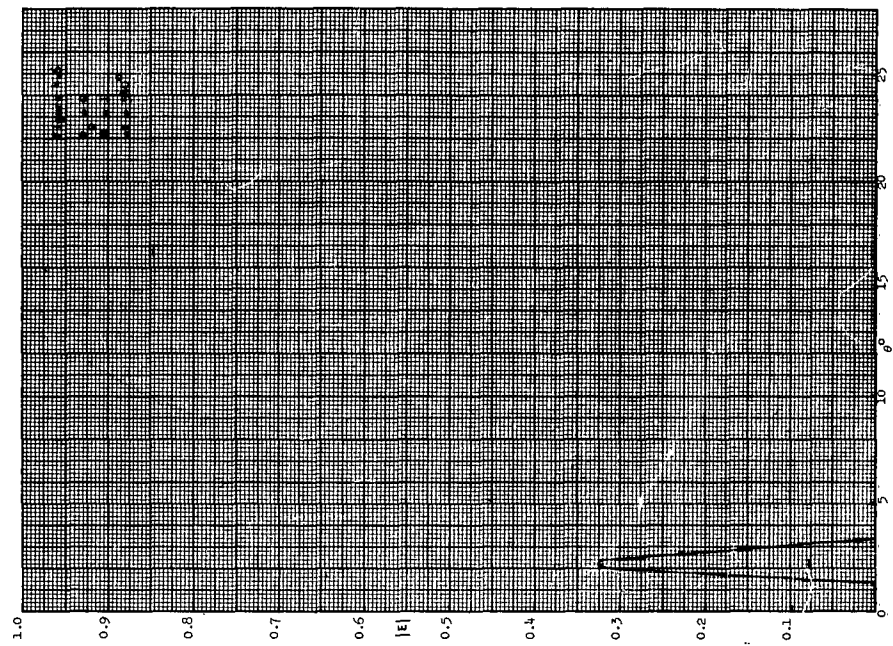
Figures 4.65 through 4.97 represent the instantaneous radiation patterns for the 45° phase case, Figures 4.65 through 4.68 for the one cycle pulse case apply to both the three-cycle and the five cycle pulse cases, and Figures 4.74 through 4.78 for the three cycle case also apply to the five cycle pulse case.

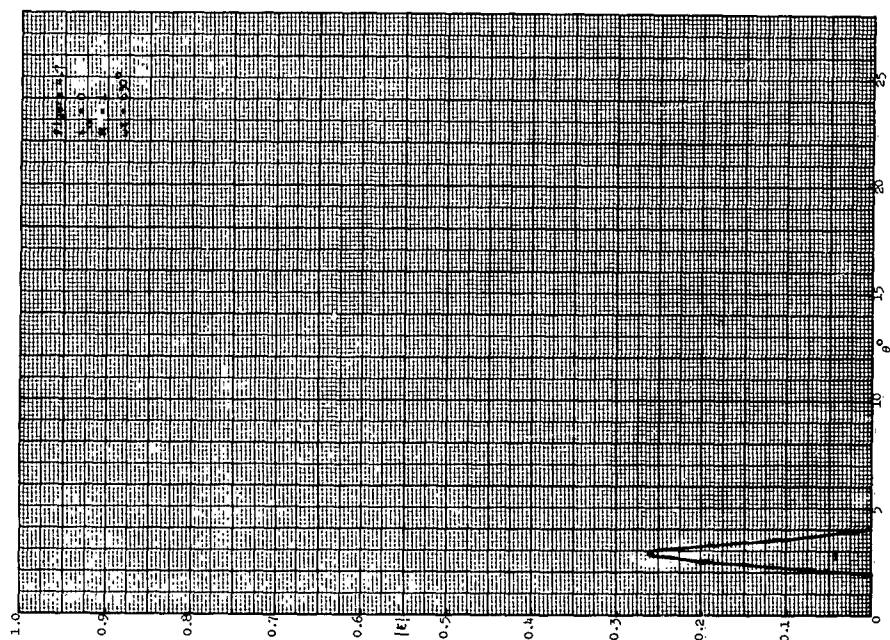
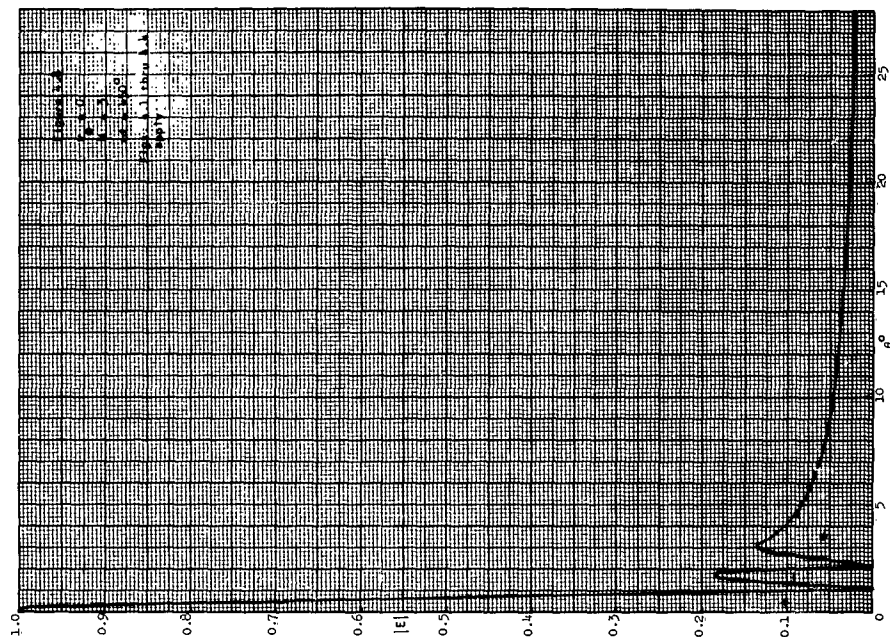
4.4 Uniform Amplitude, 60° Progressive Phase Radiation Patterns

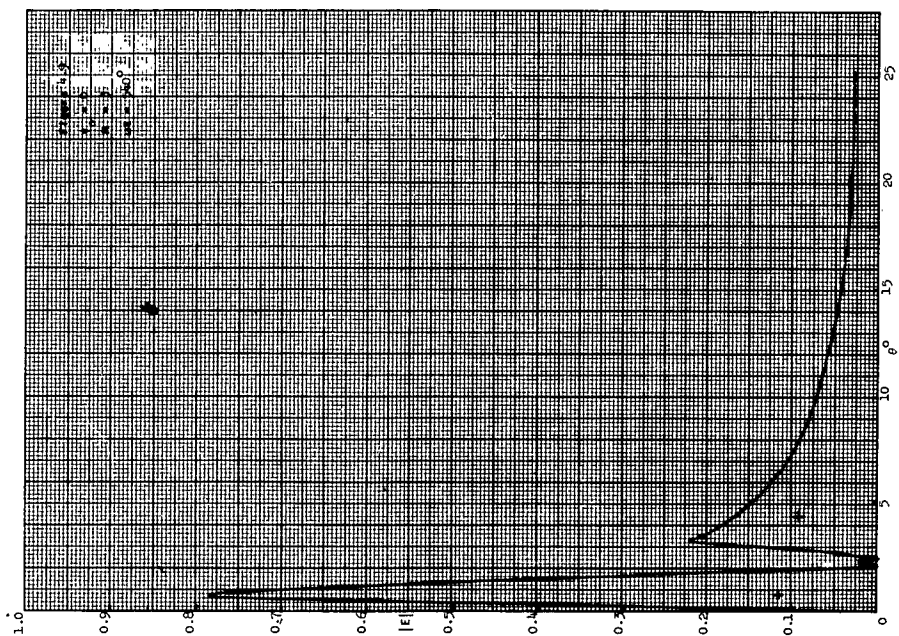
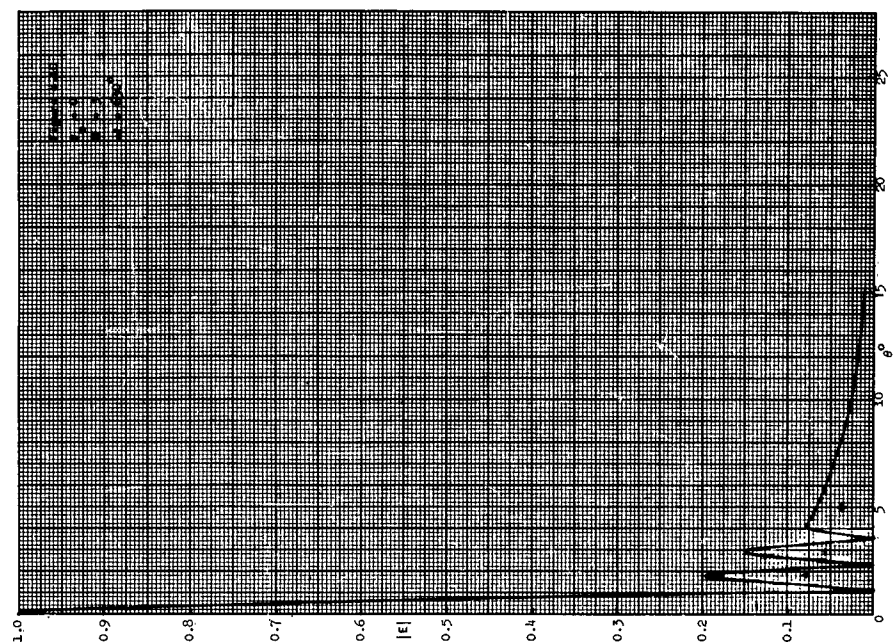
Figures 4.98 through 4.138 represent the instantaneous radiation patterns for the 60° phase case. Figures 4.98 through 4.101 apply to both the three cycle and the five cycle pulse cases, and Figures 4.107 through 4.110 apply to the five cycle pulse case.

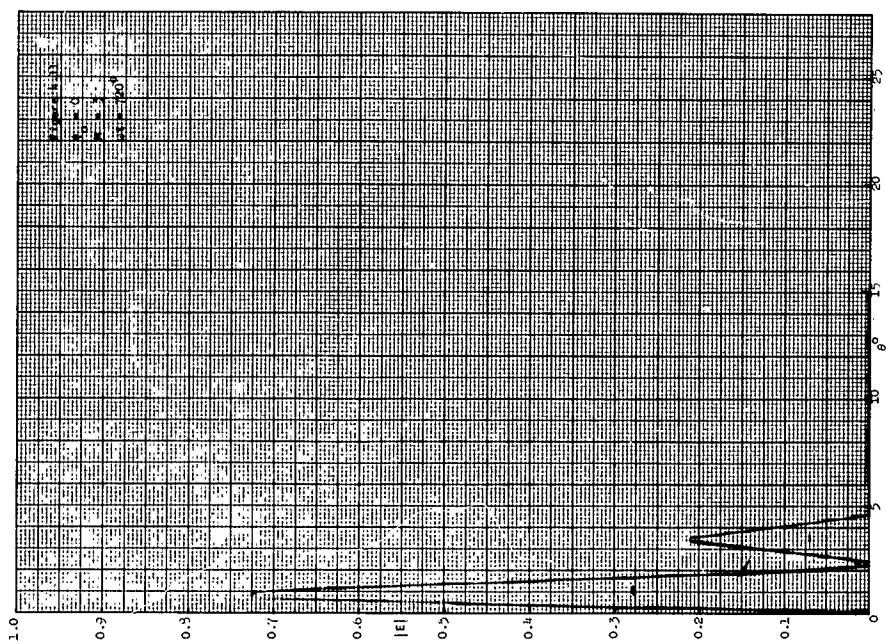
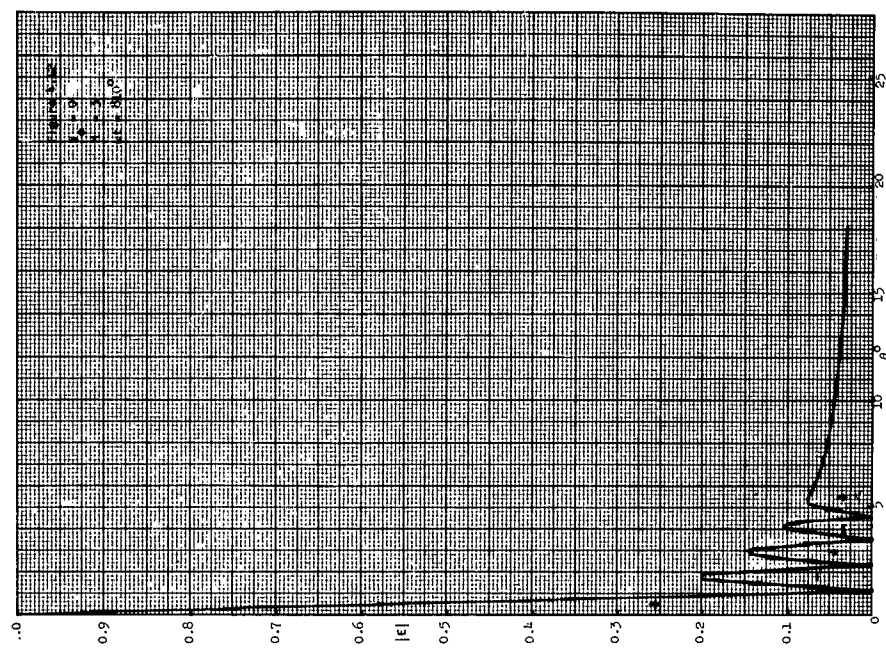


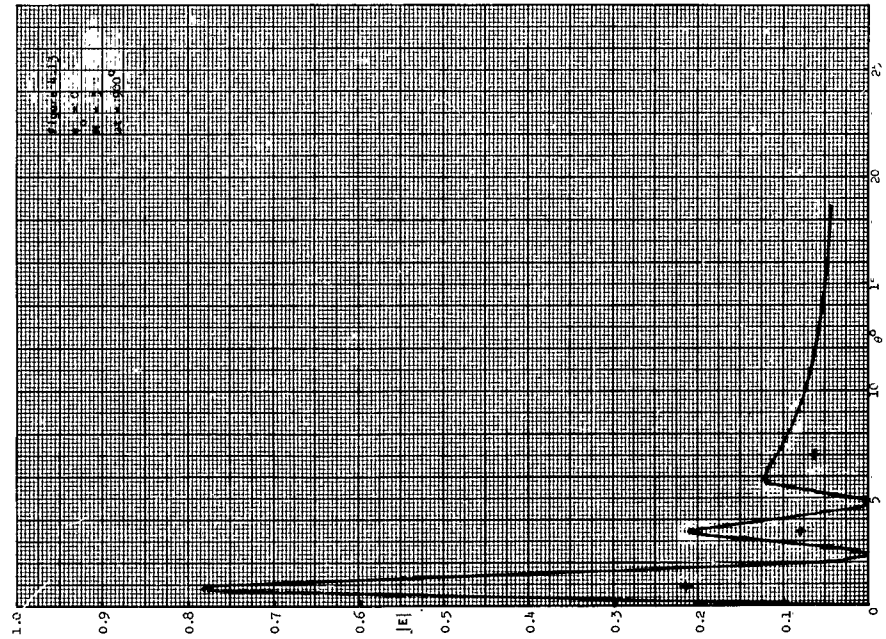
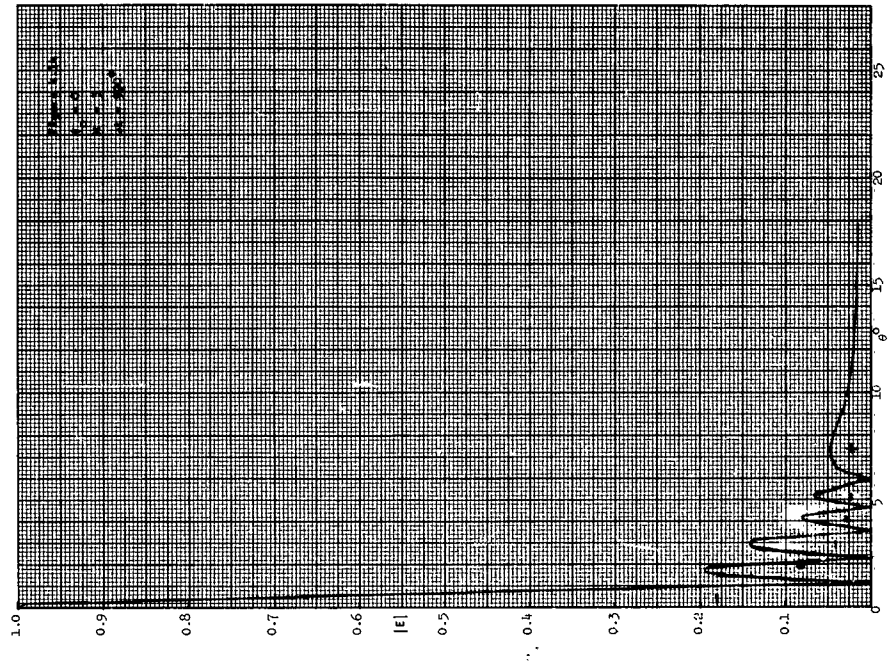


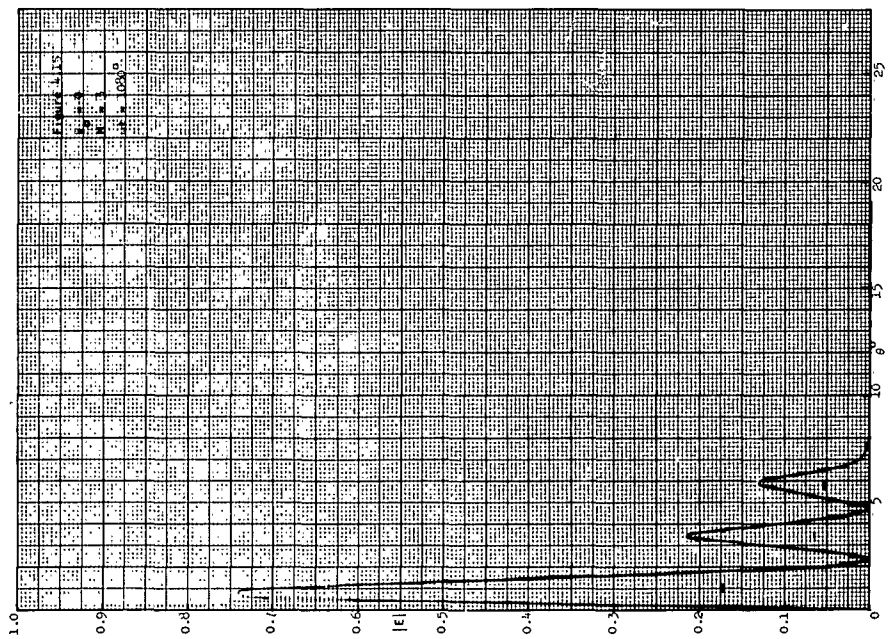
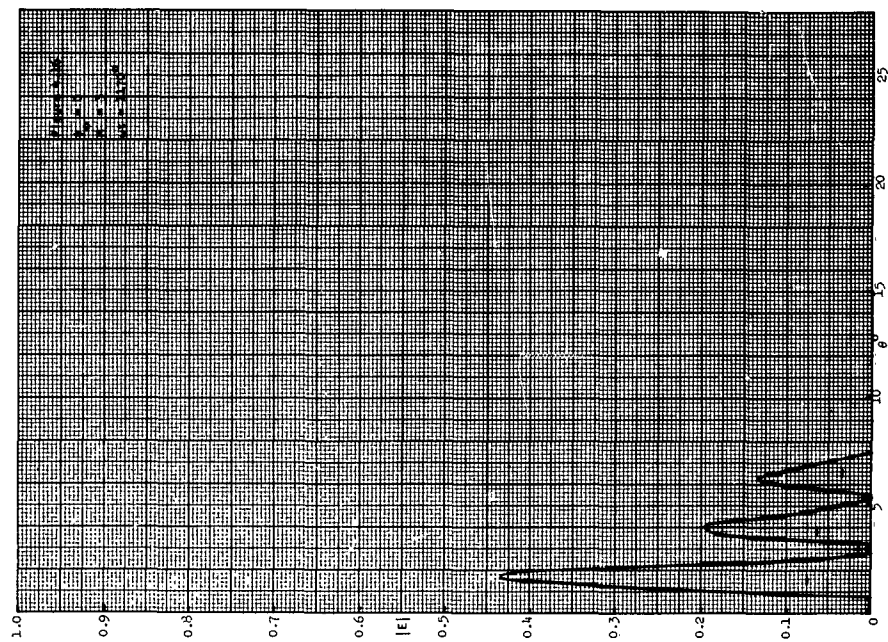


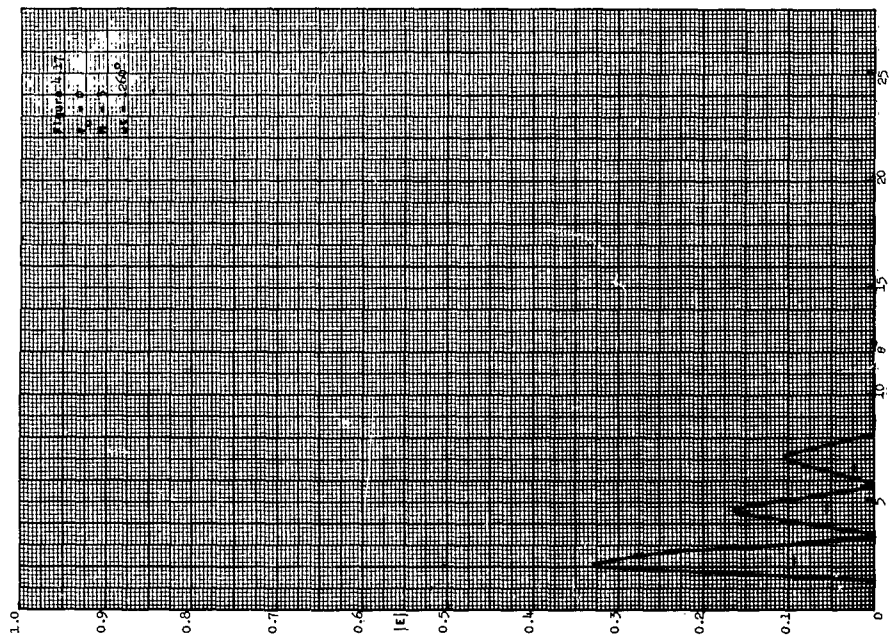
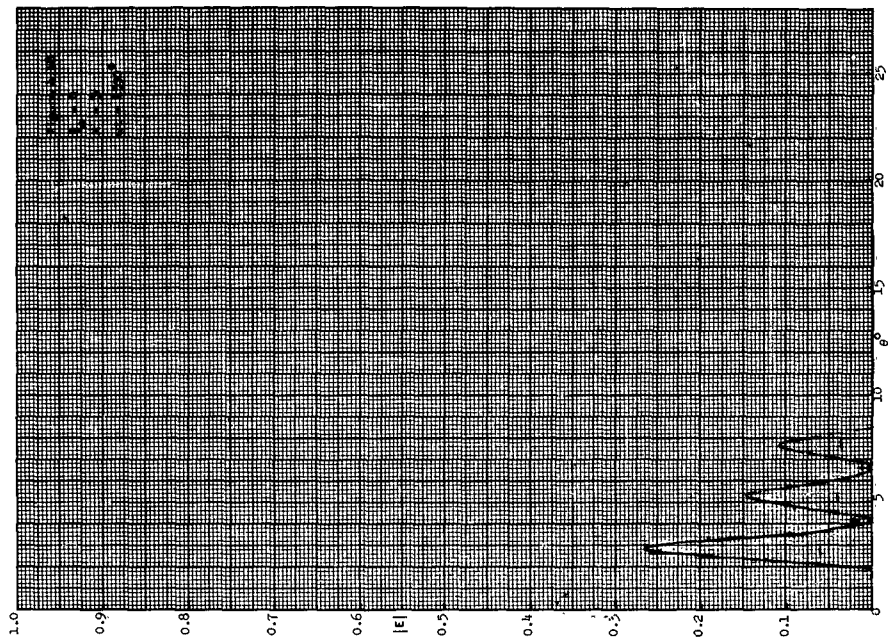


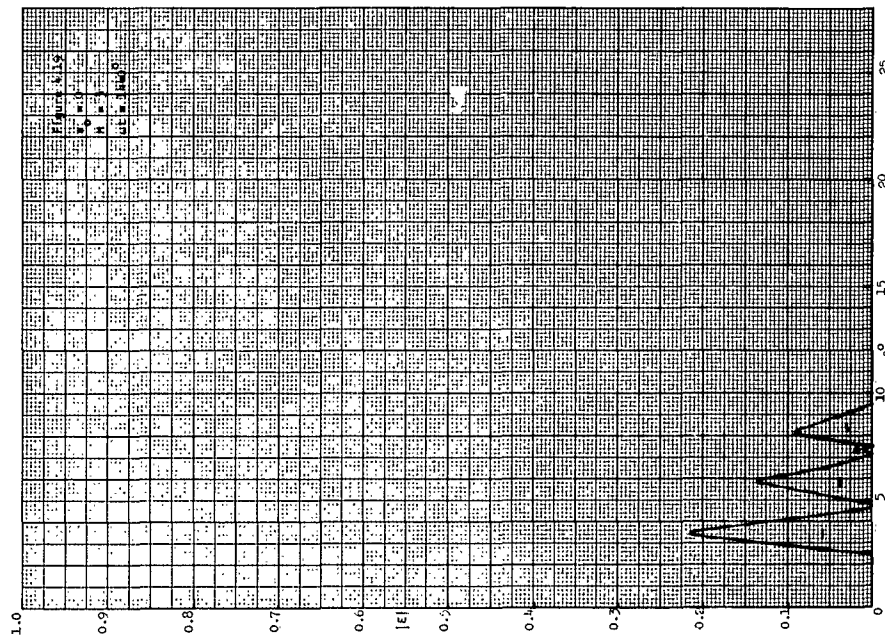
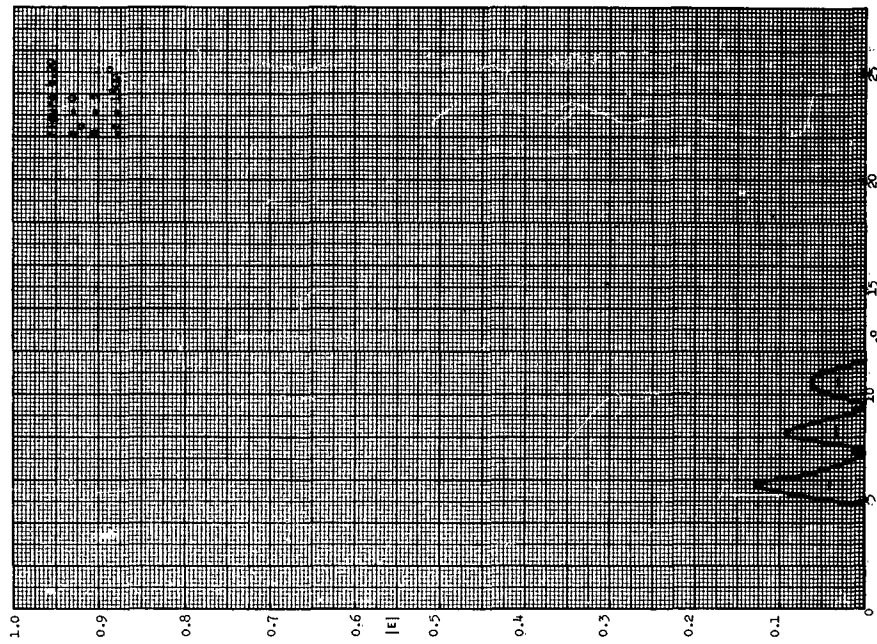


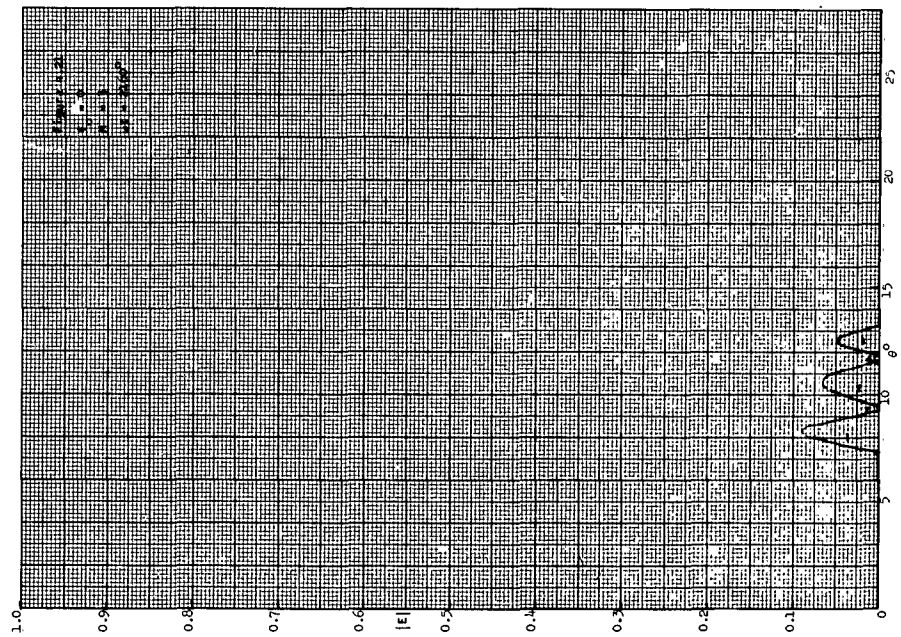
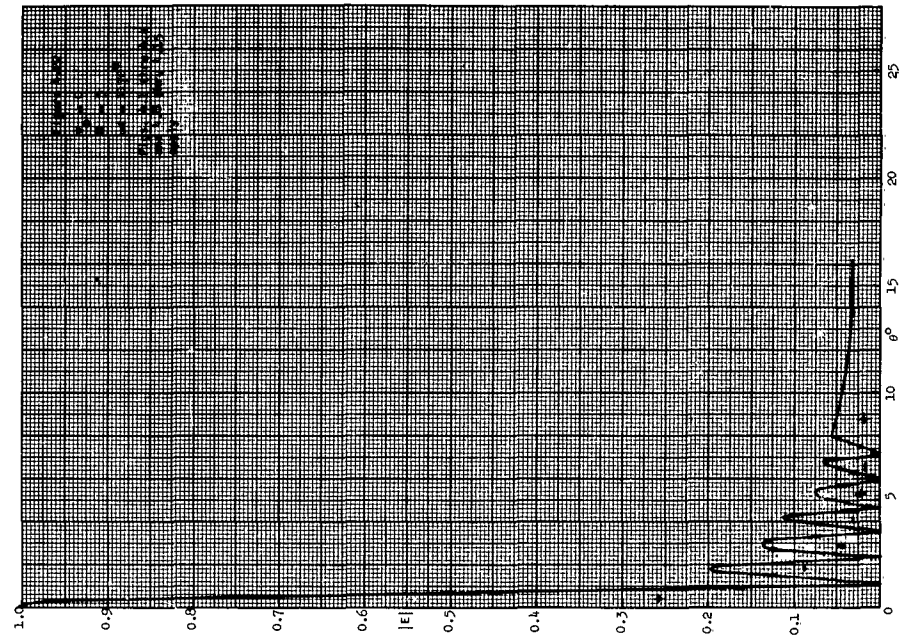


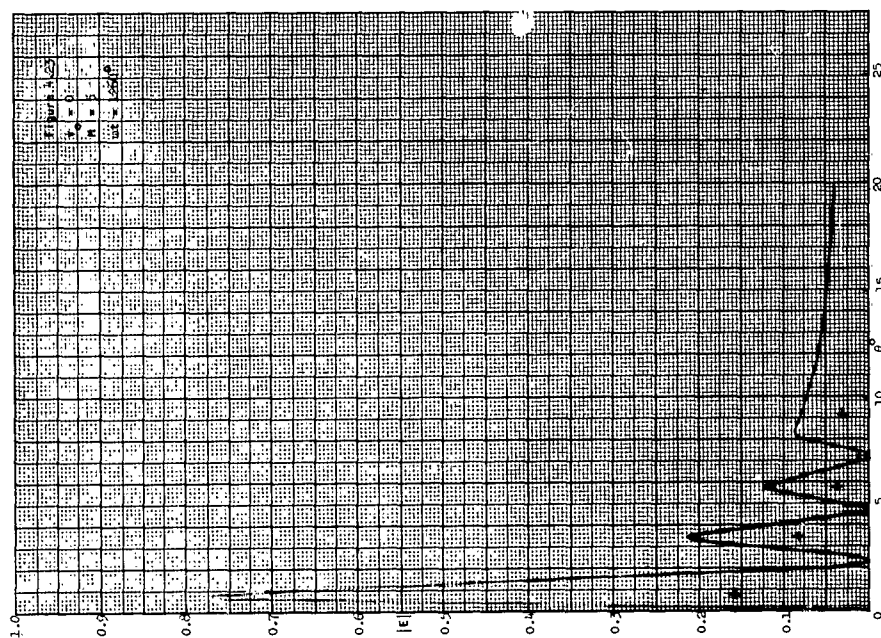
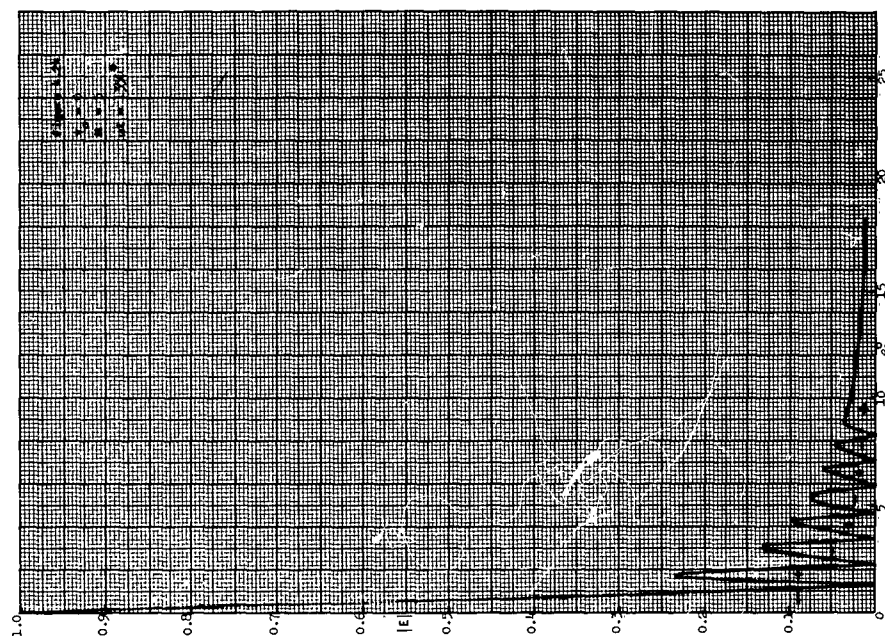


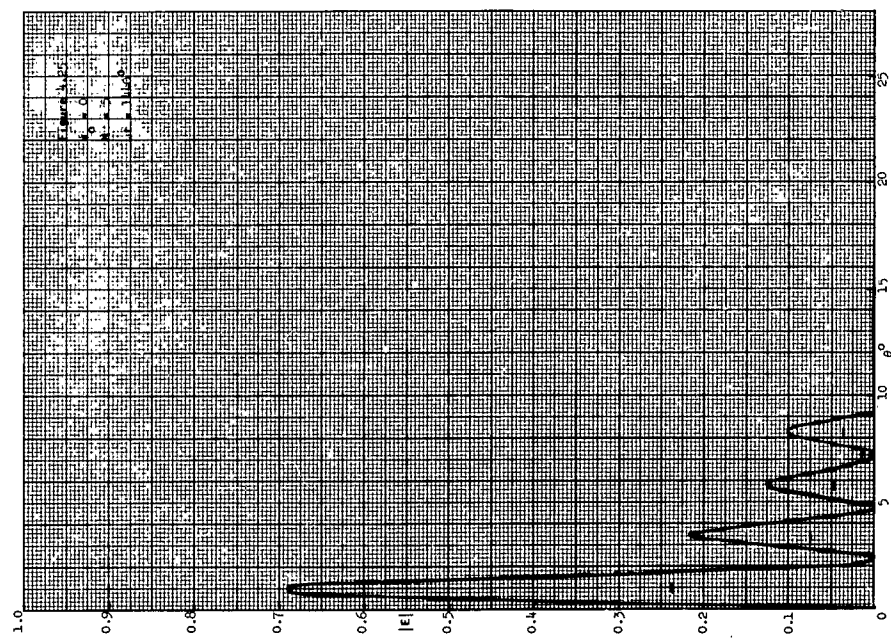
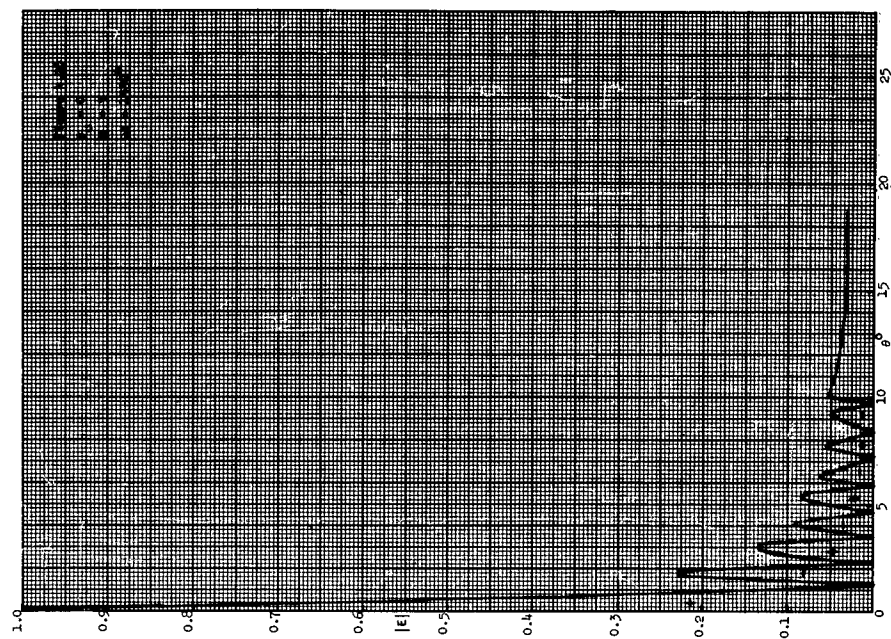


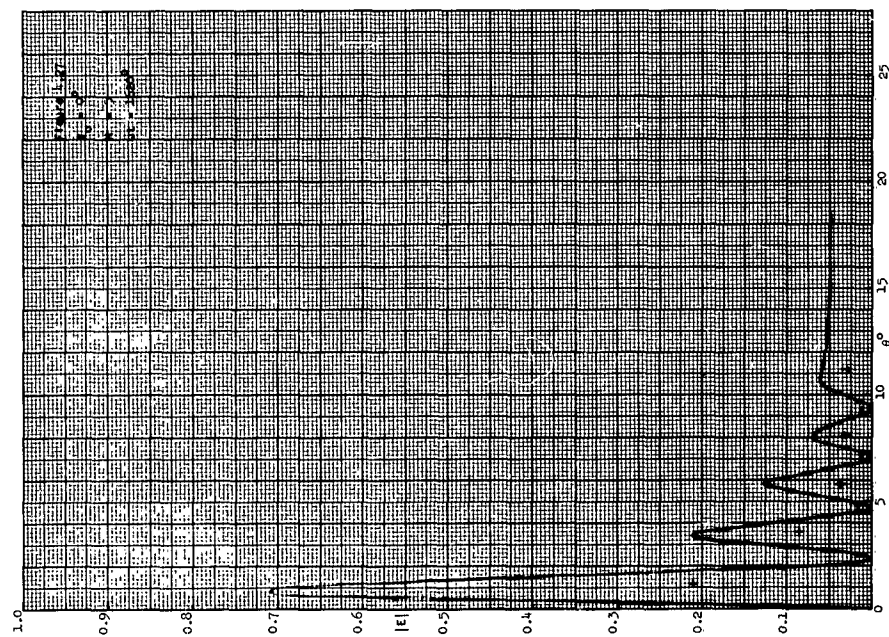
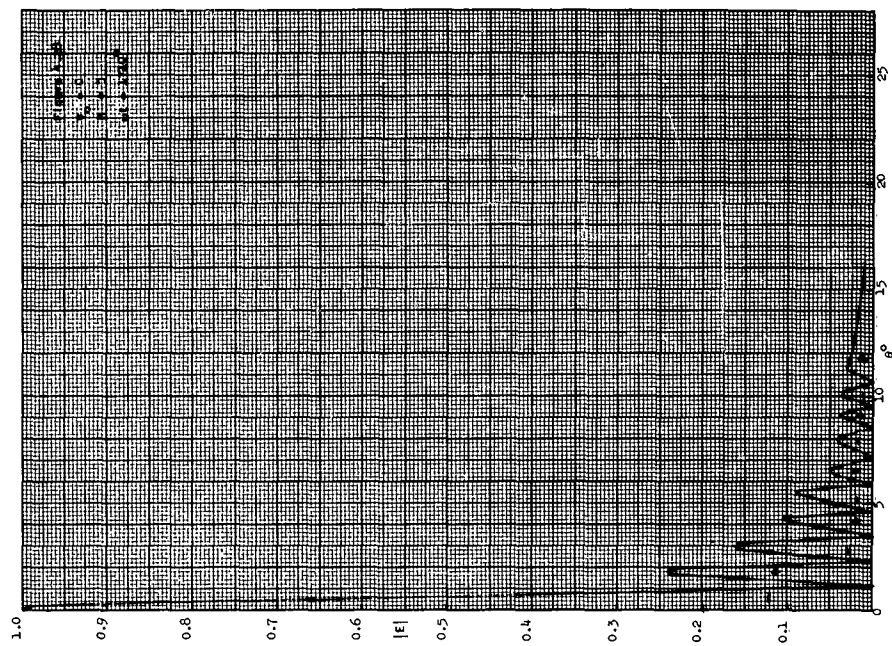


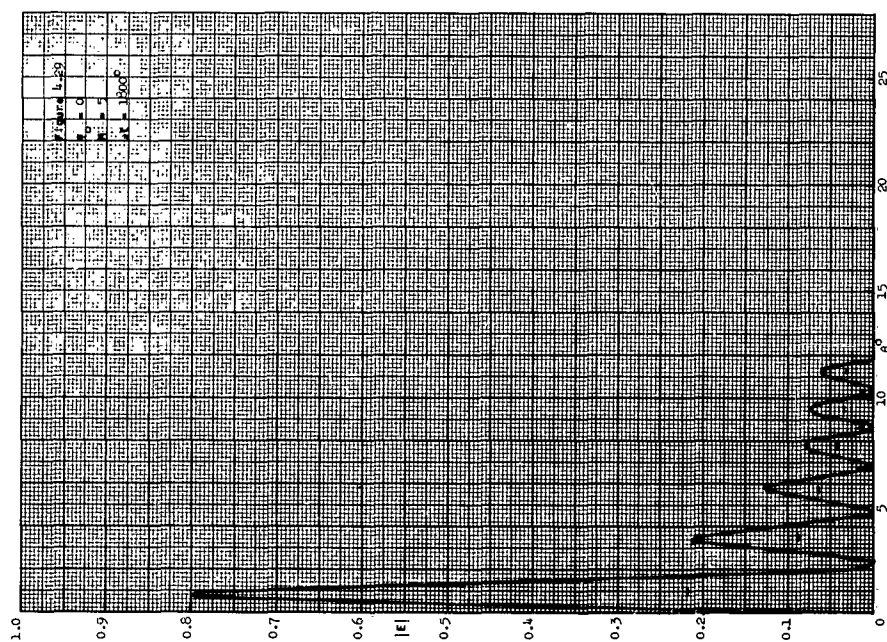
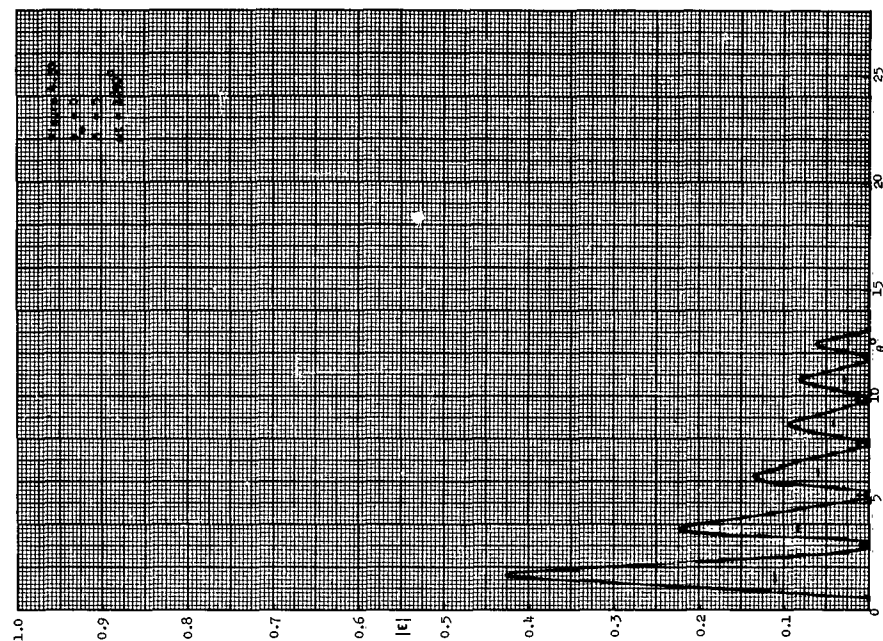


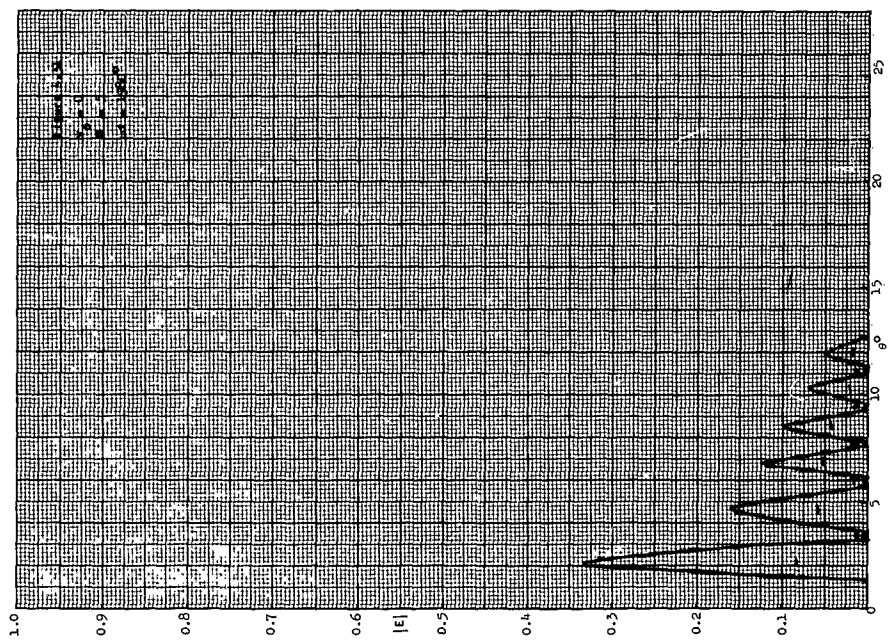
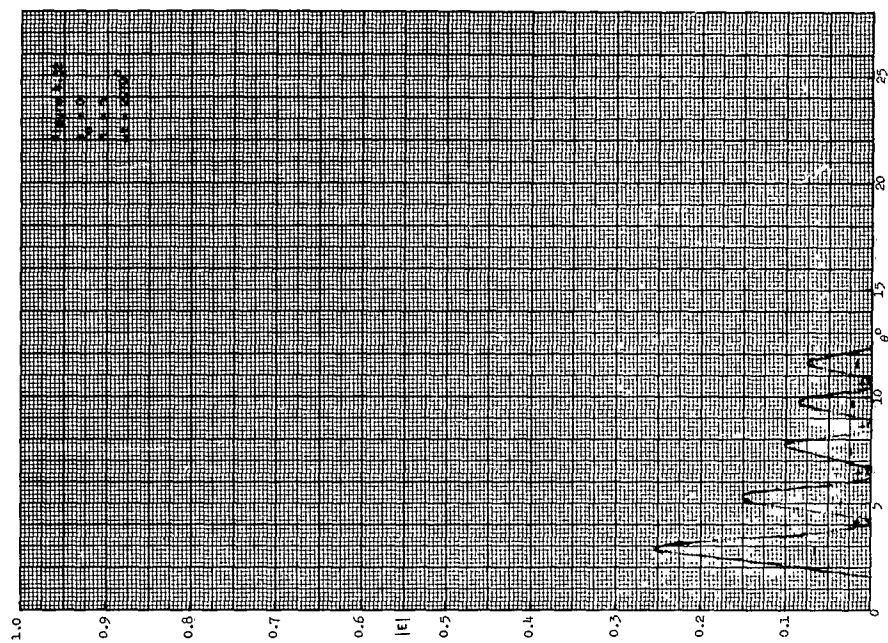


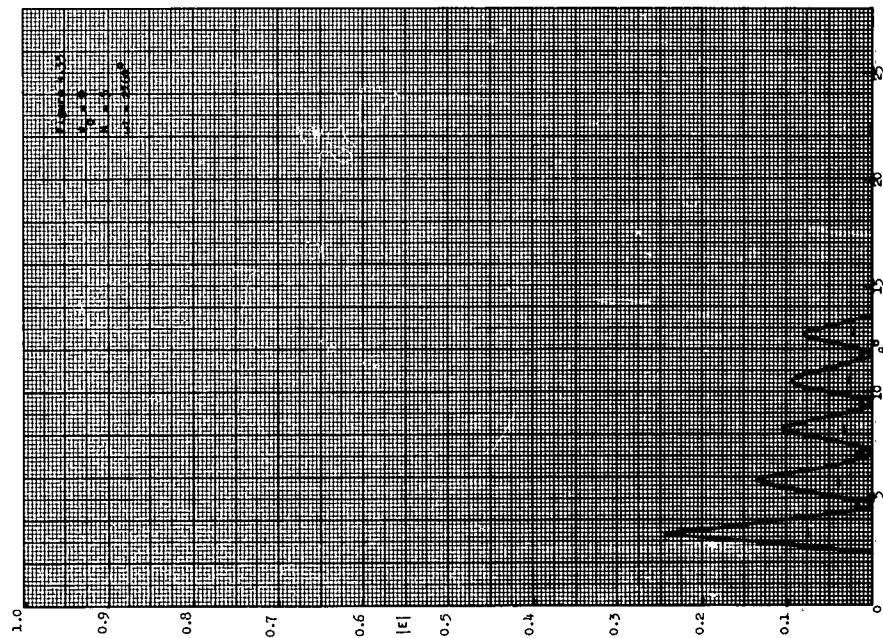
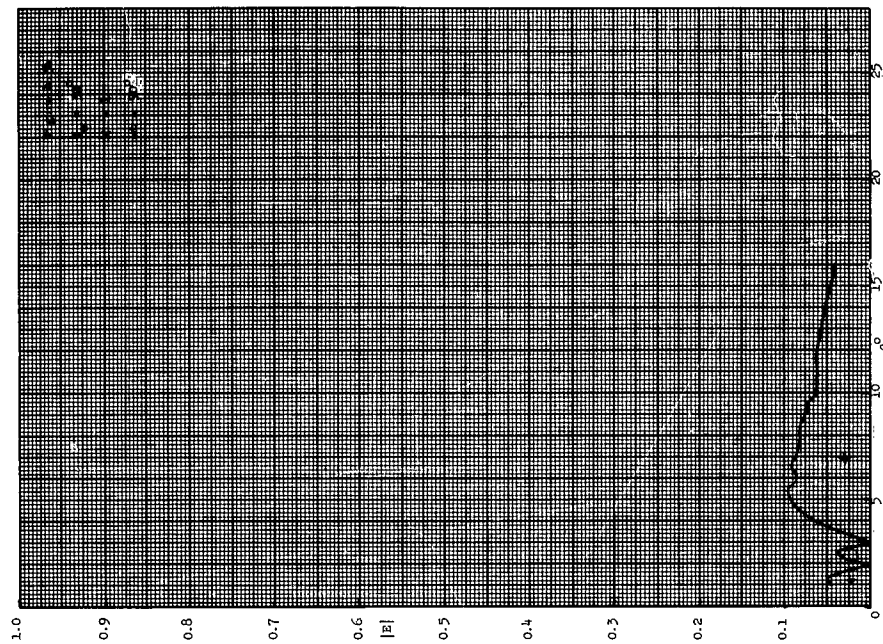


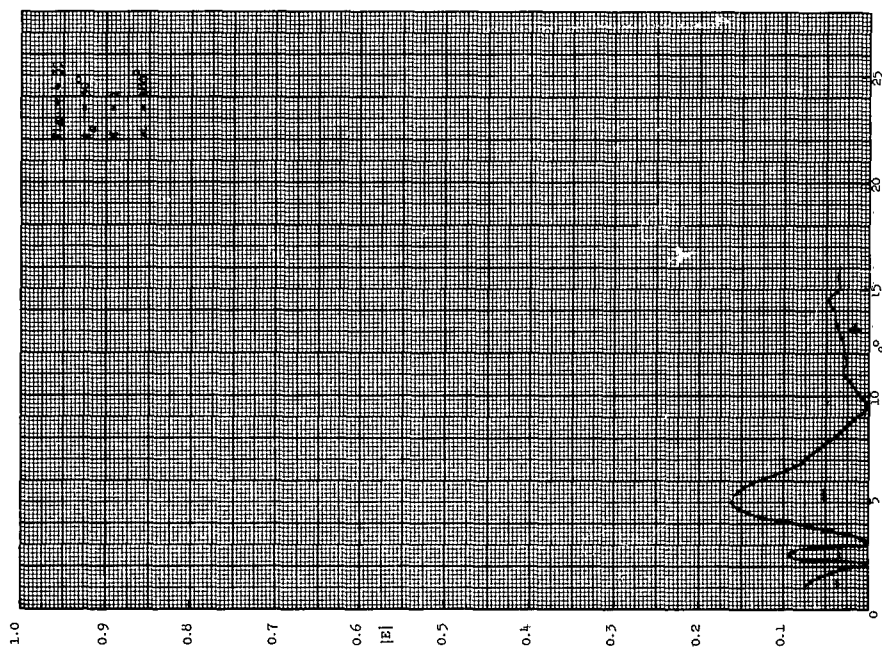
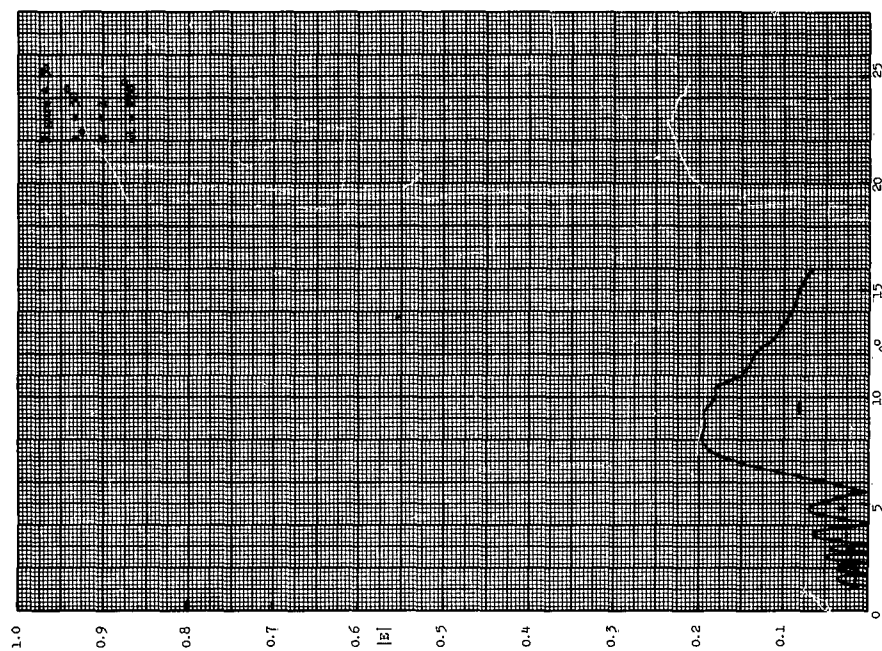


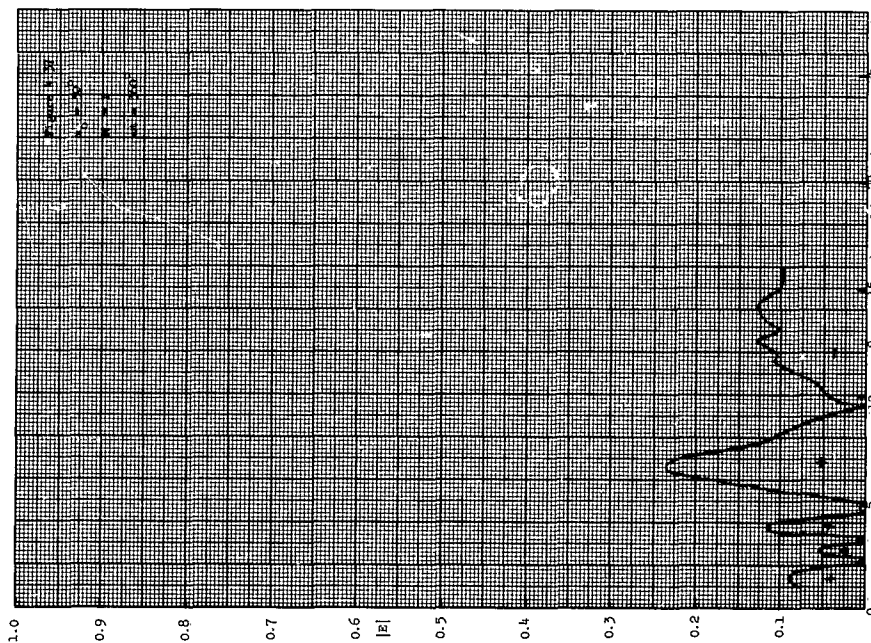
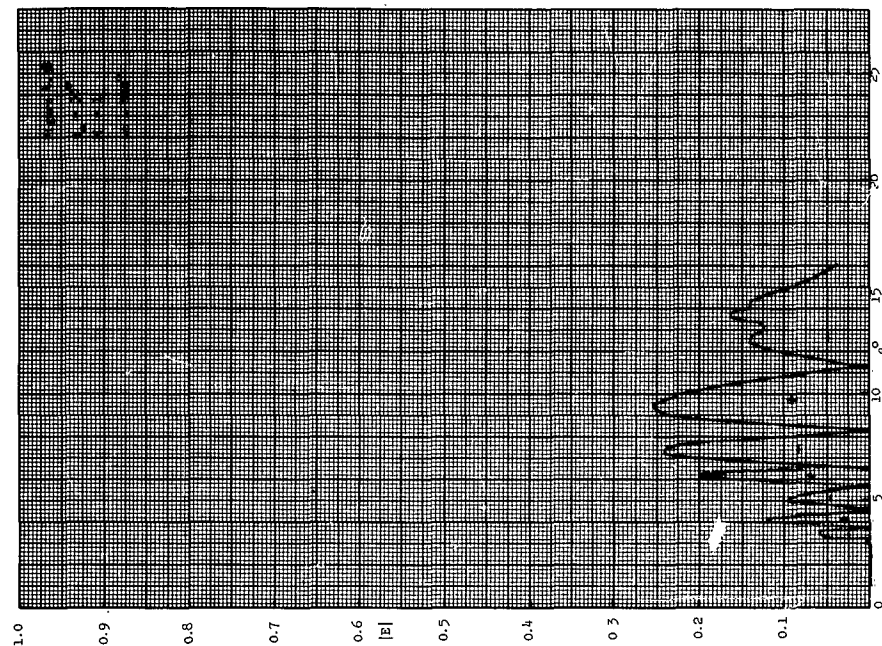


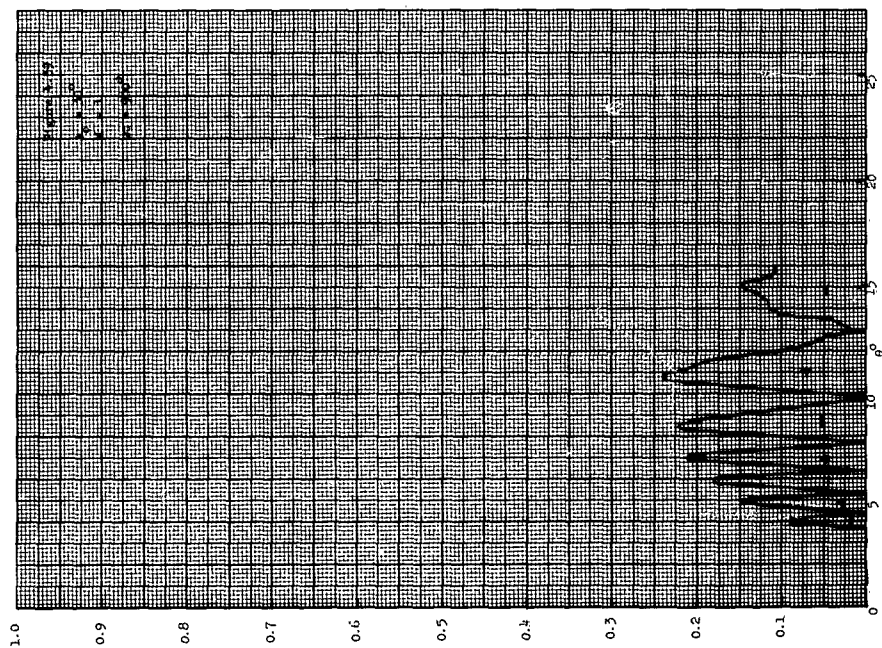
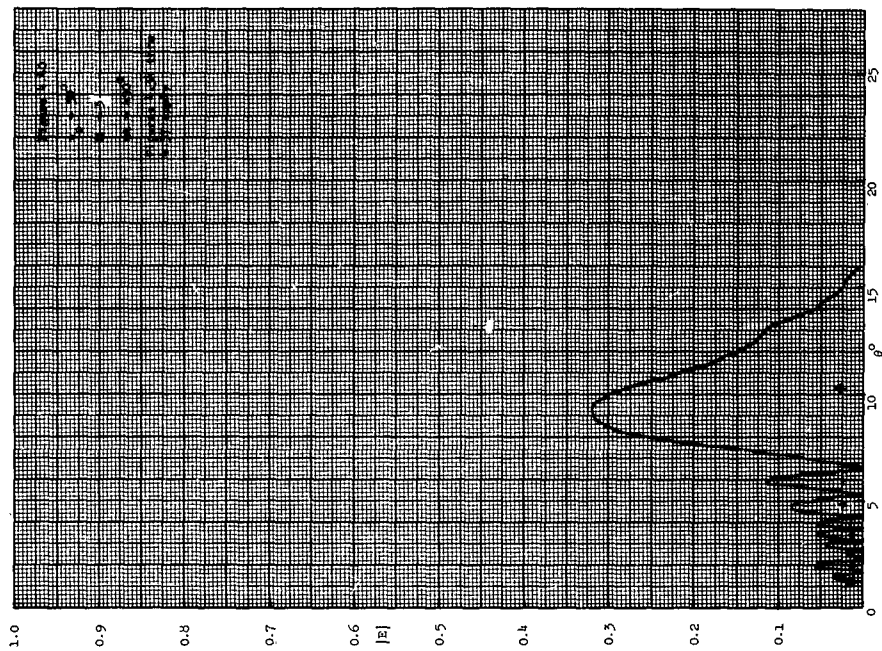


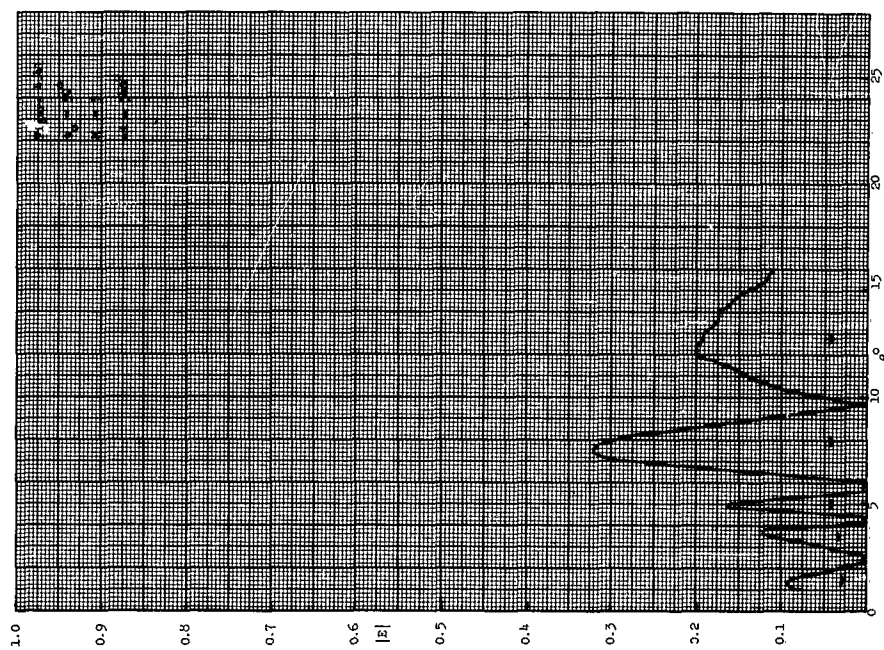
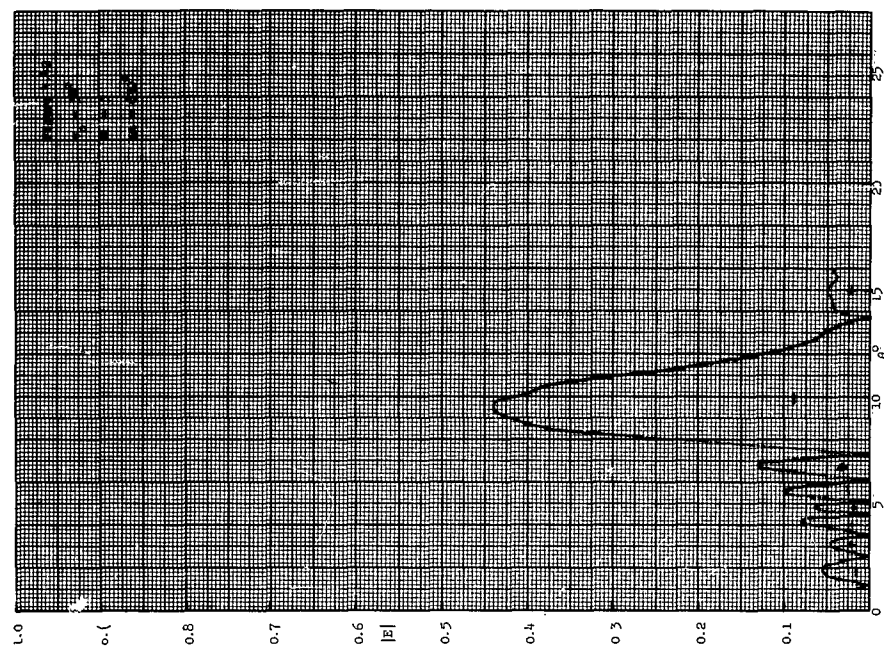


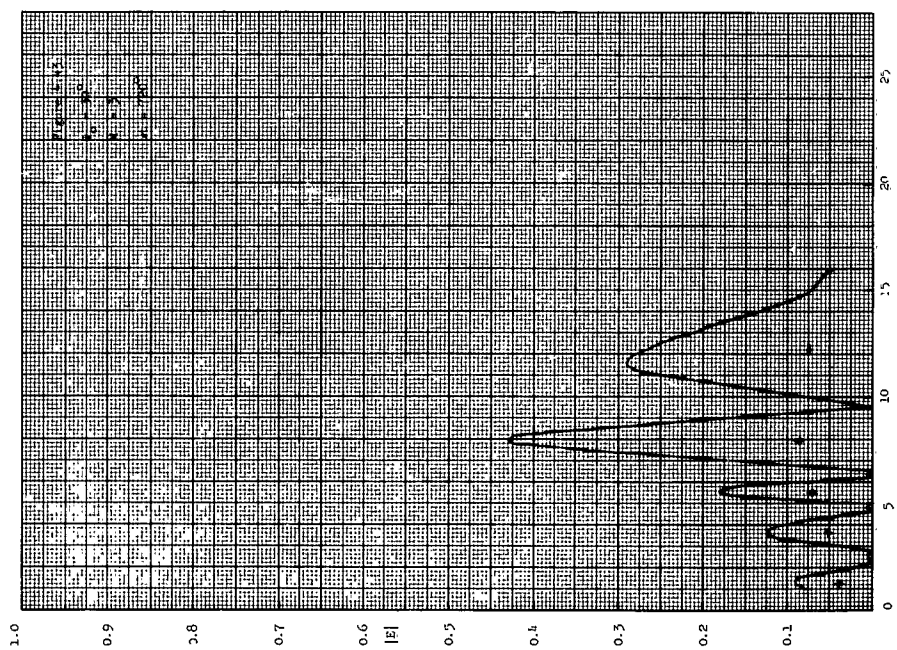
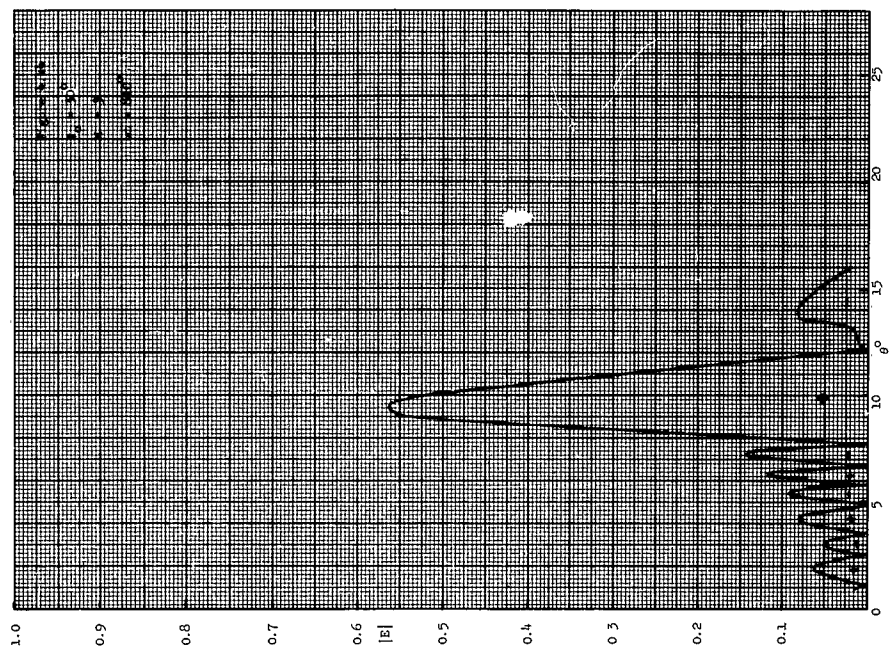


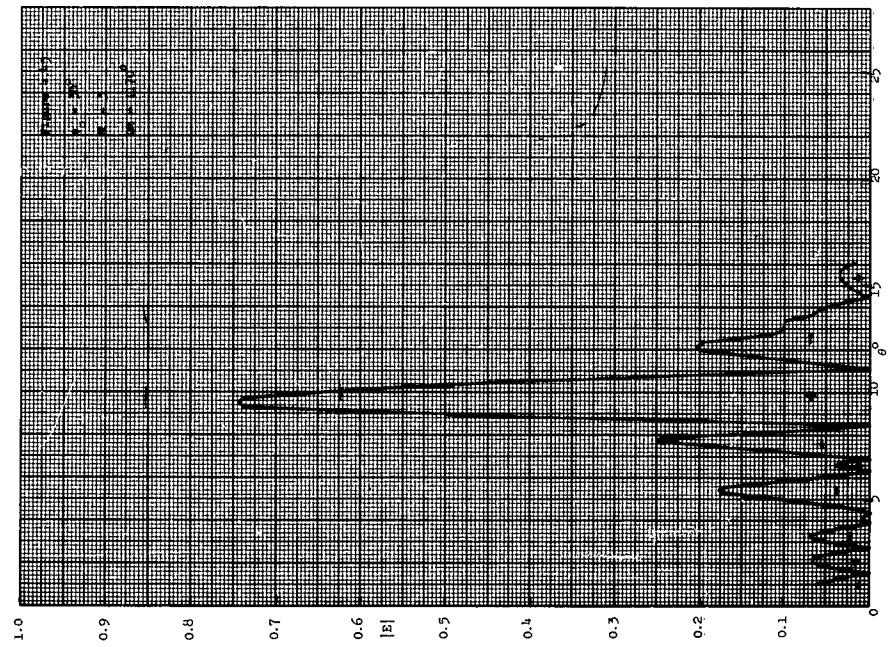
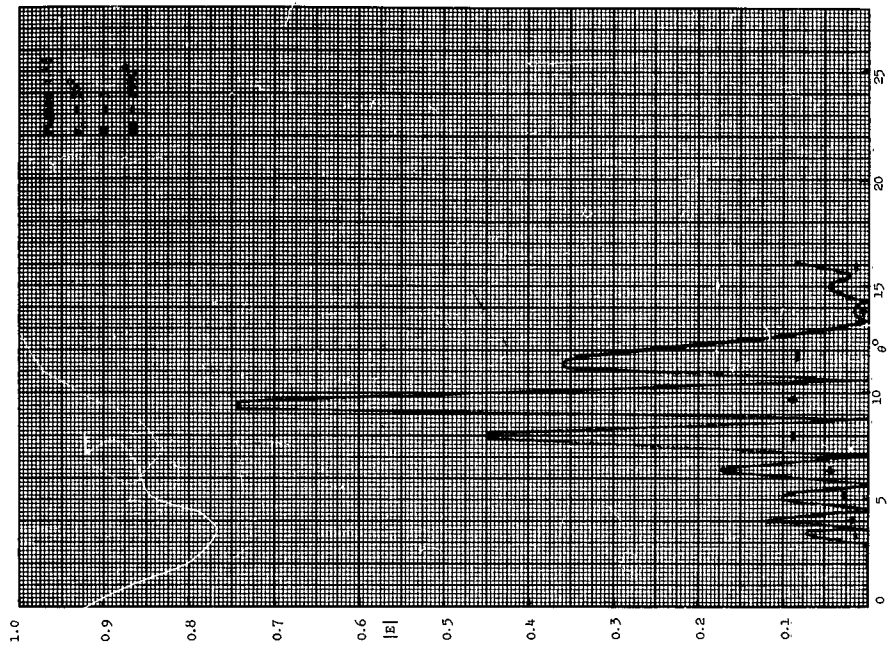


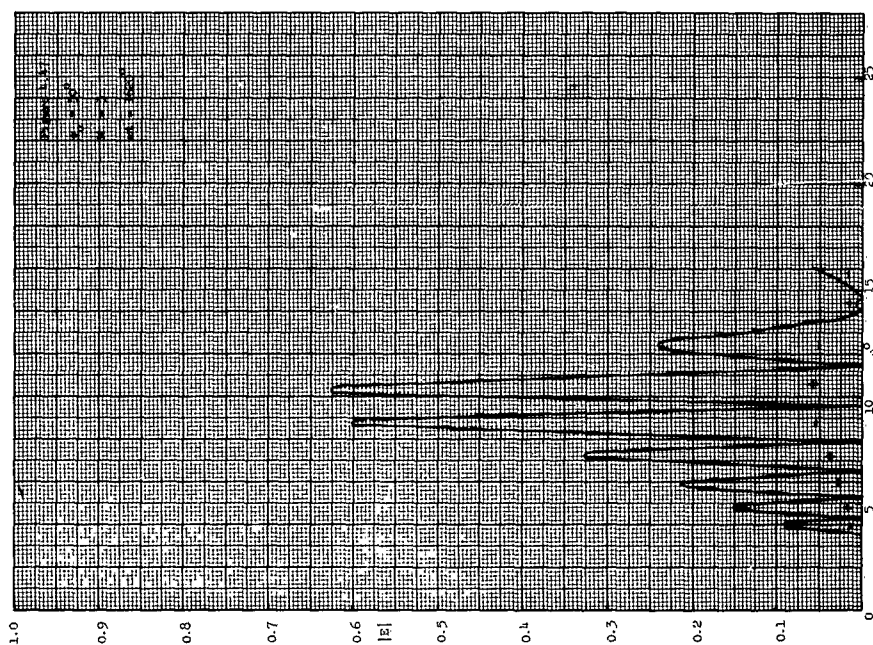
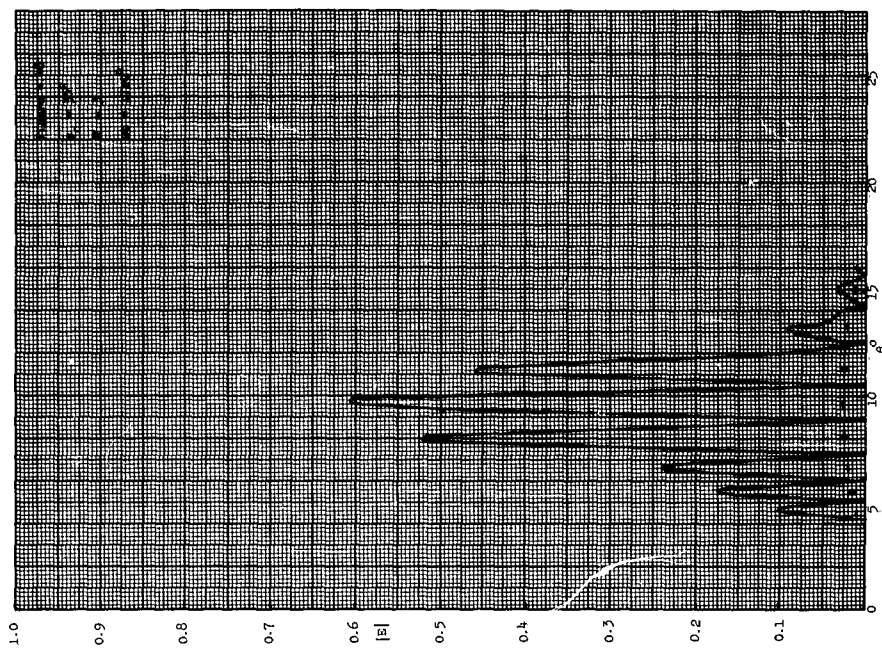


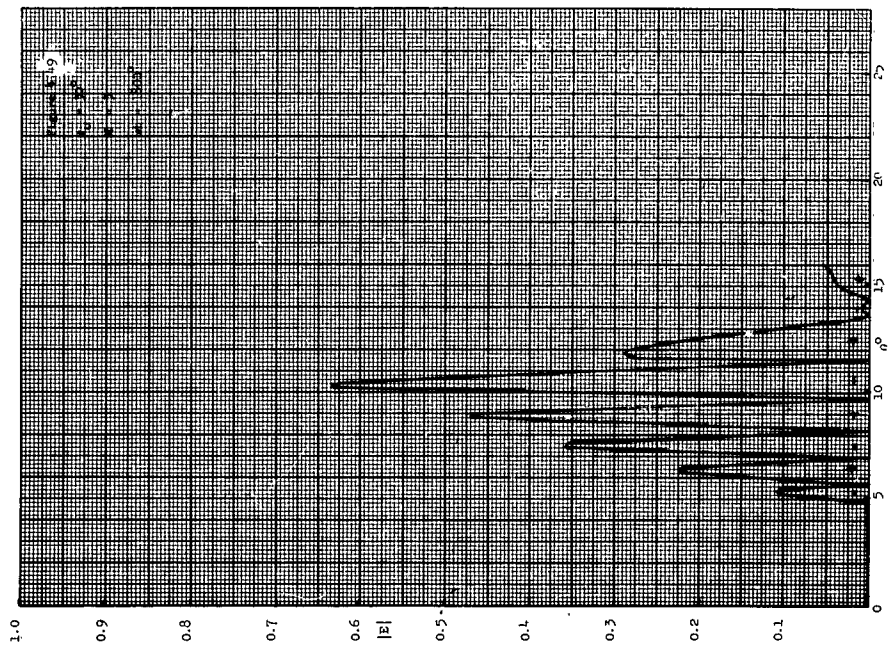
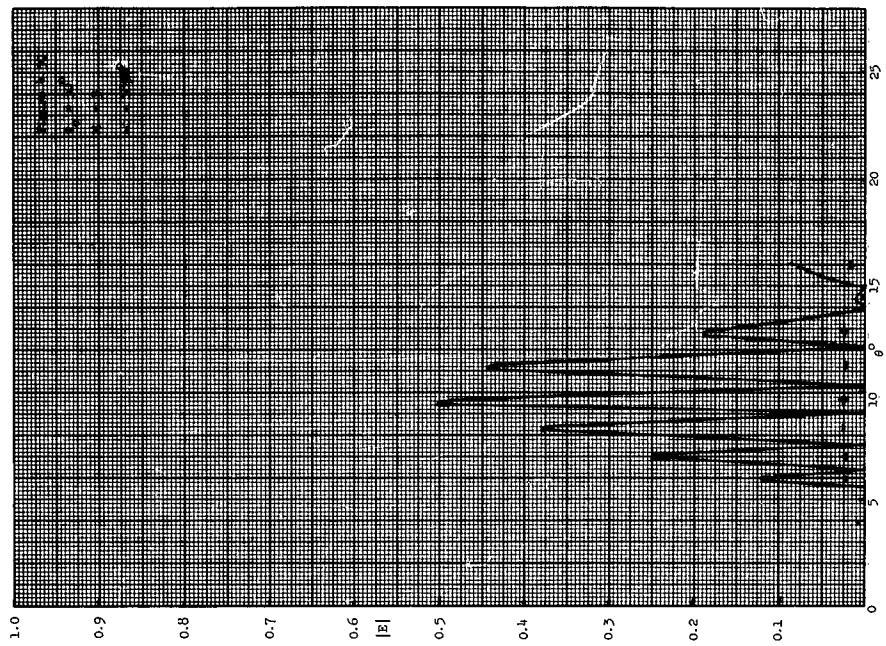


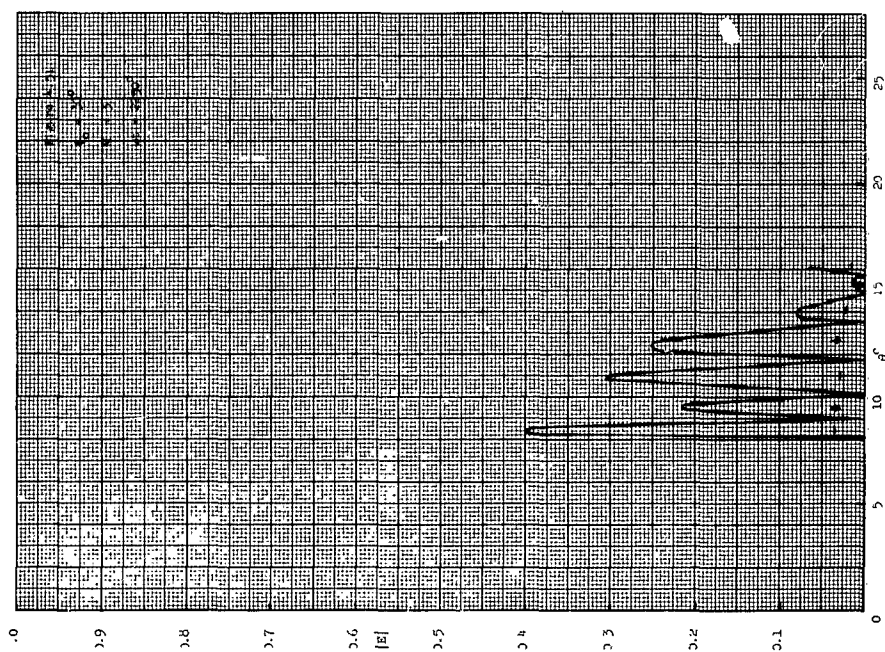
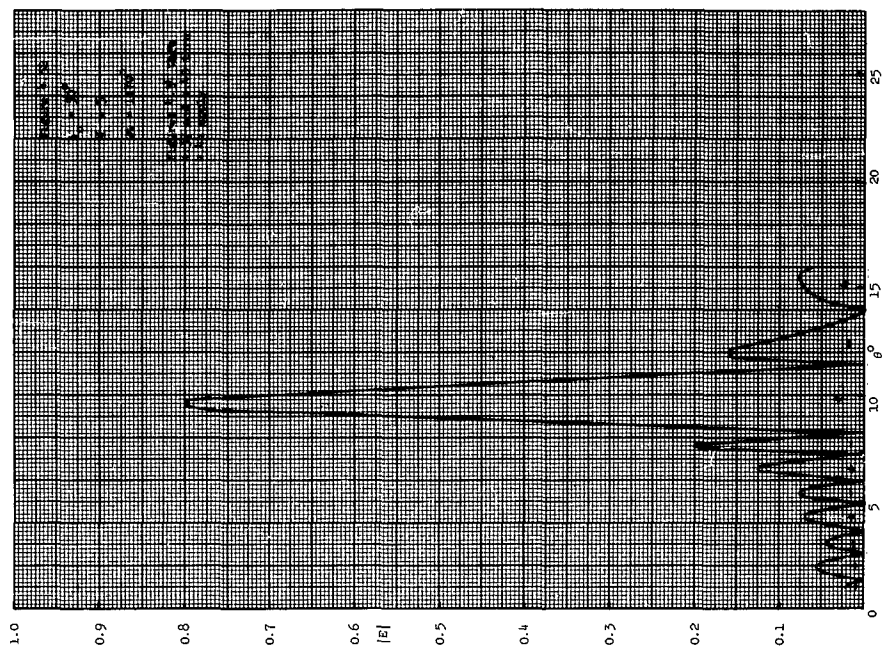


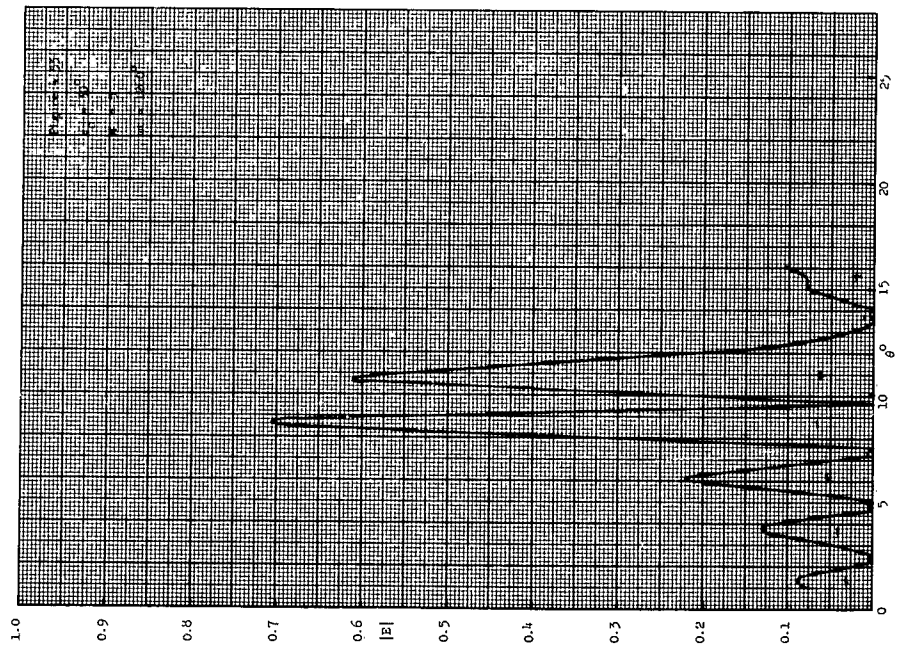
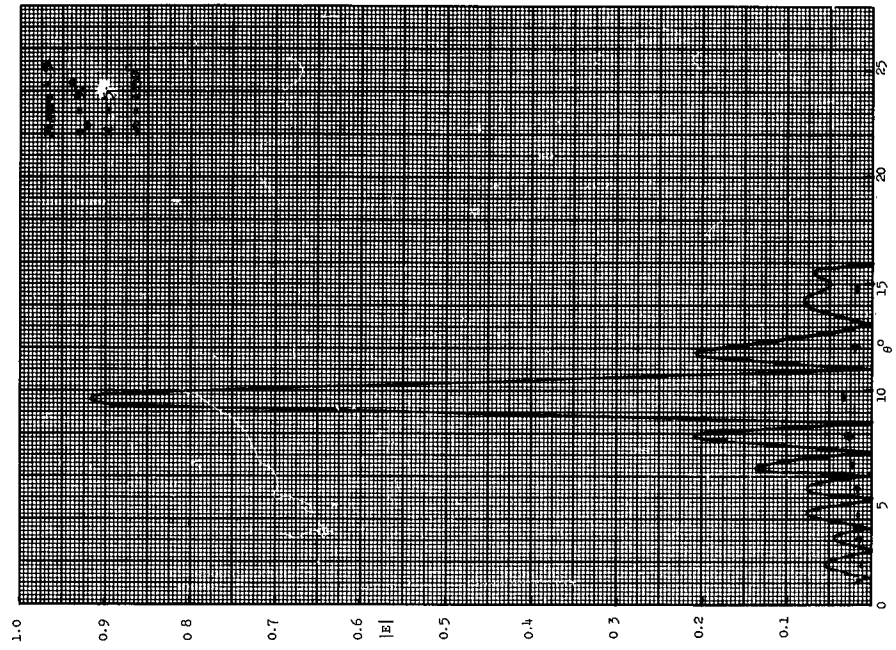


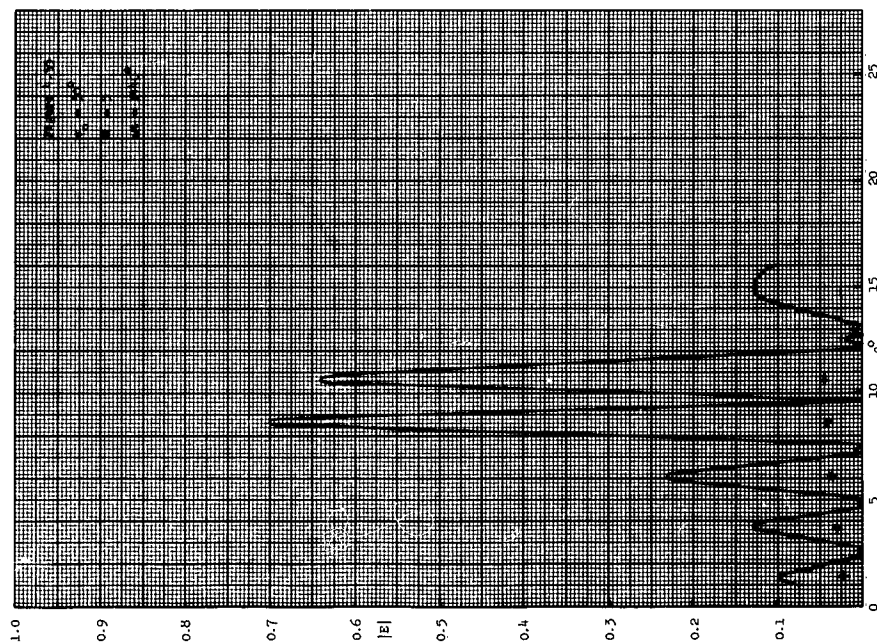
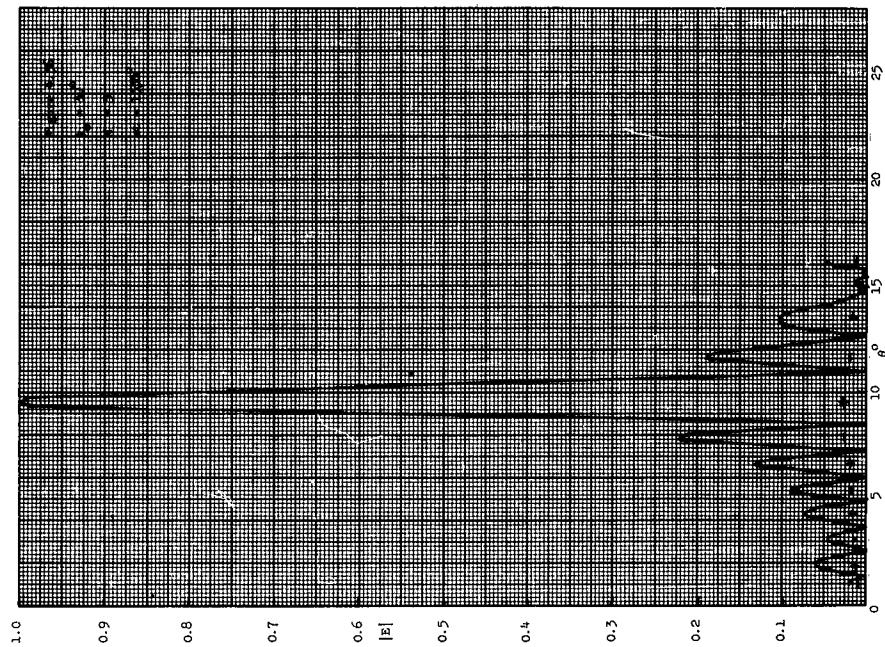


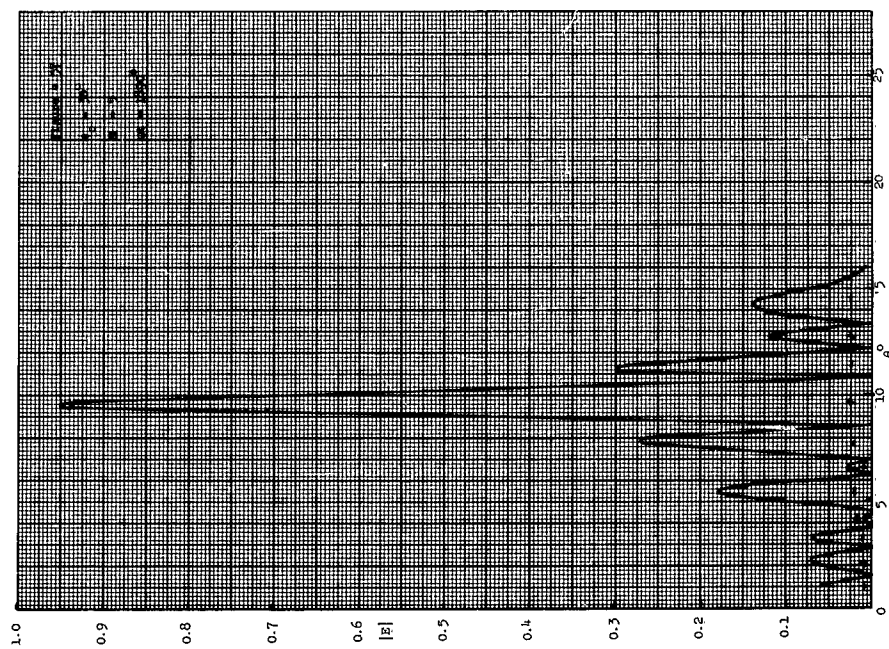
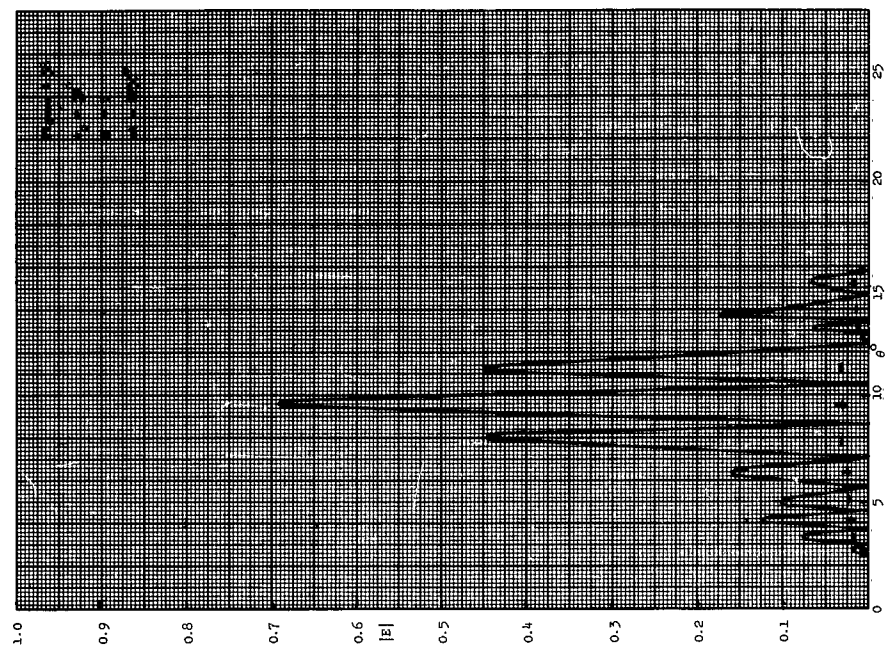


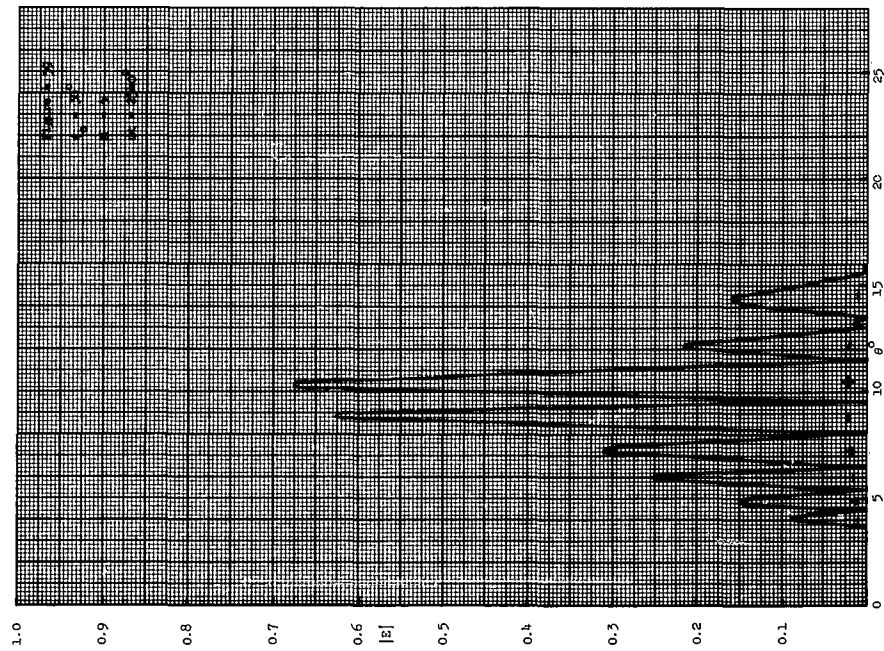
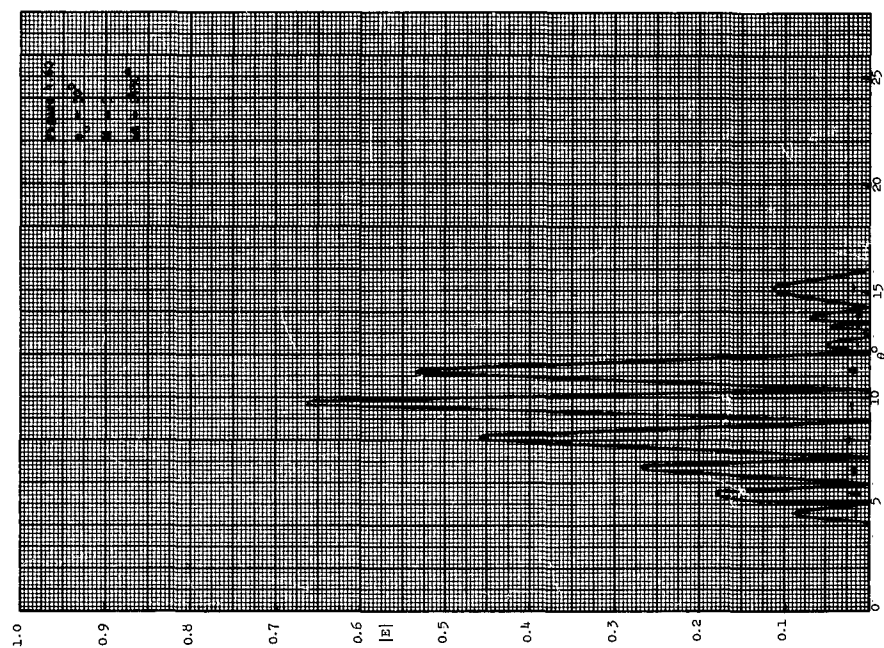


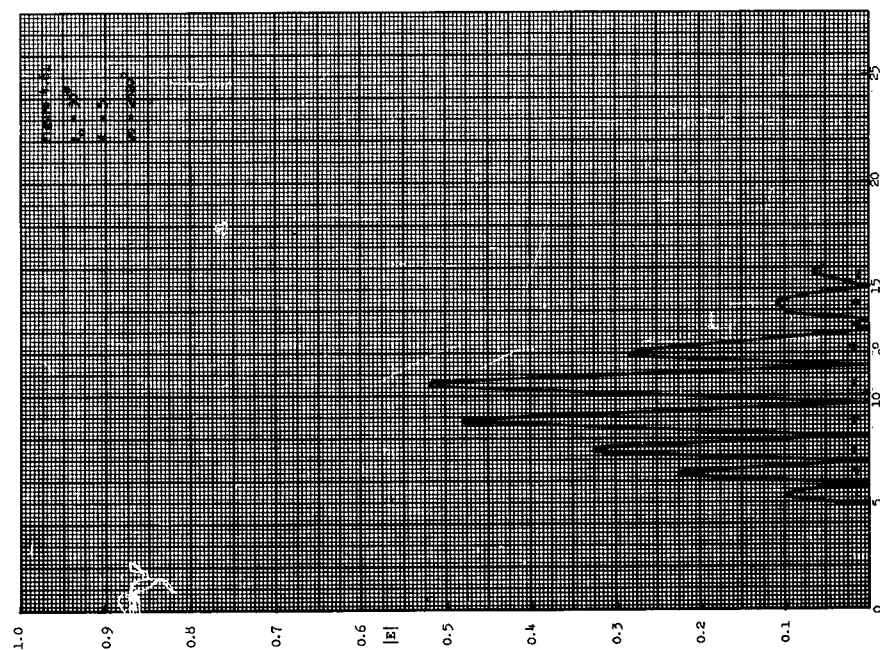
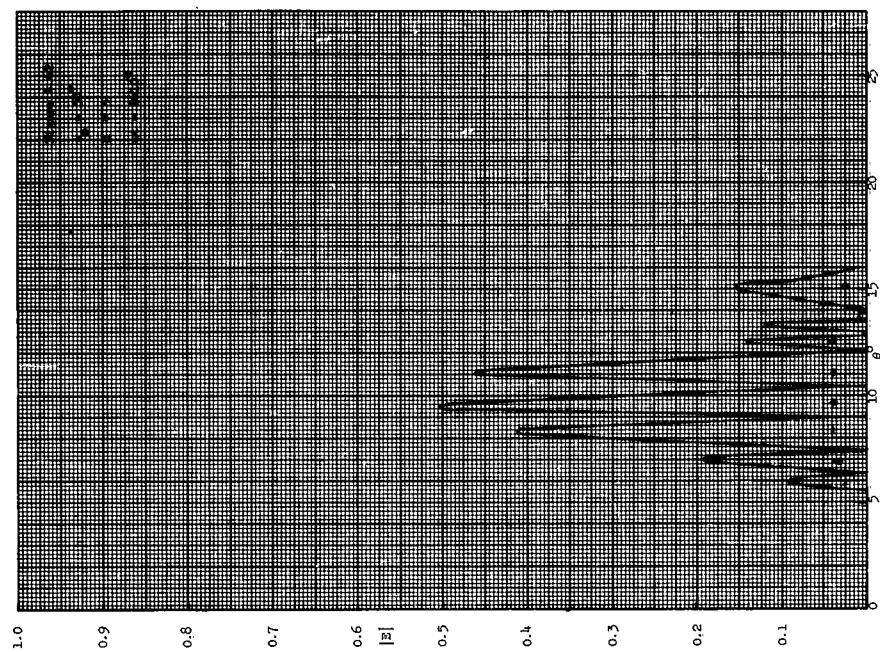


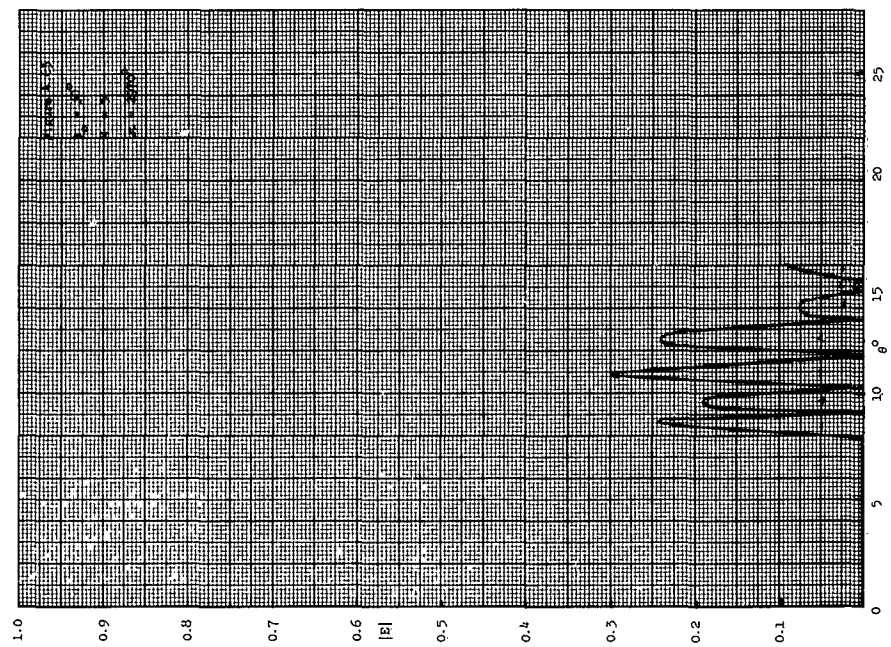
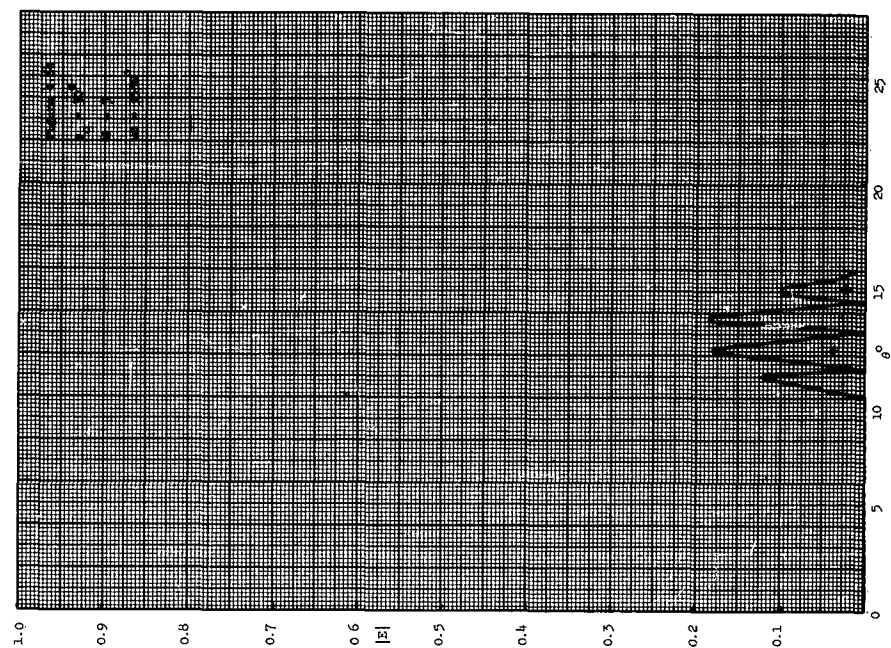


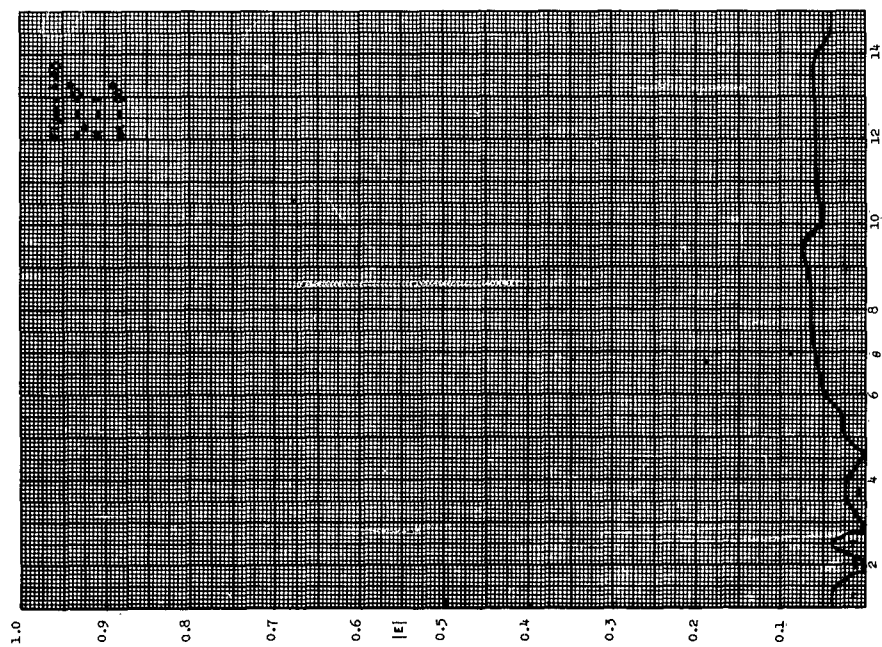
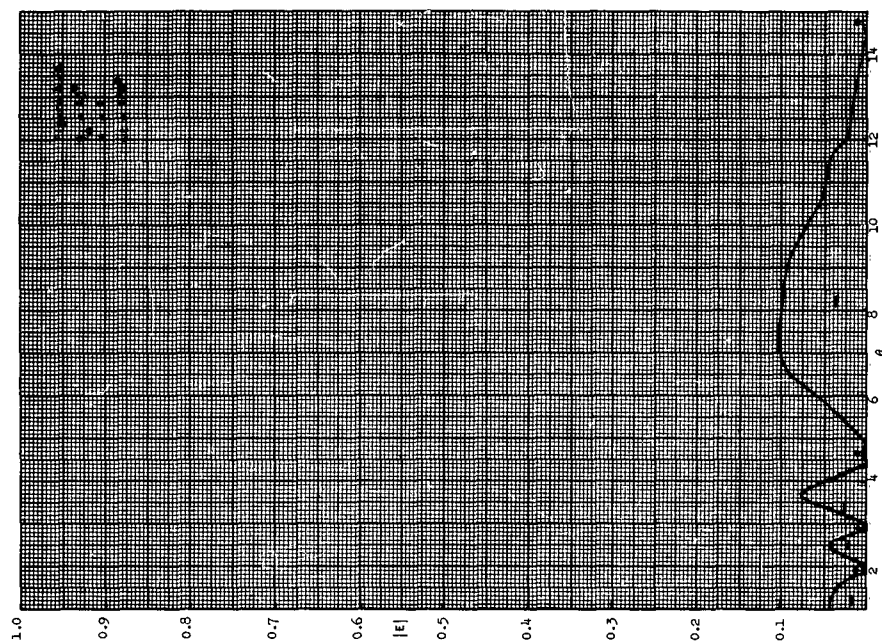


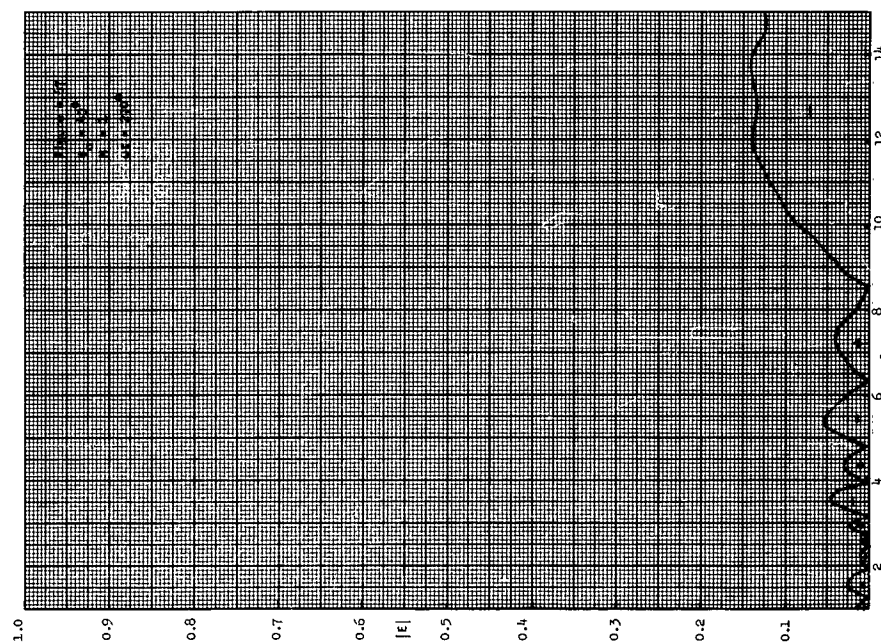
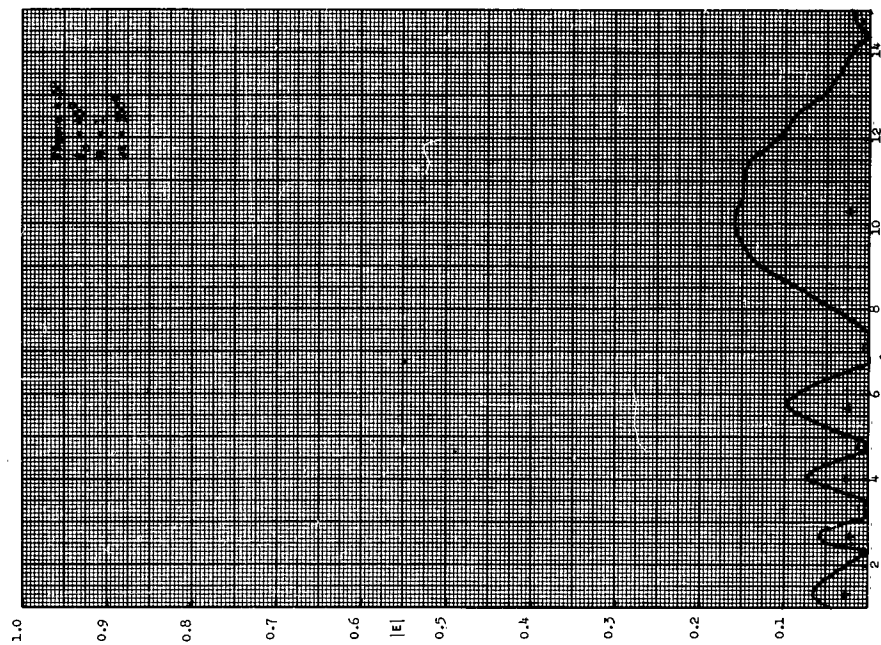


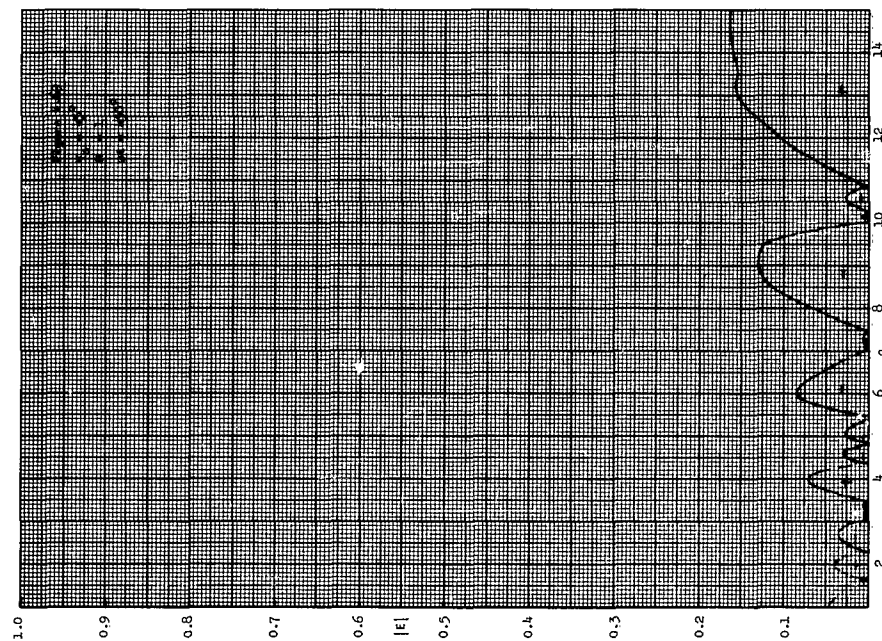
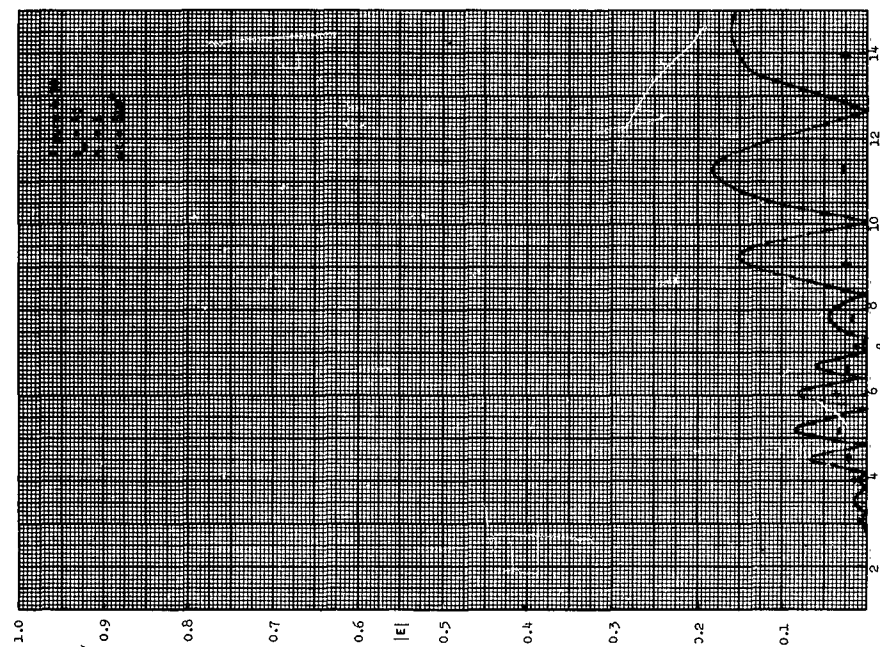


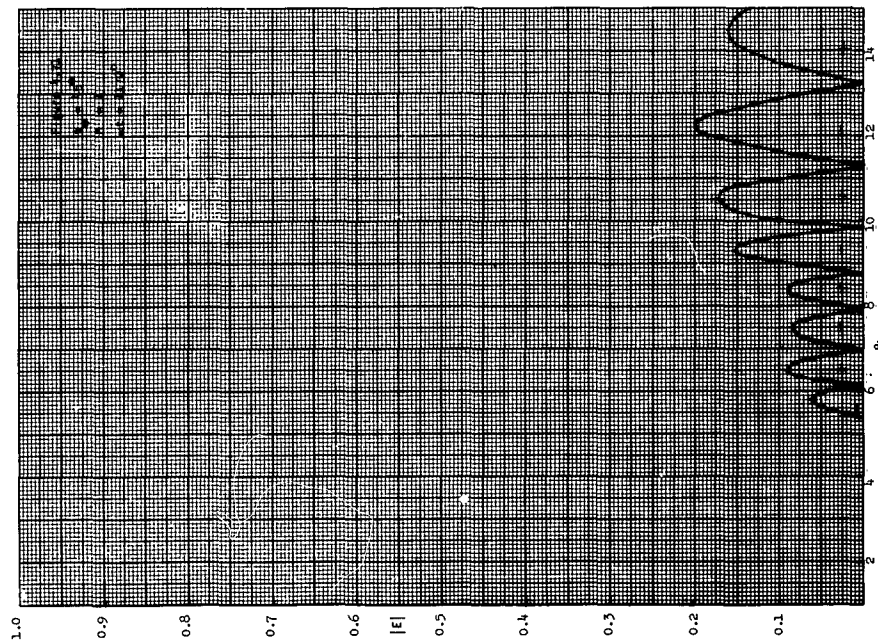
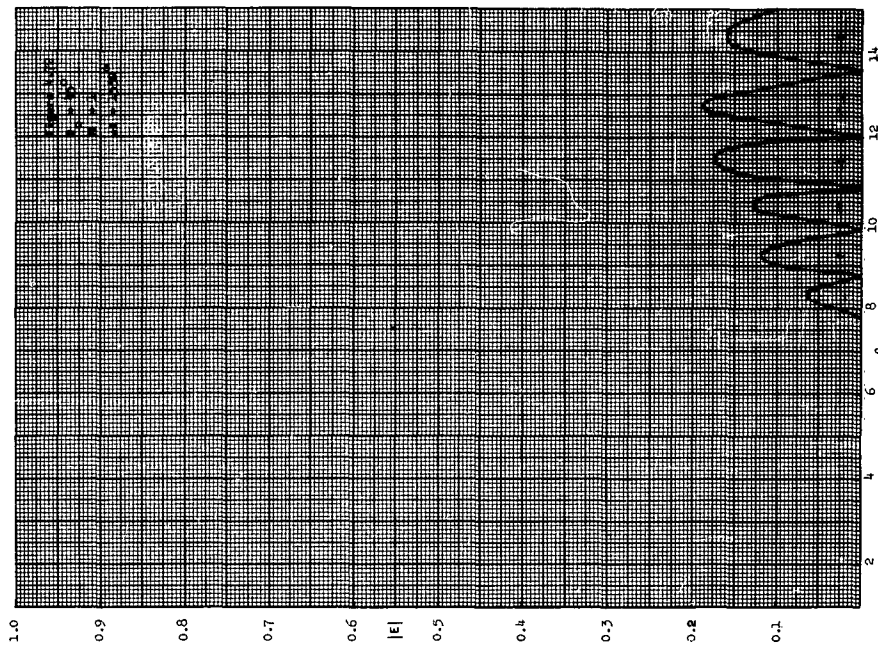


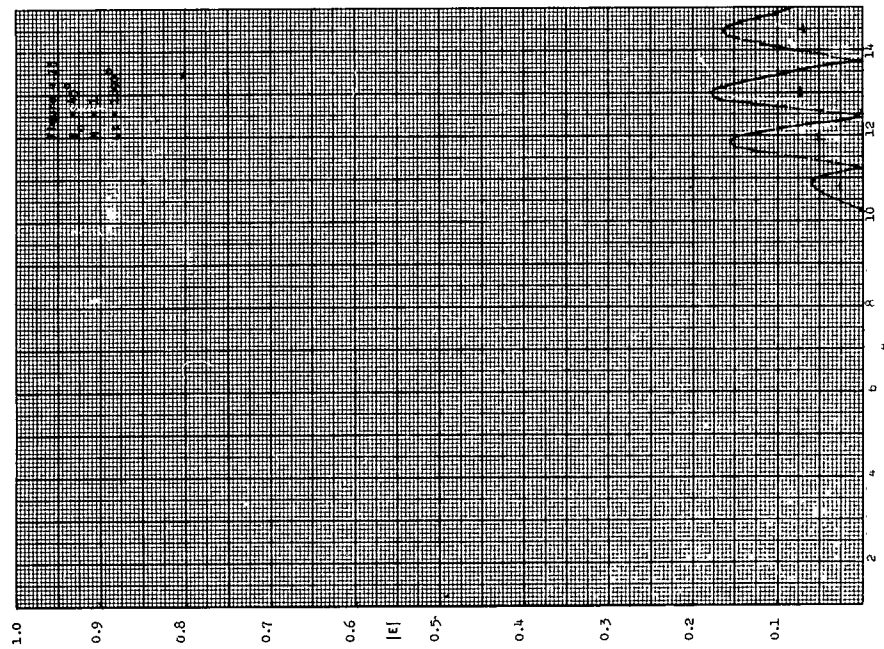
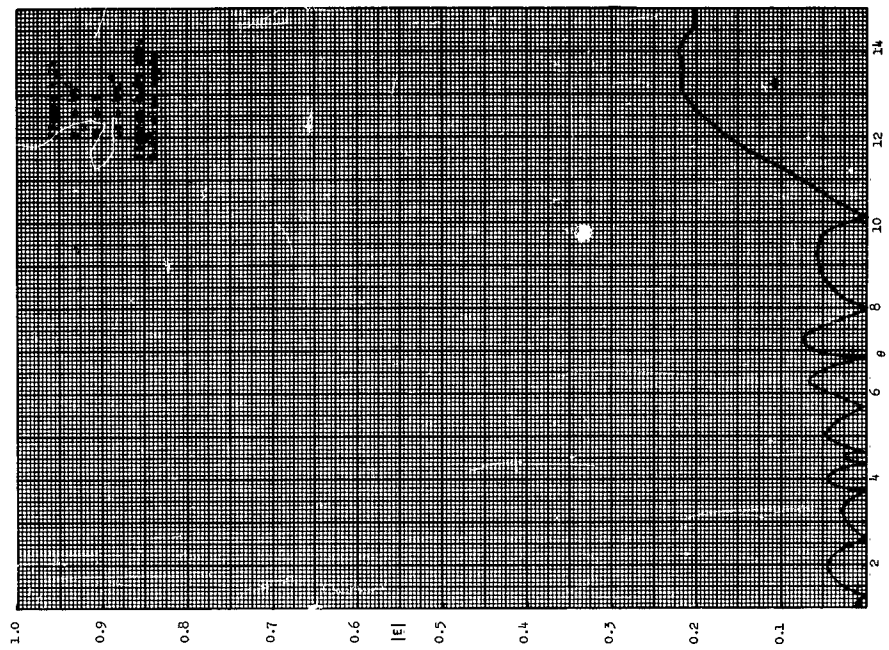


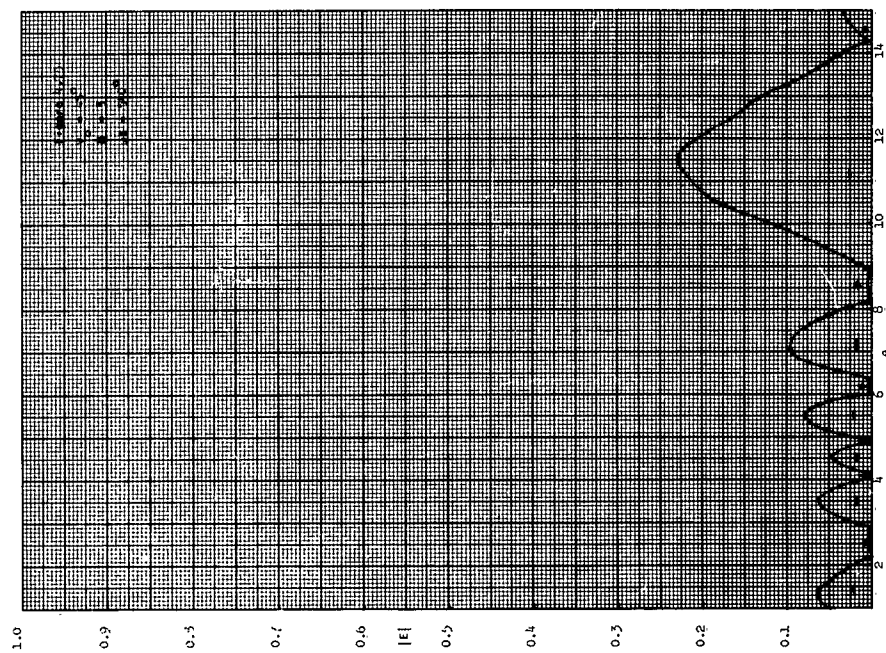
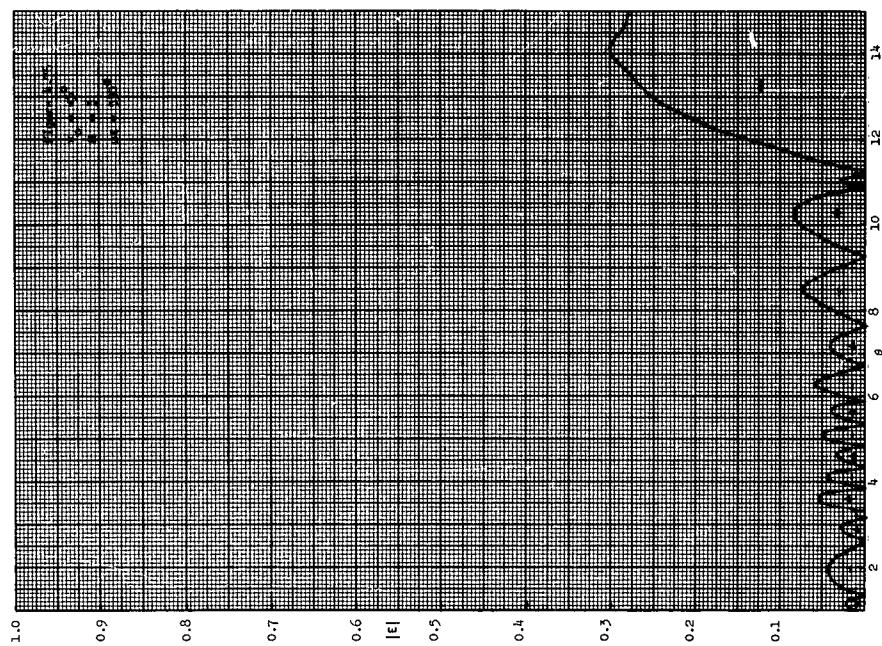


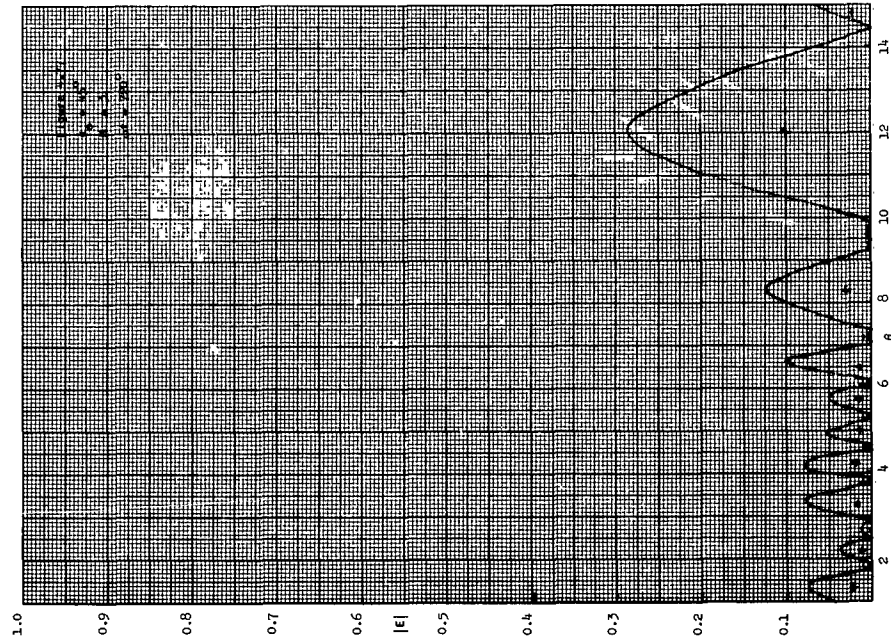
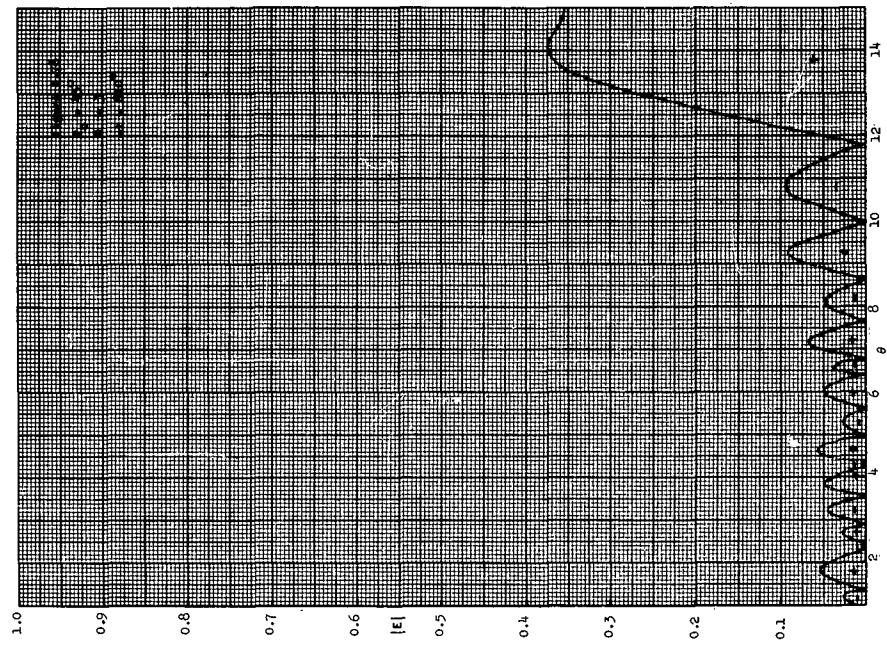


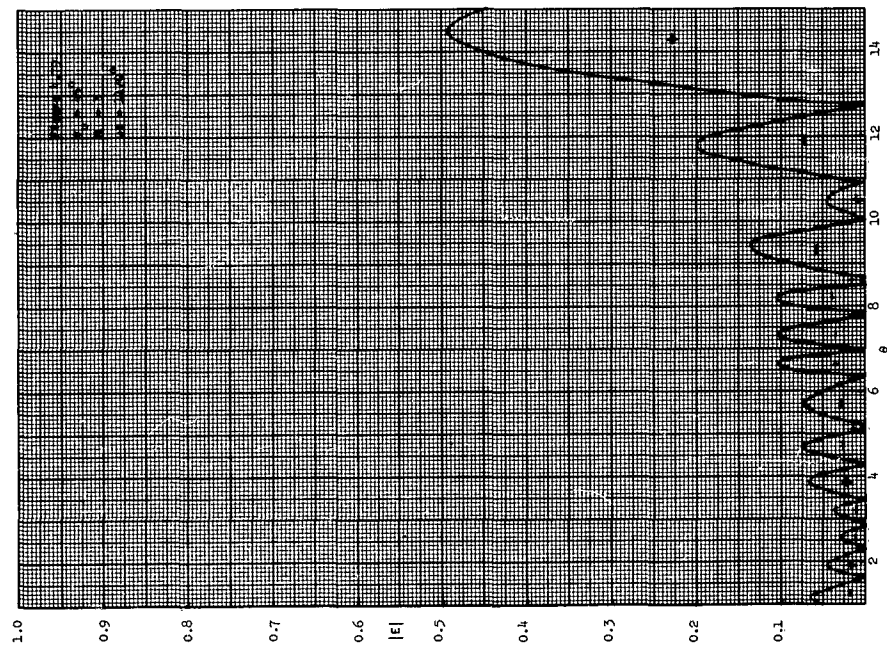
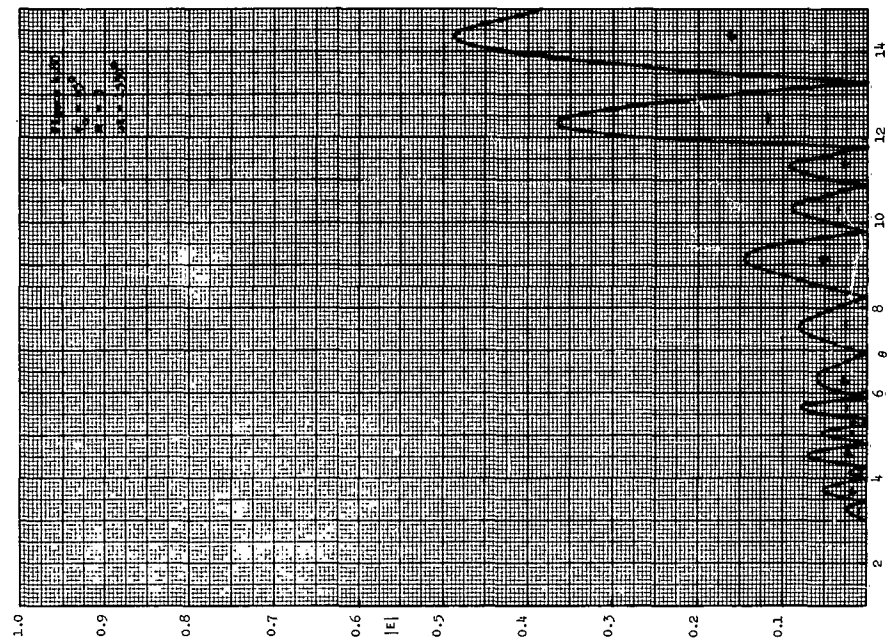


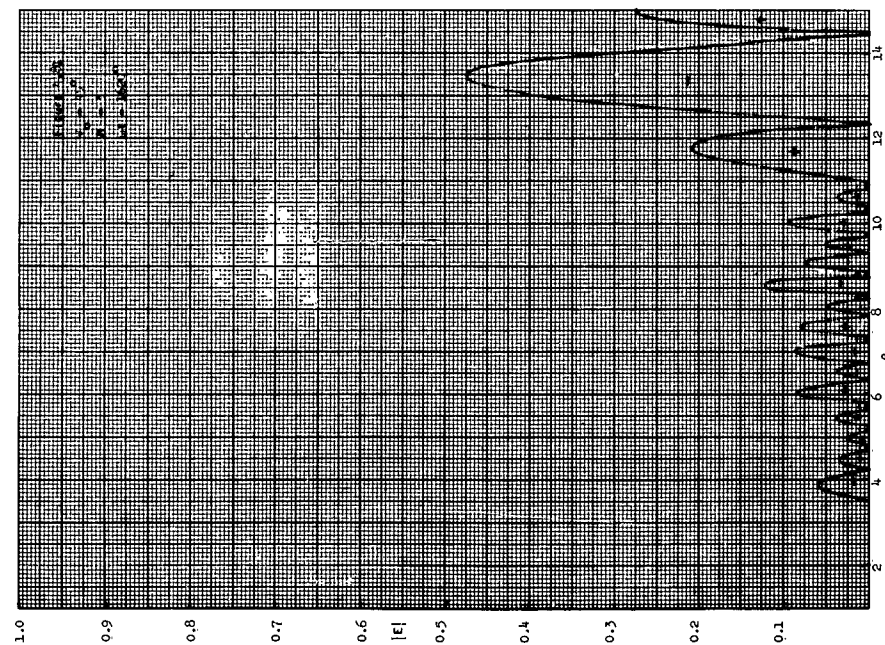
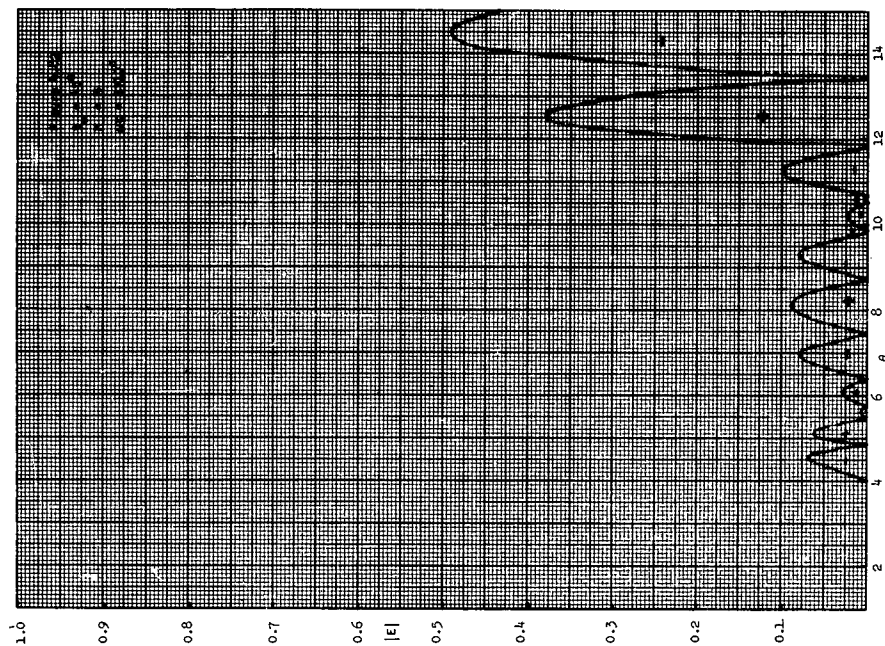


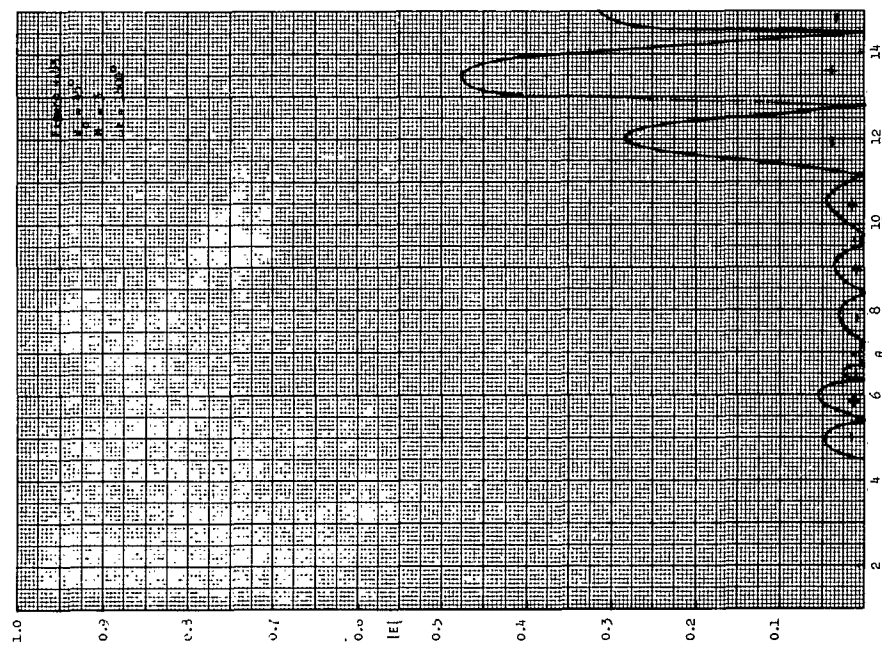
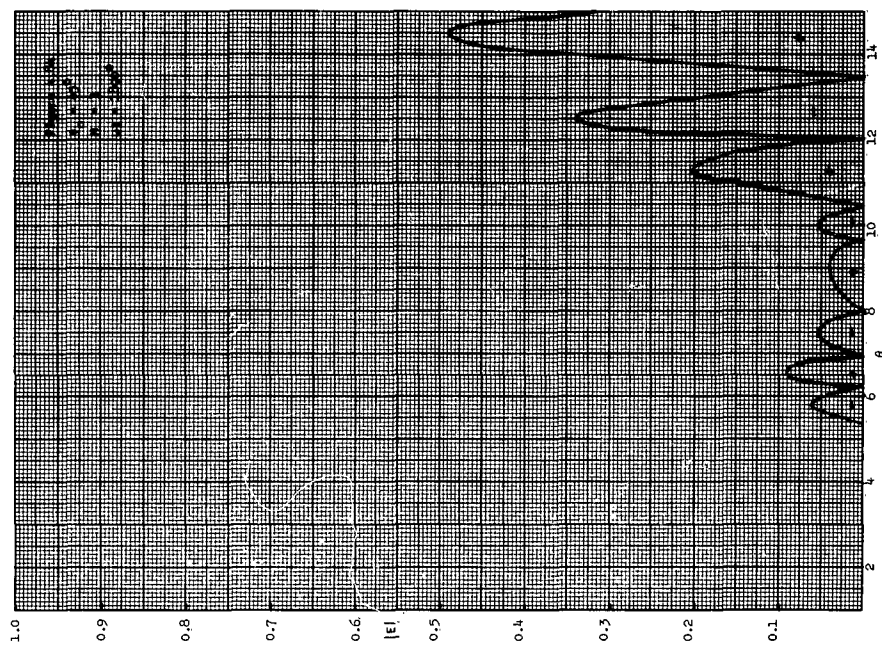


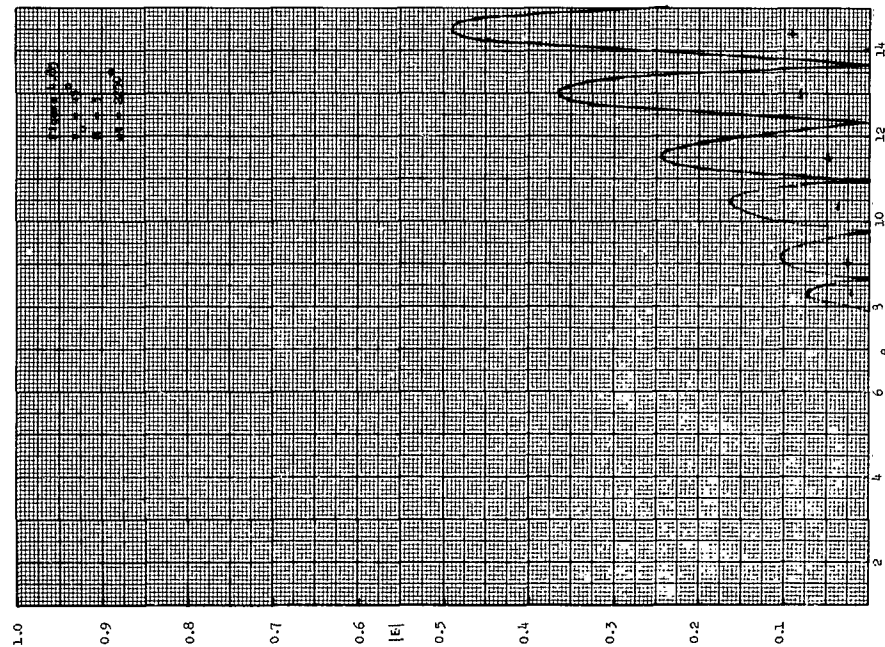
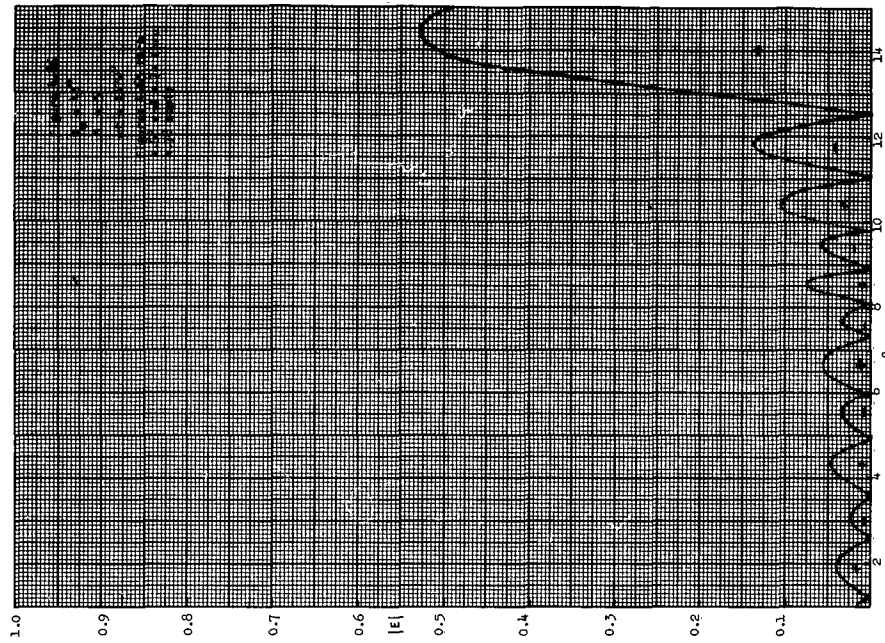


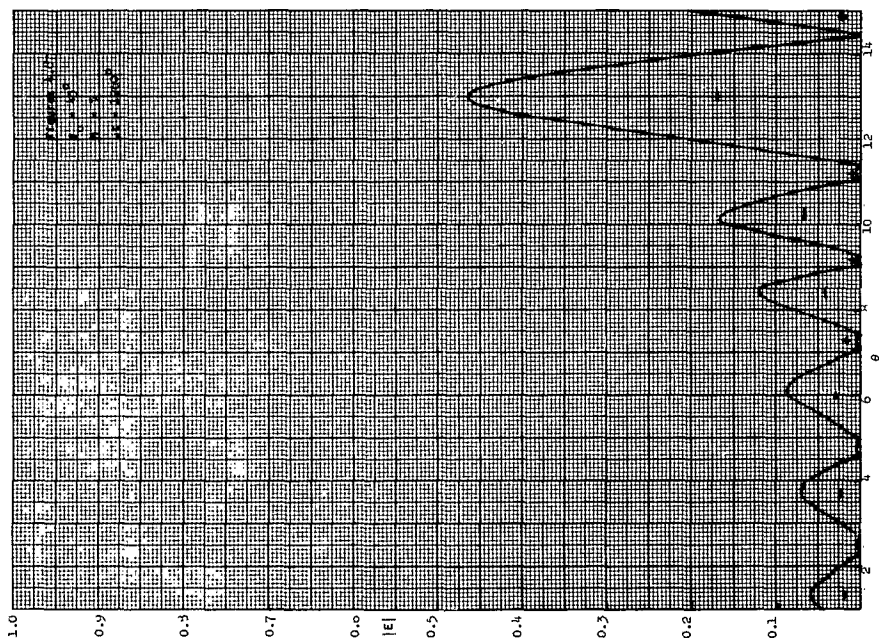
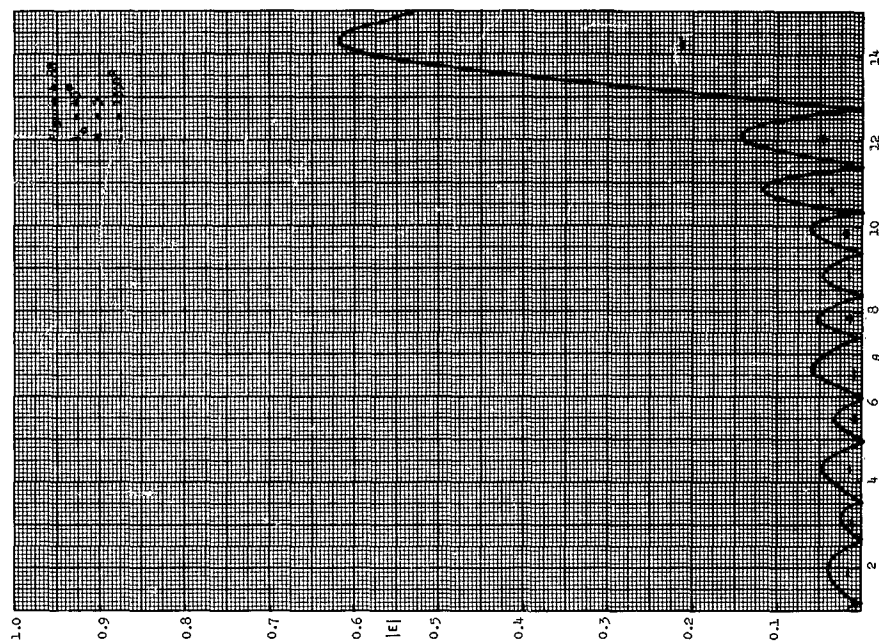


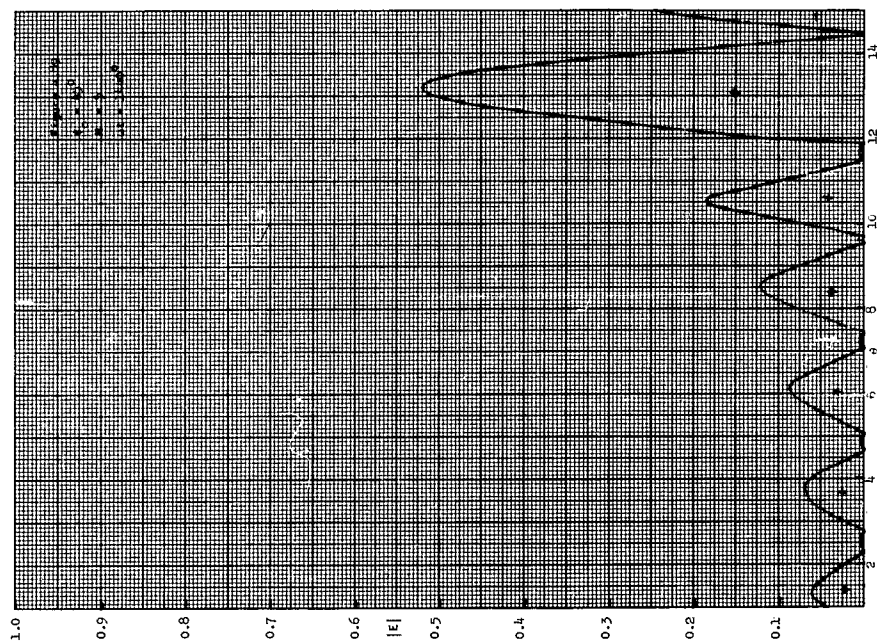
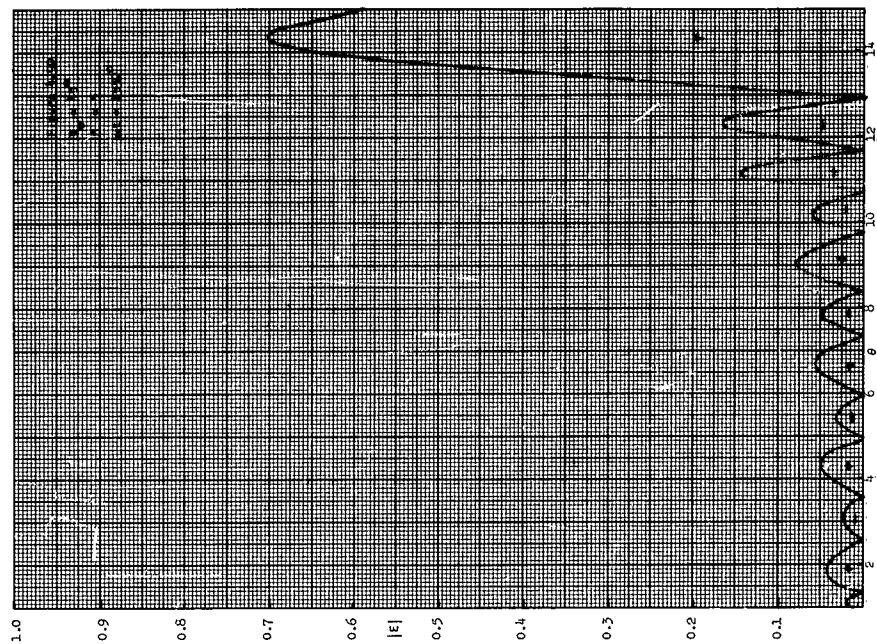


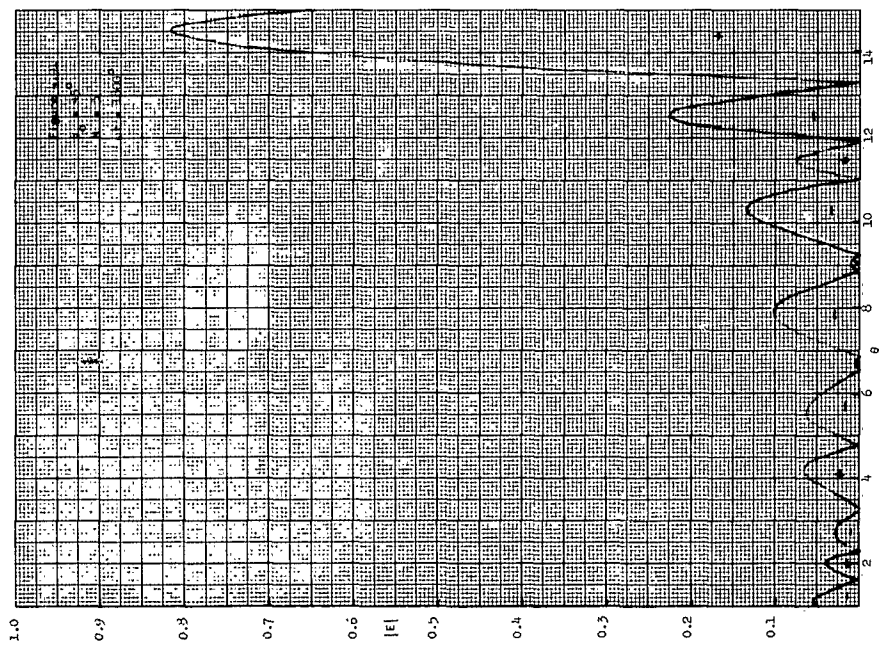
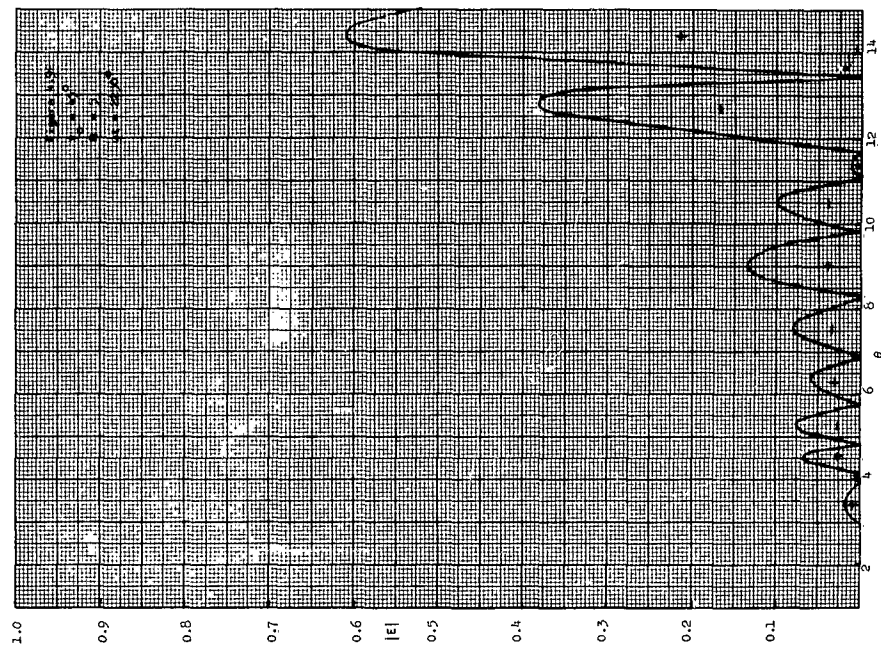


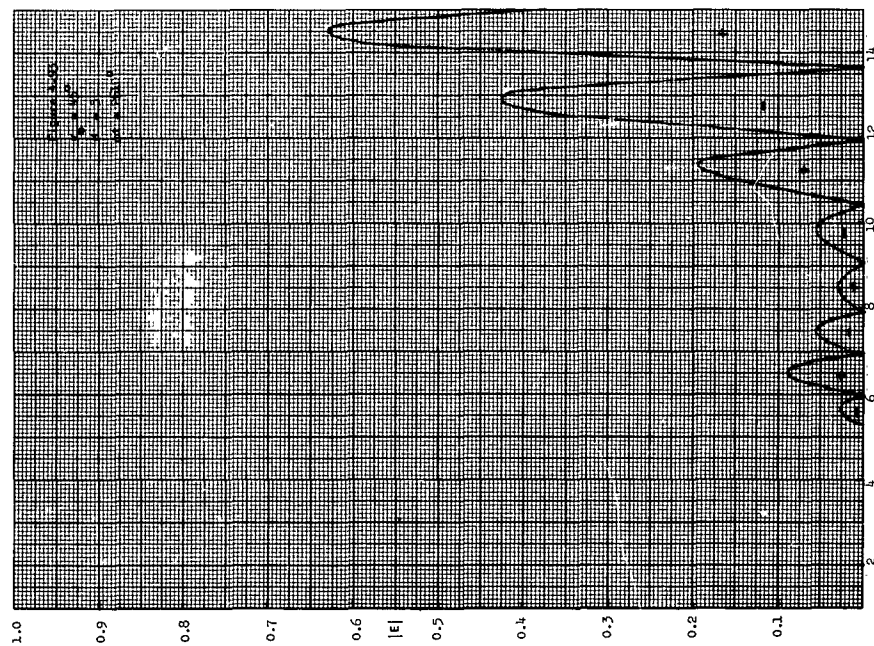
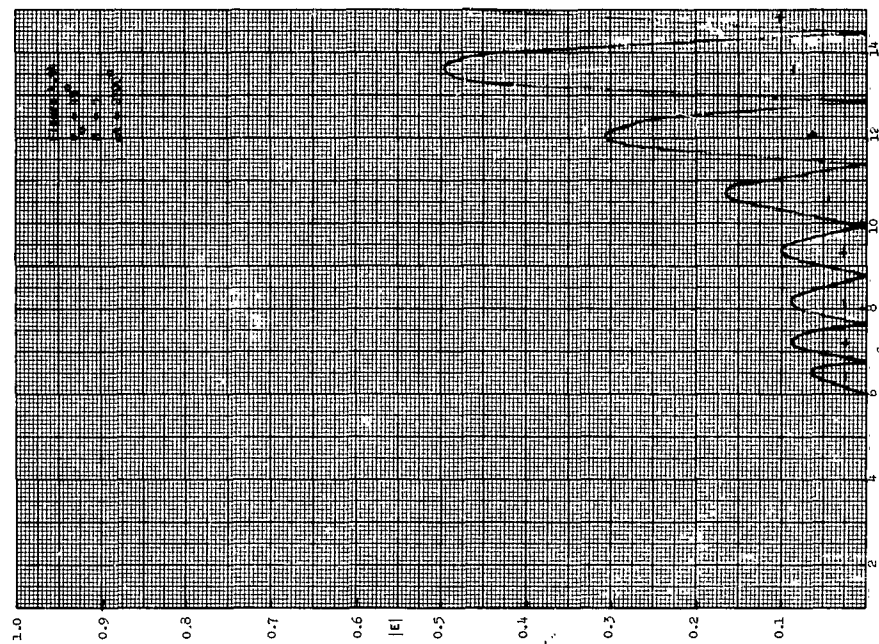


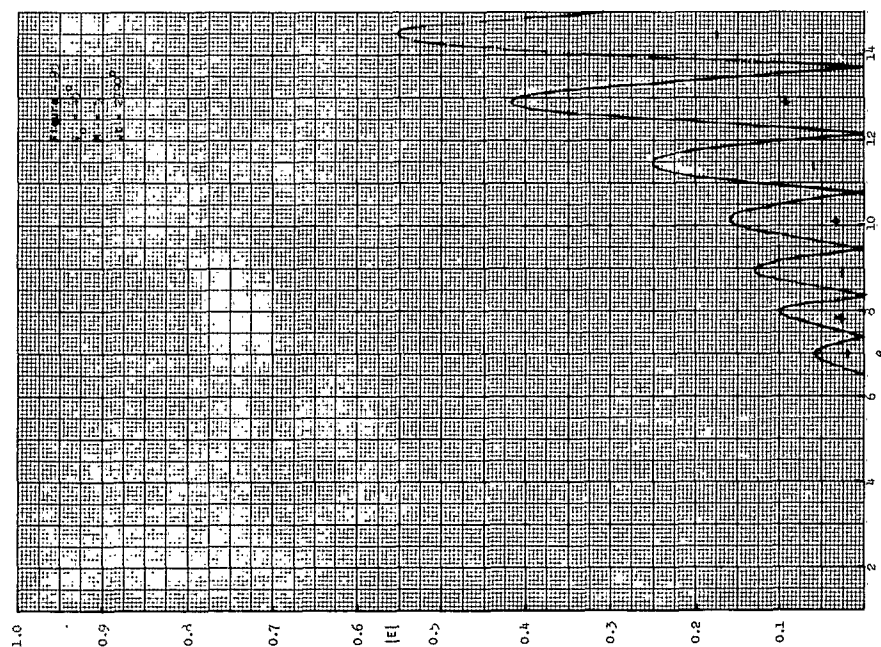
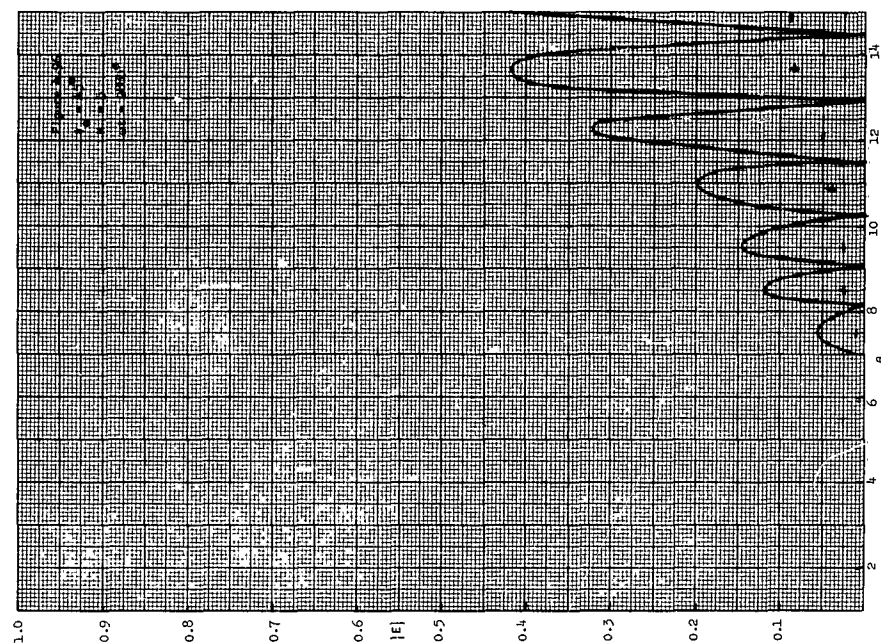


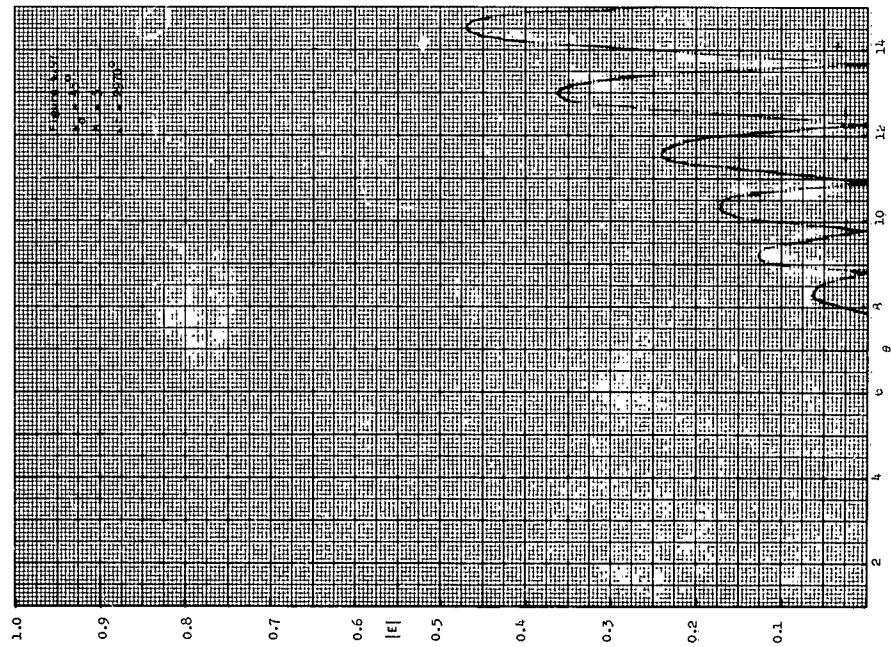
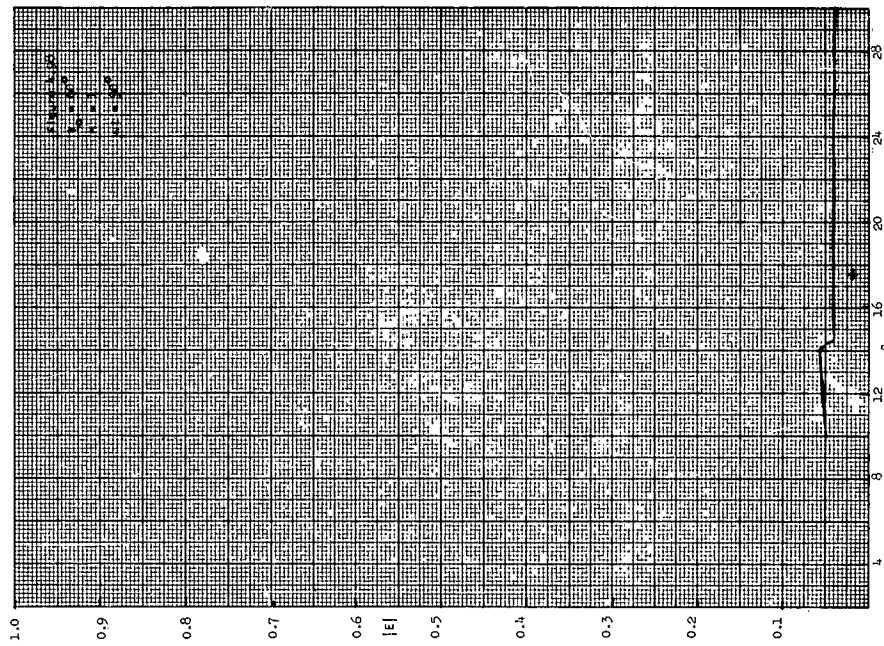


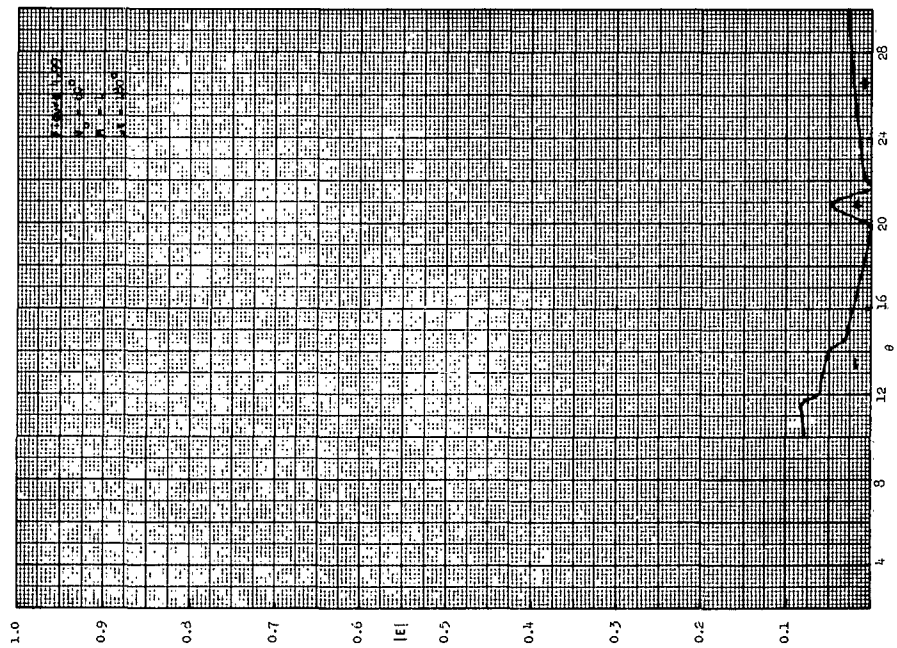
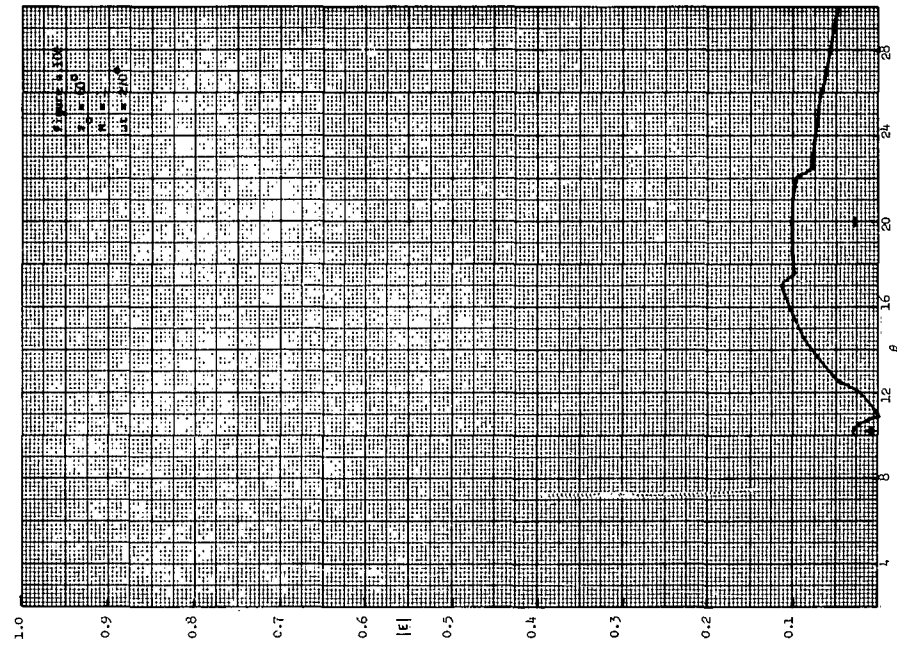


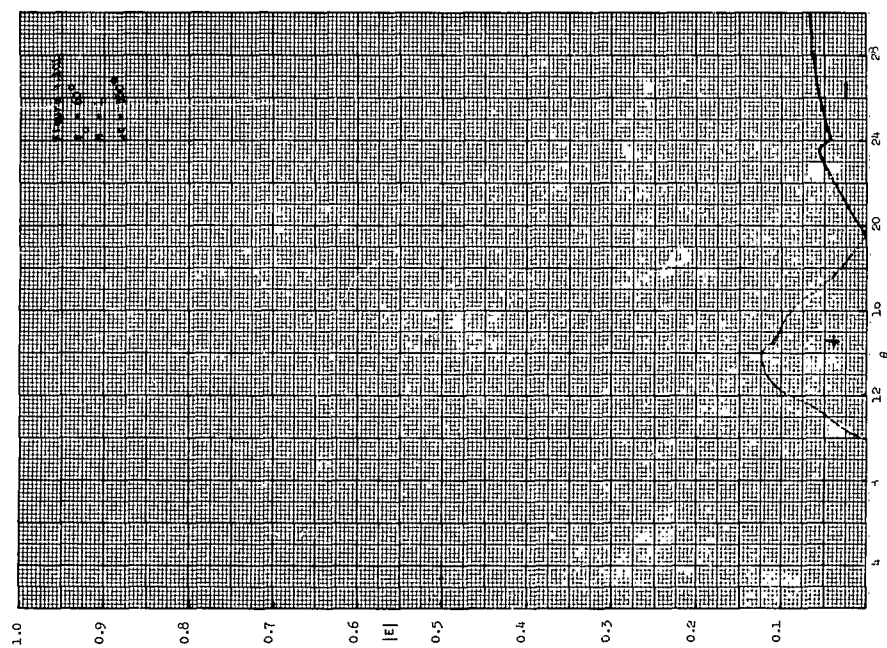
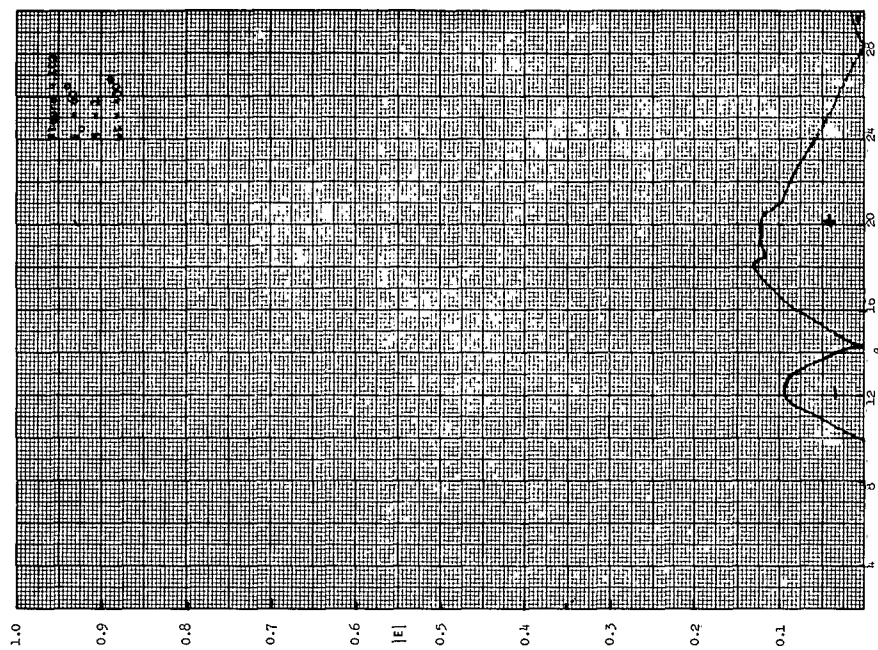


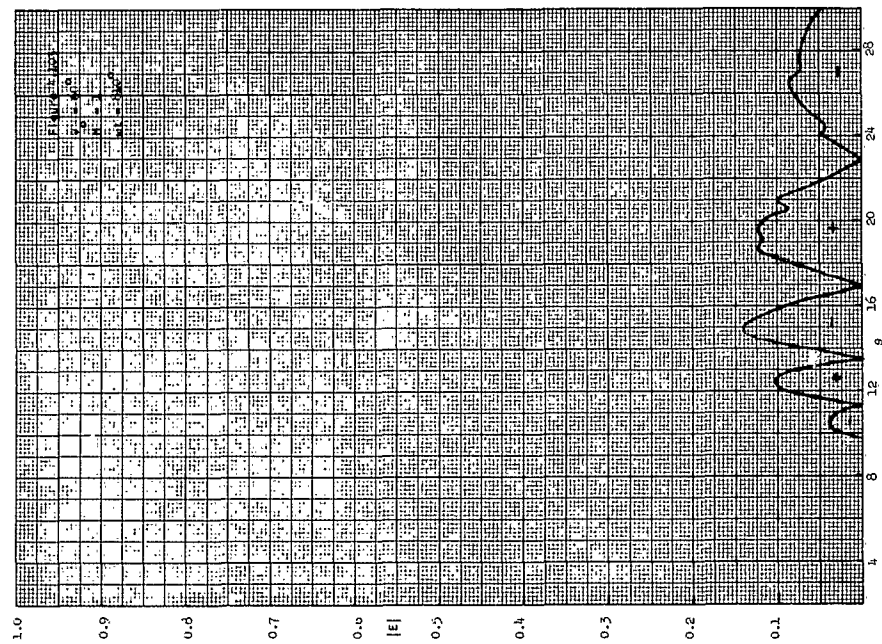
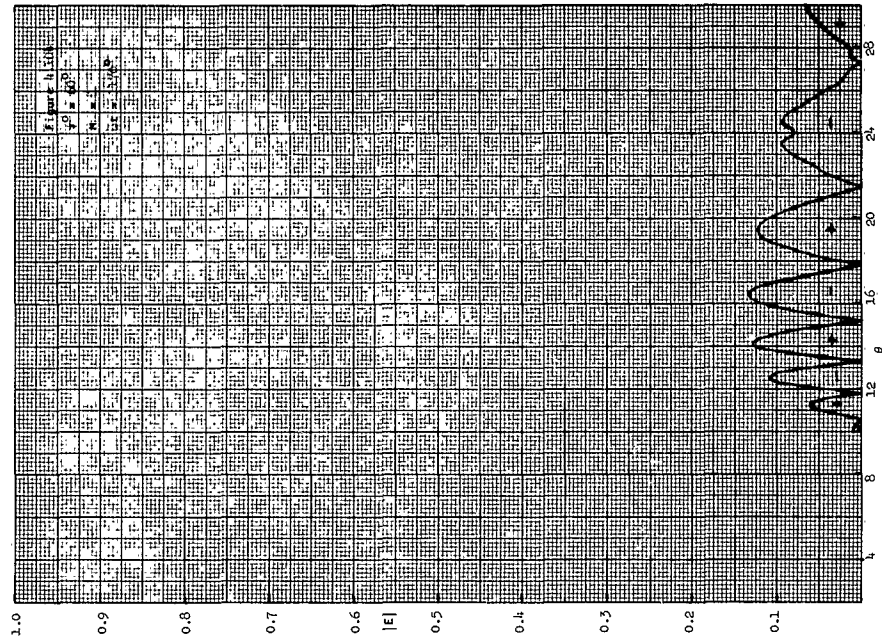


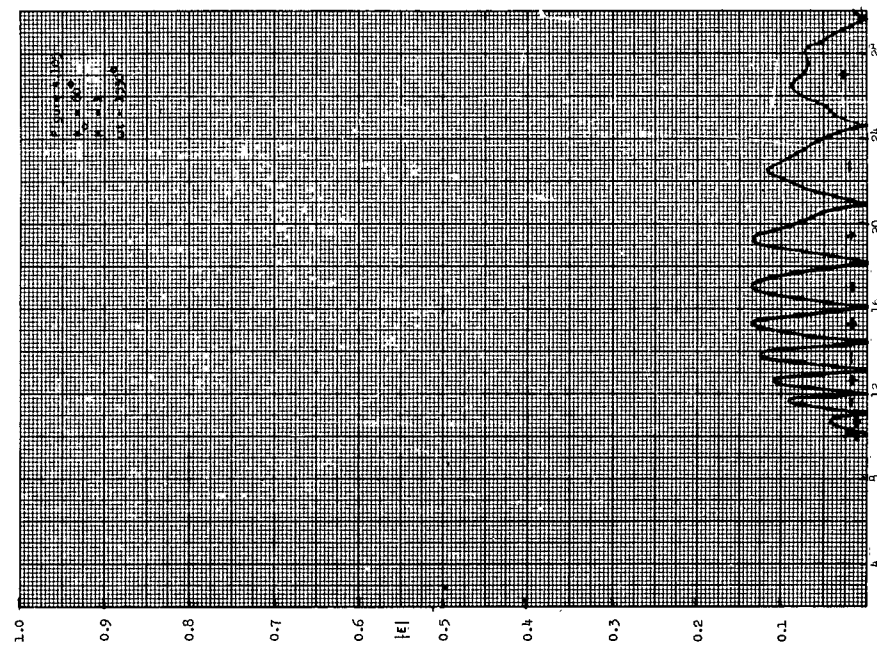
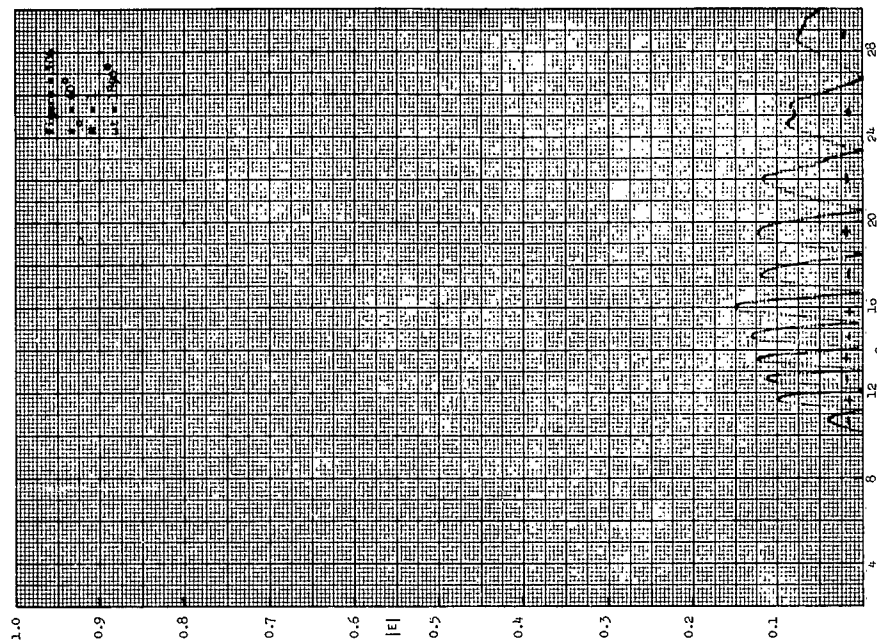


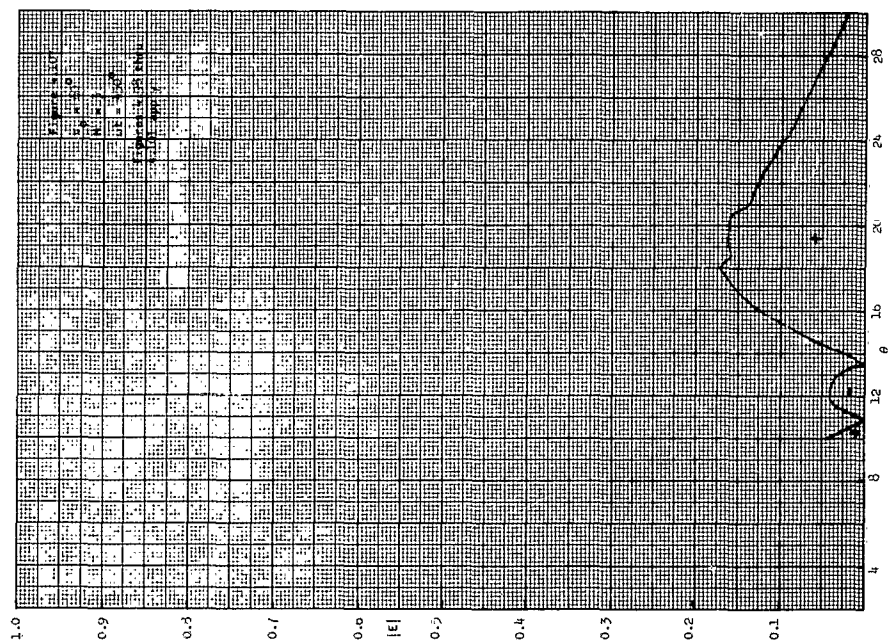
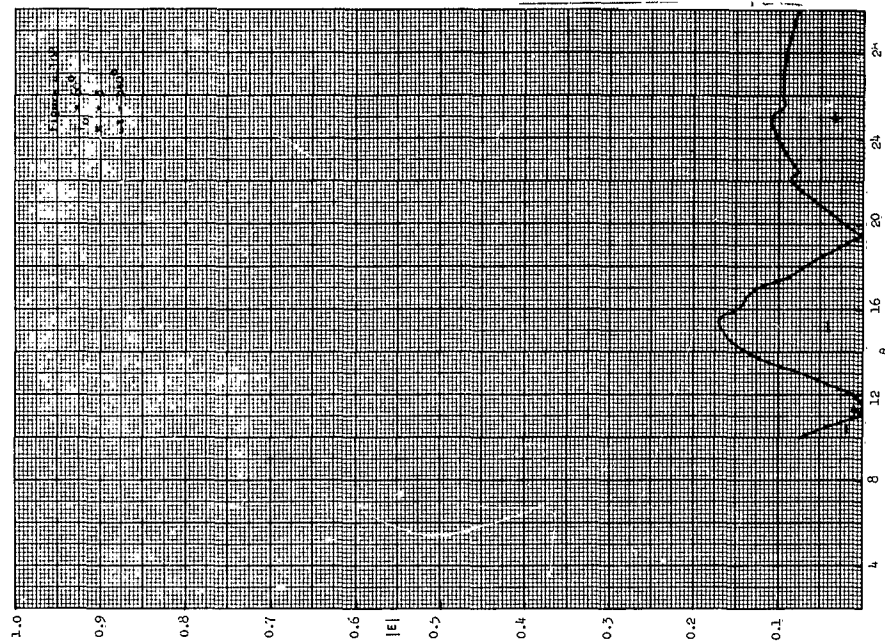


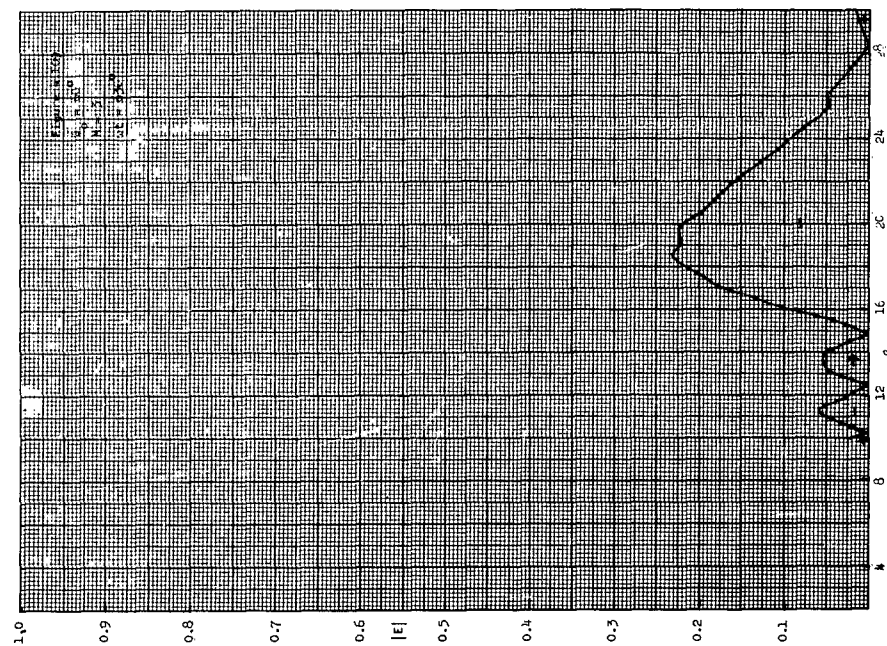
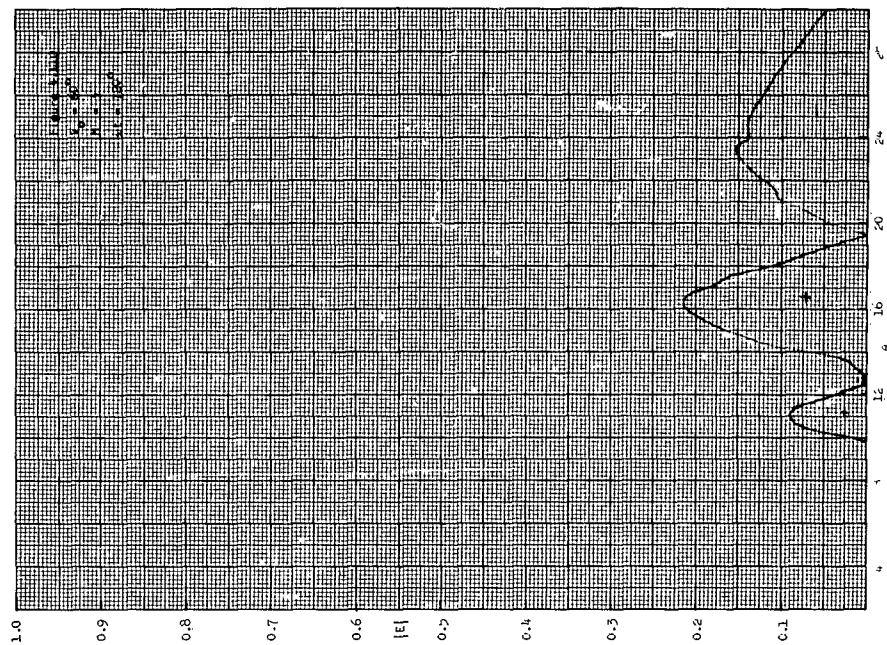


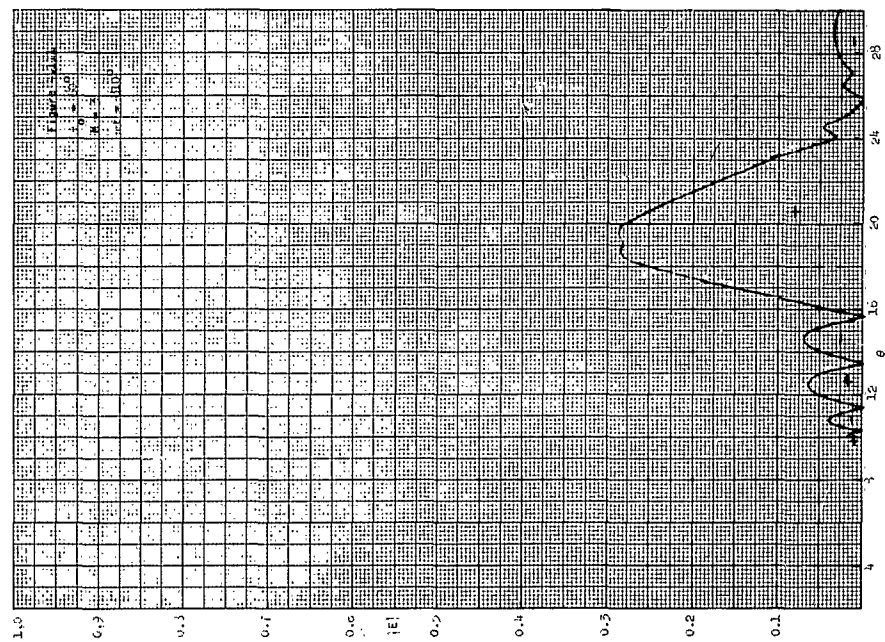
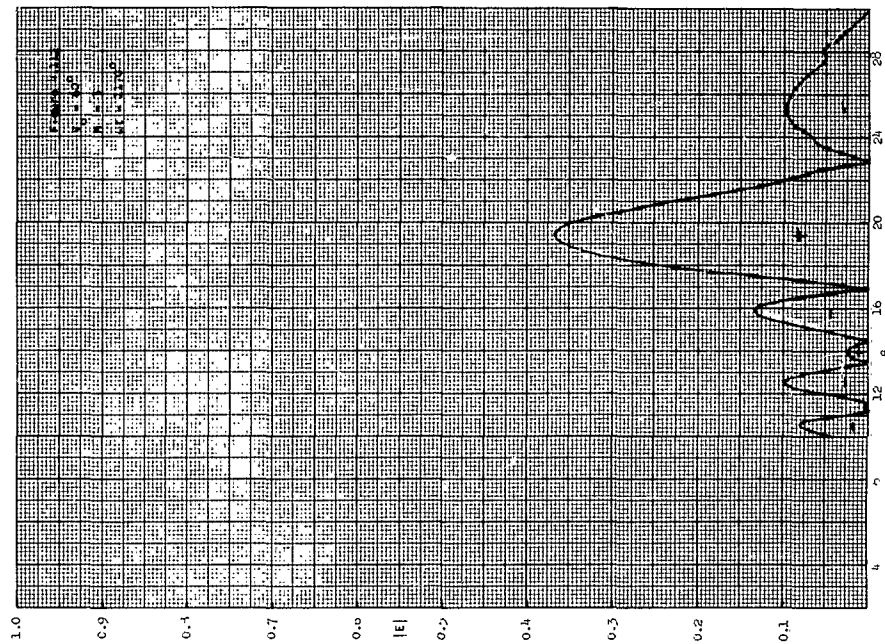


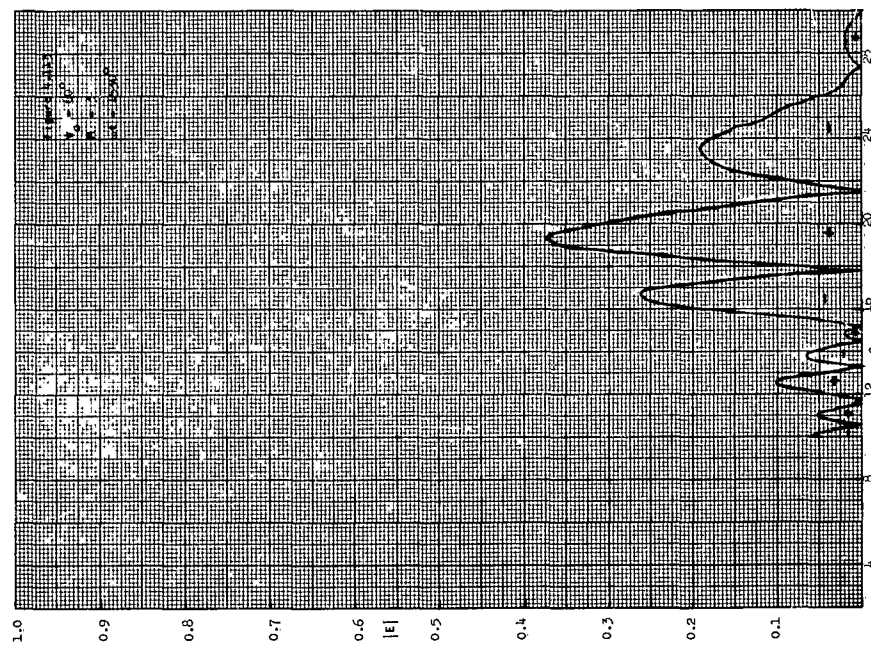
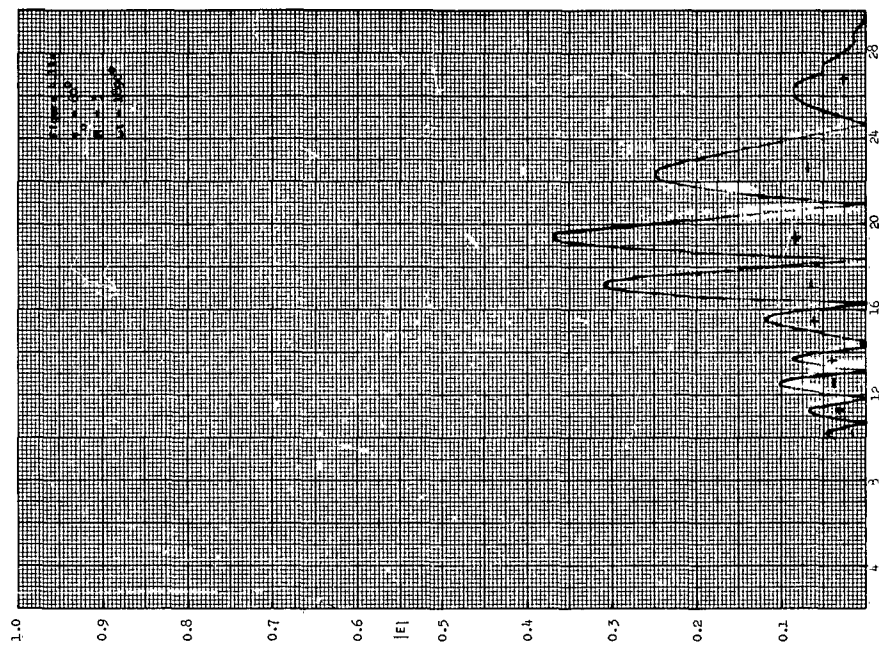


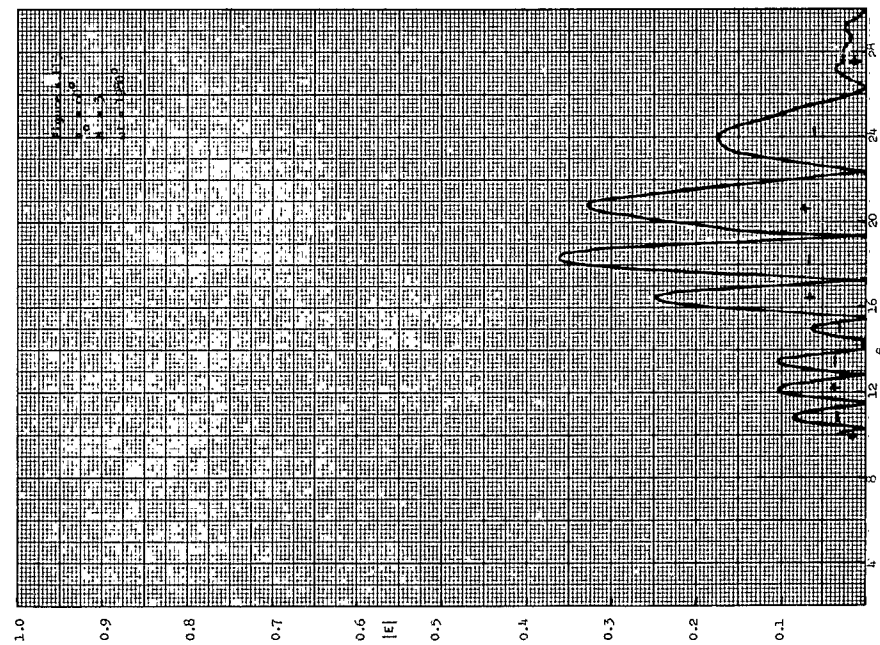
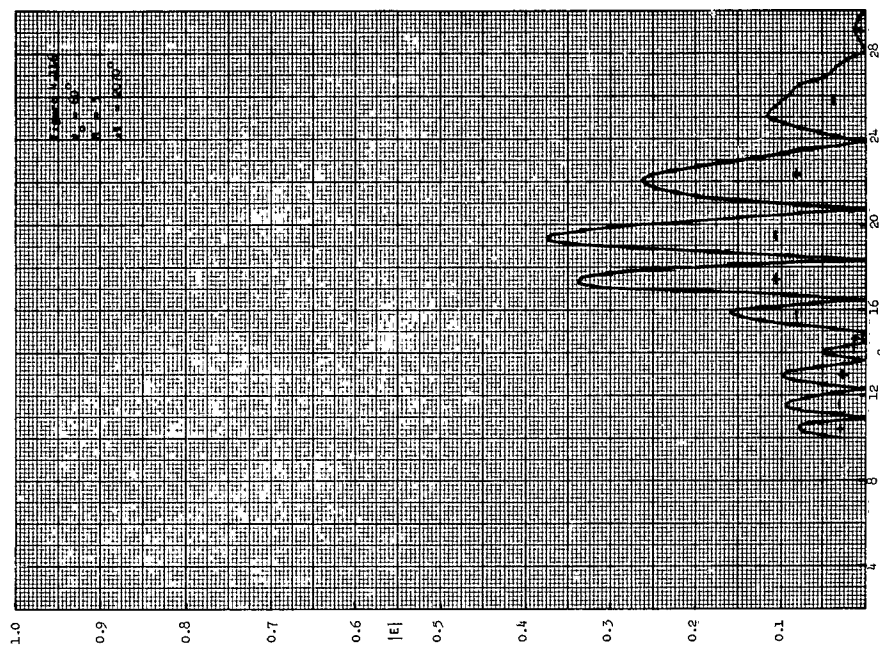


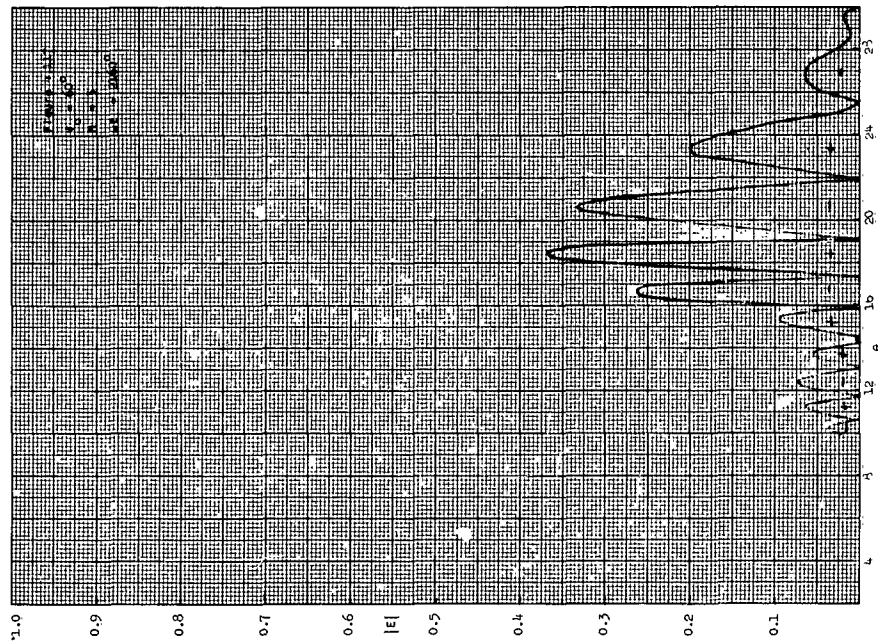
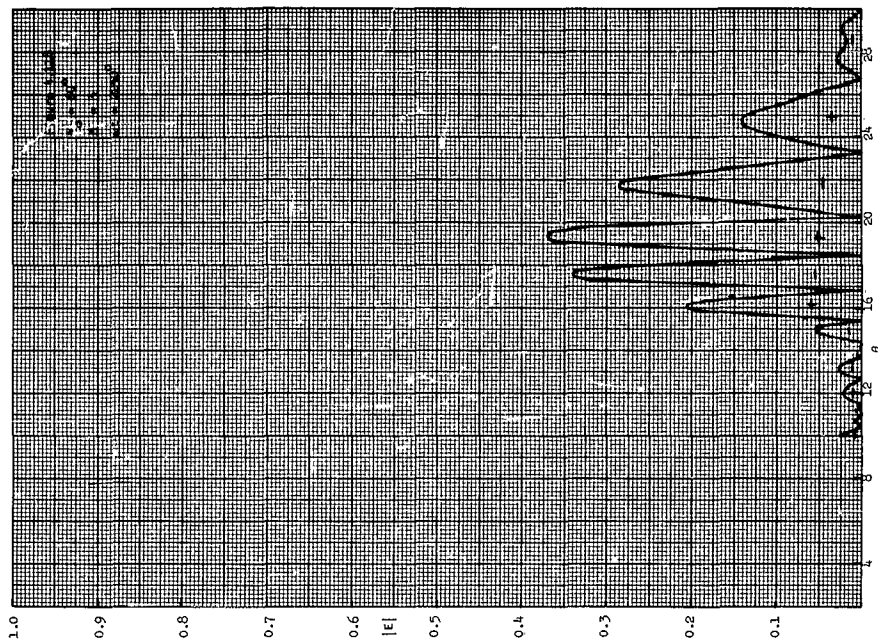


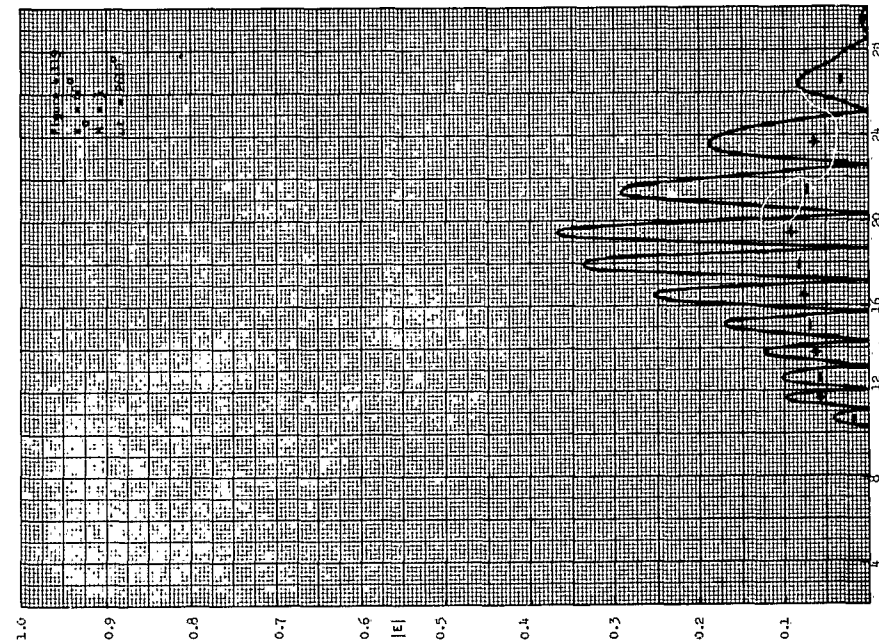
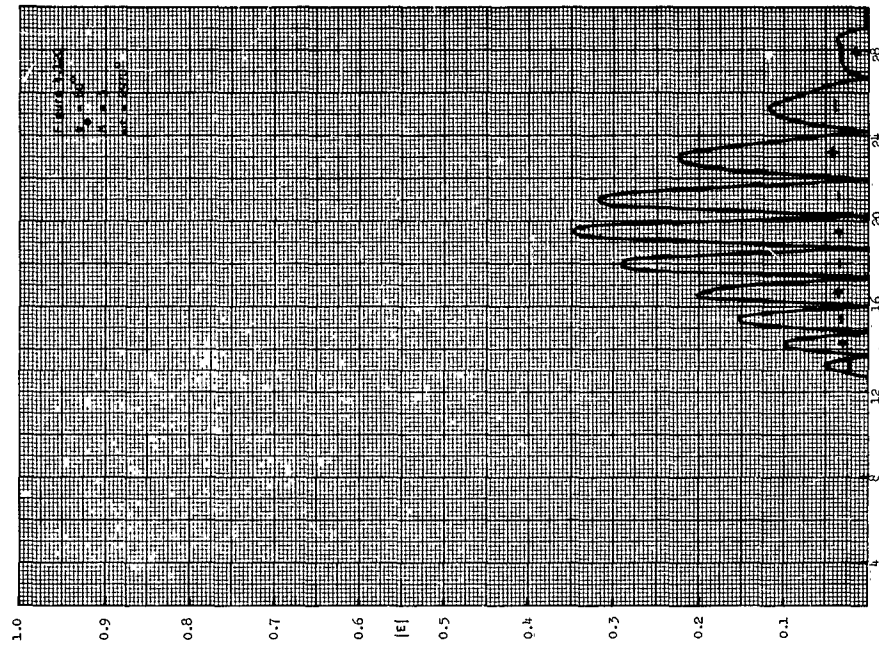


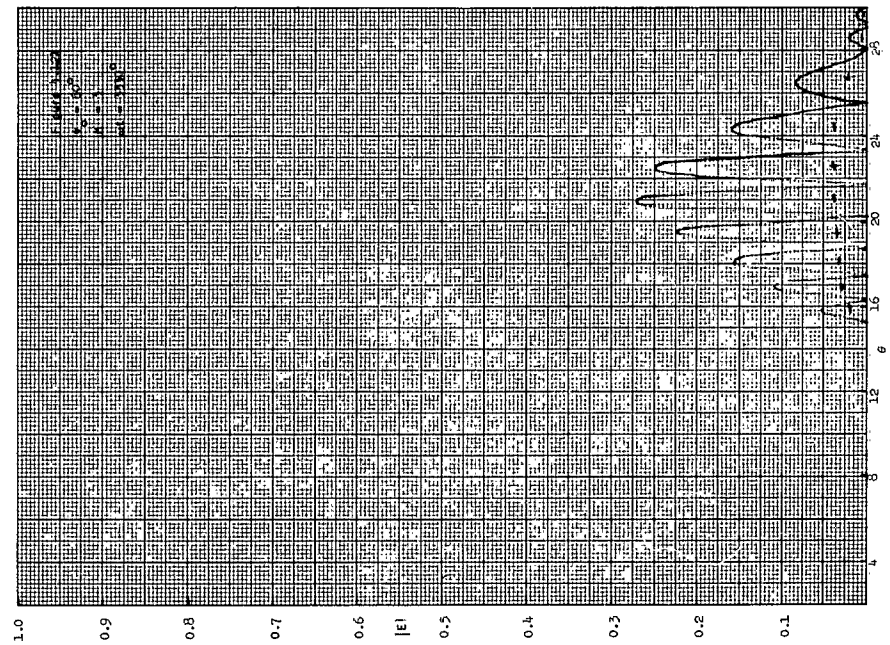
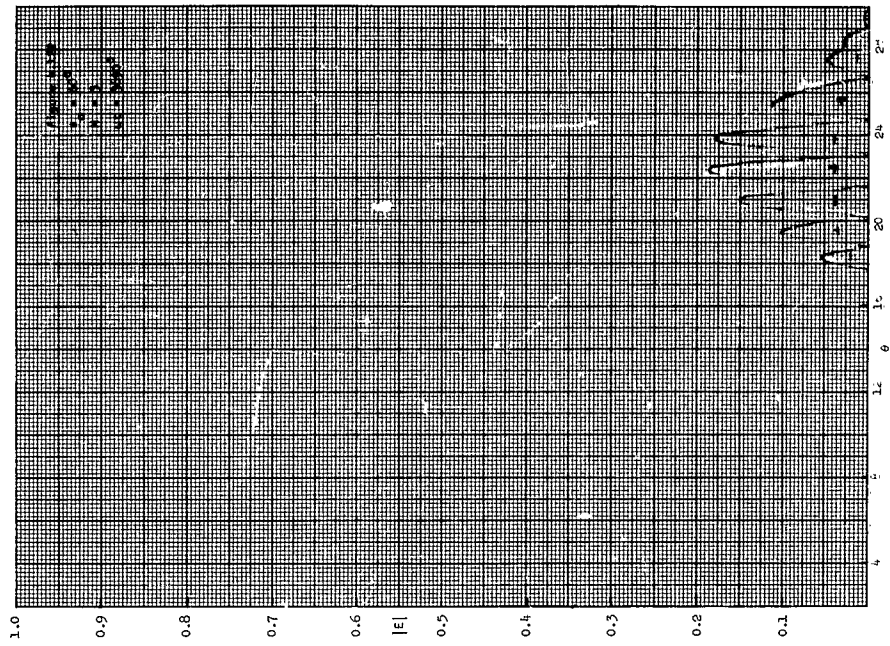


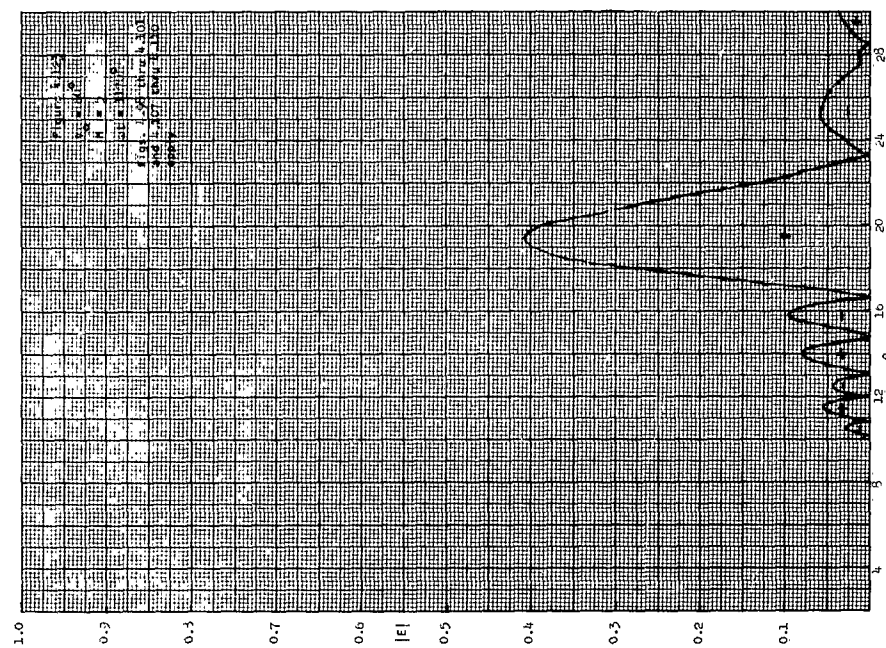
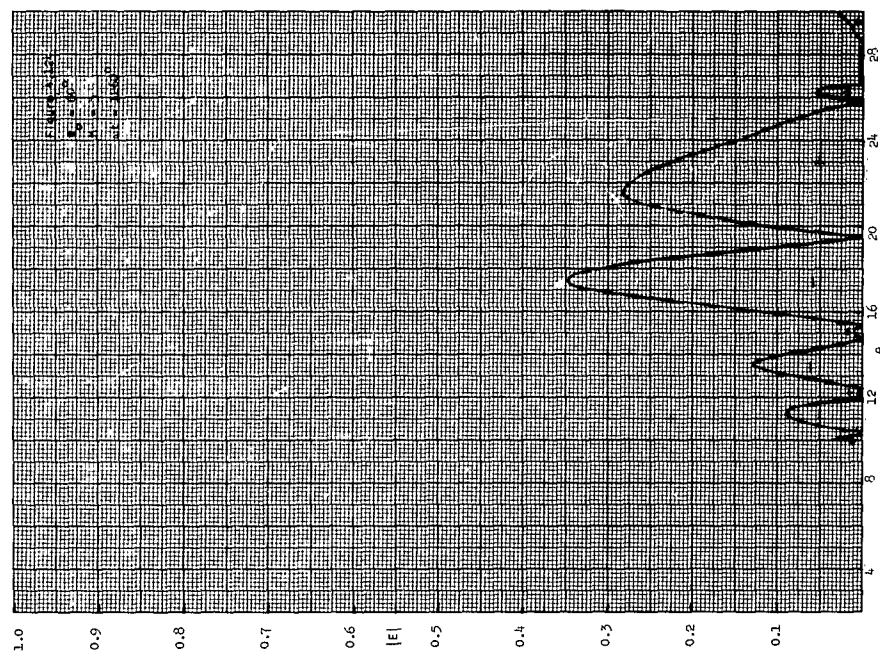


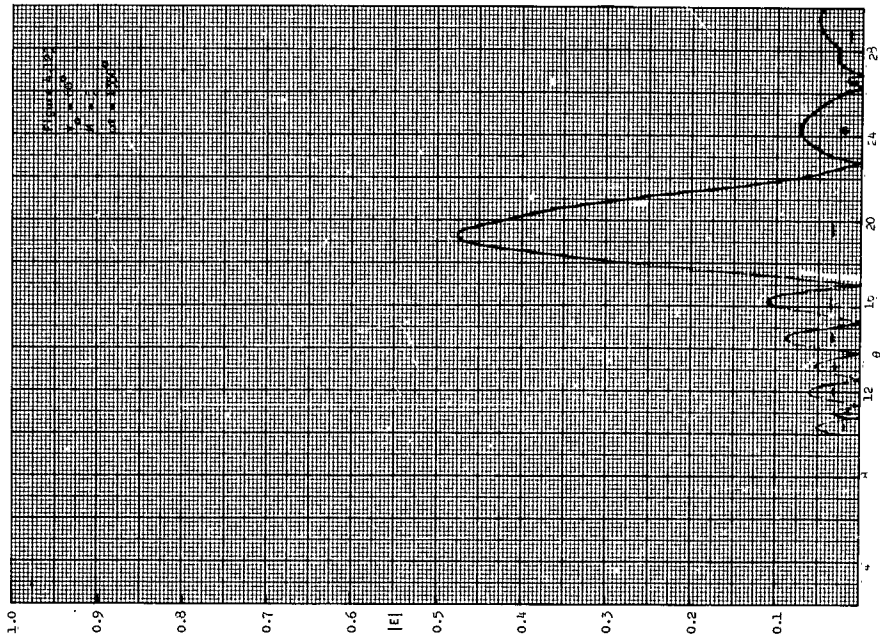
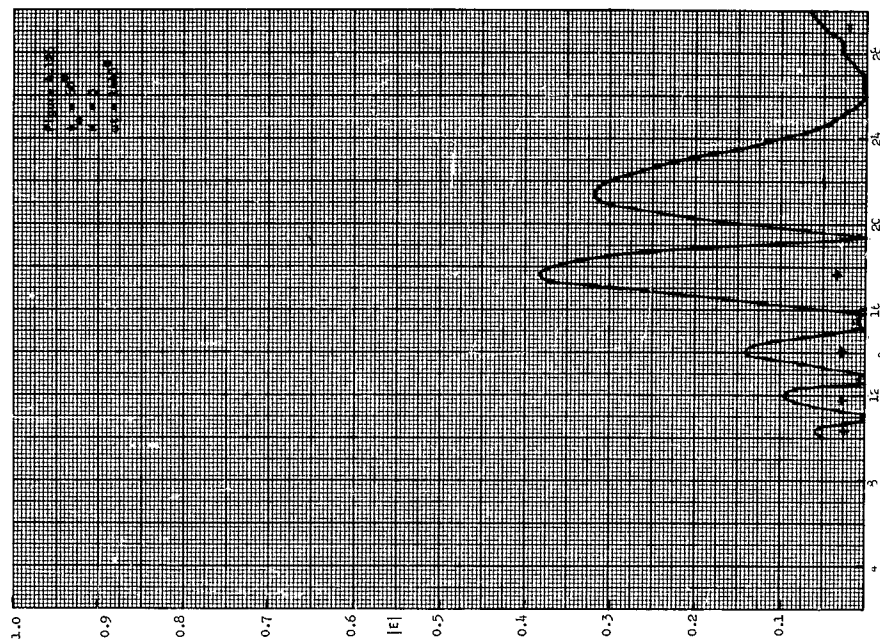


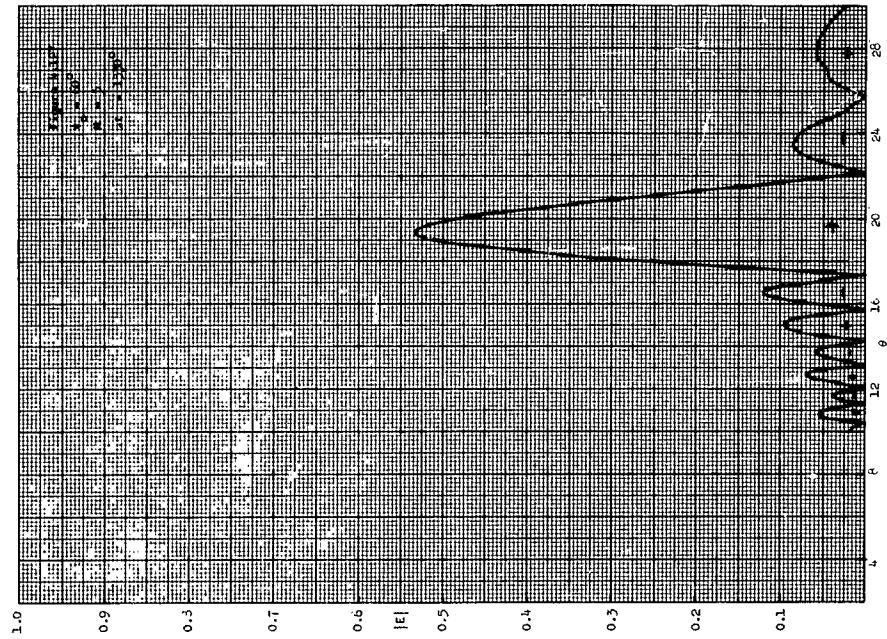
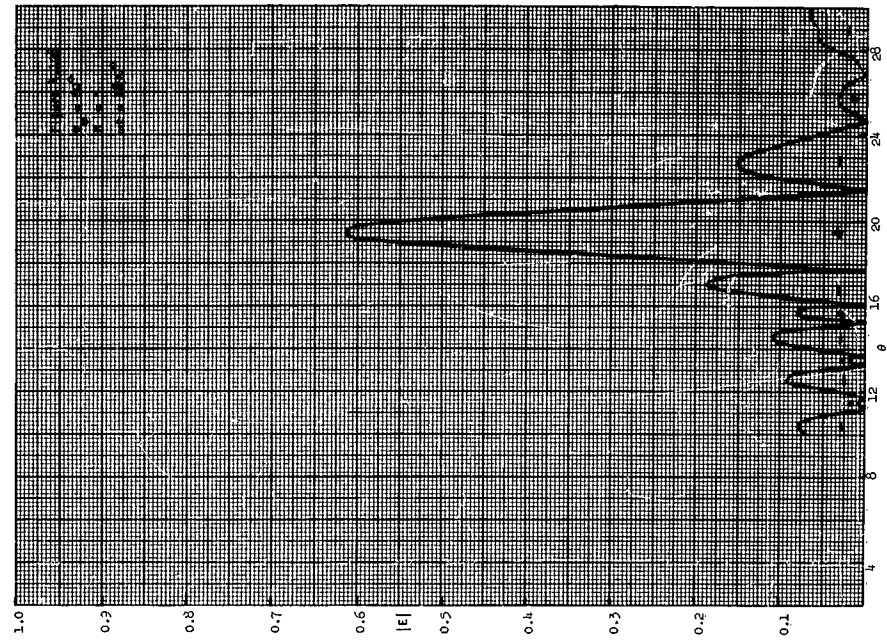


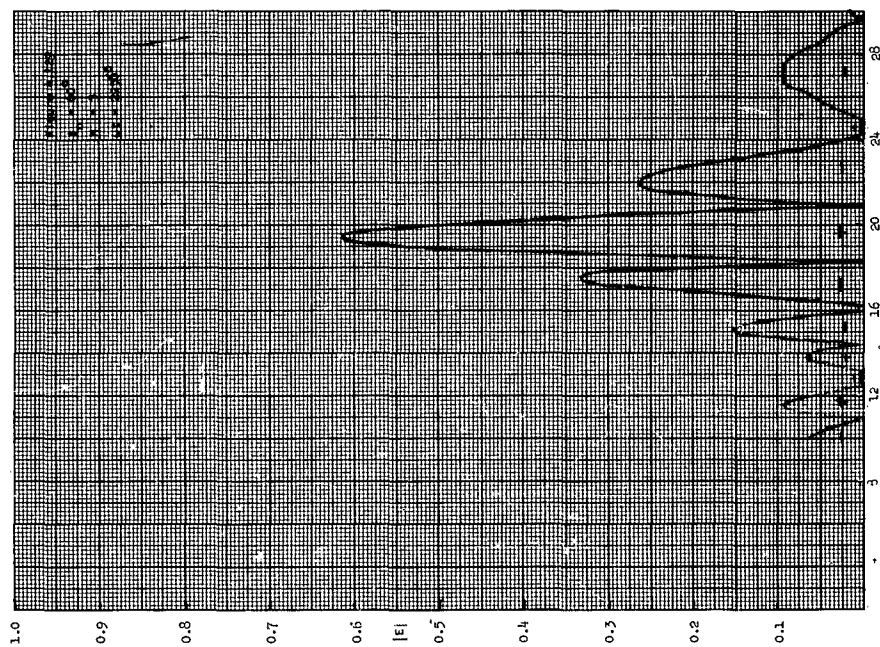
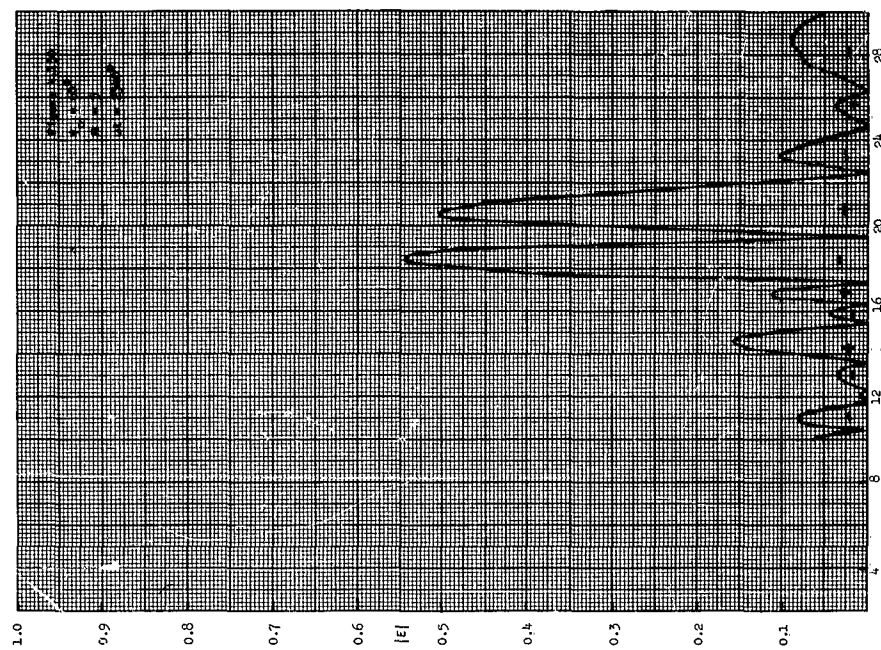


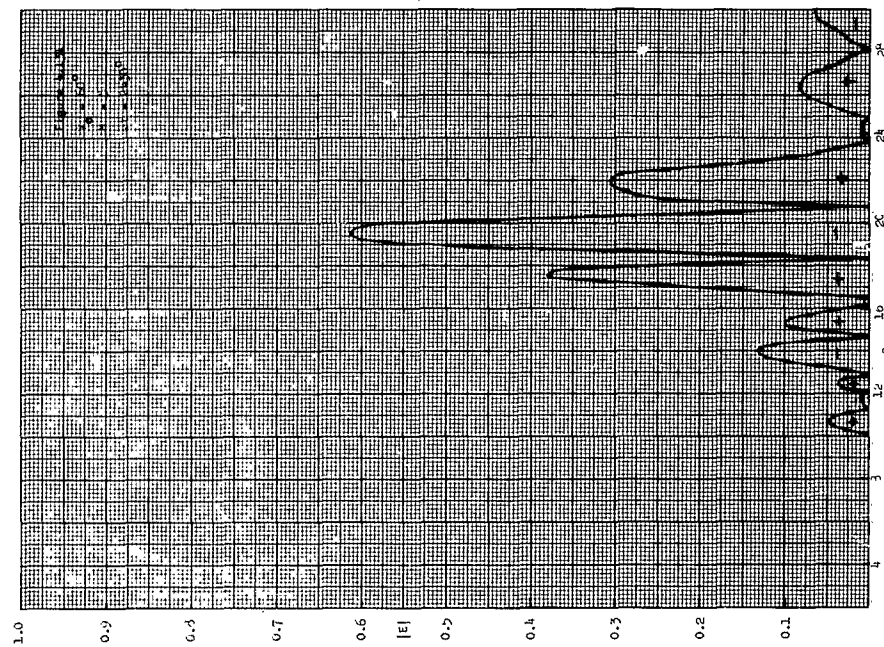
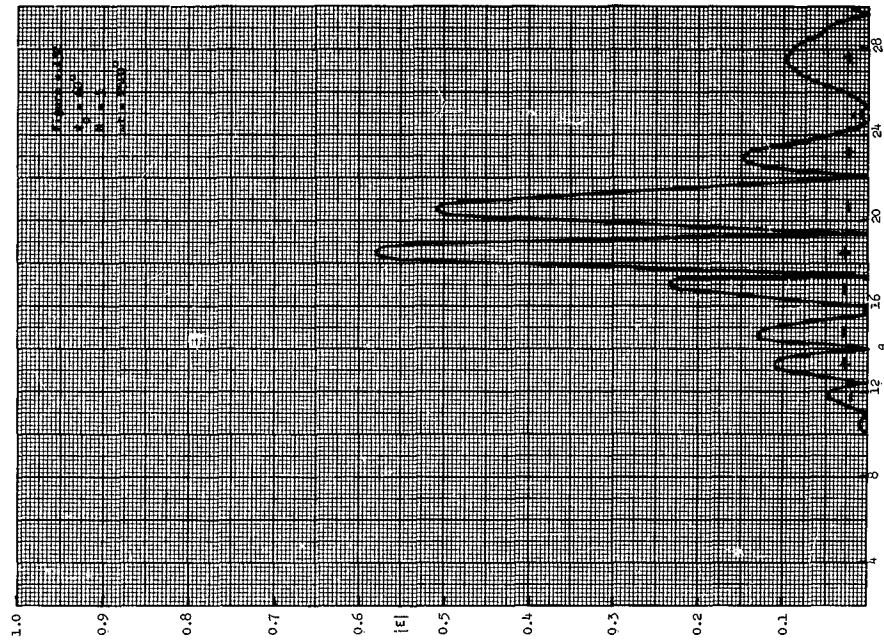


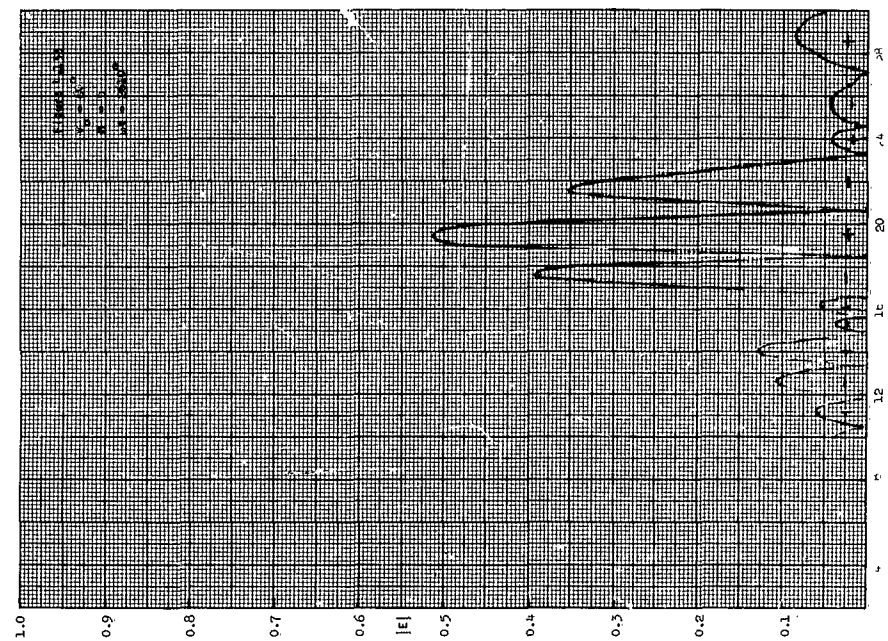
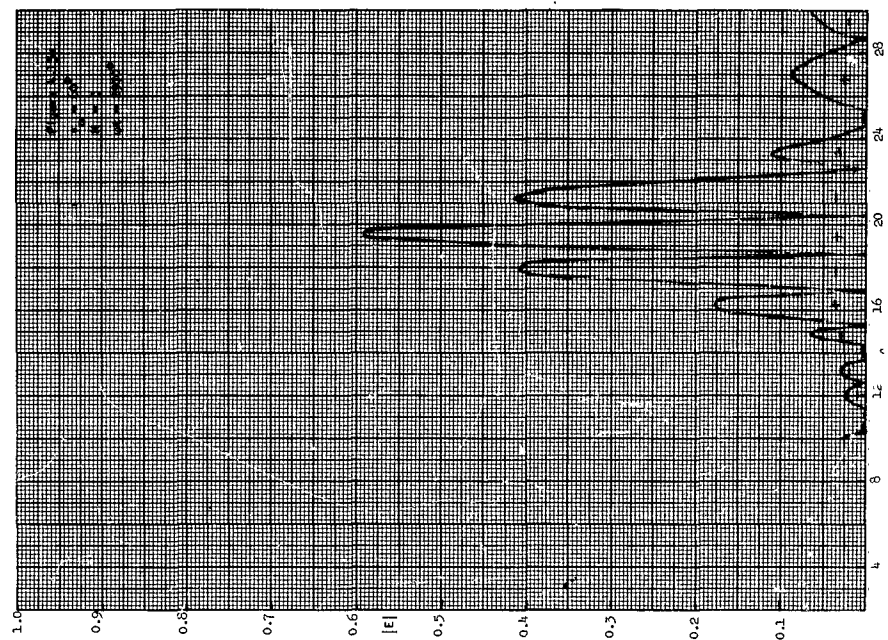


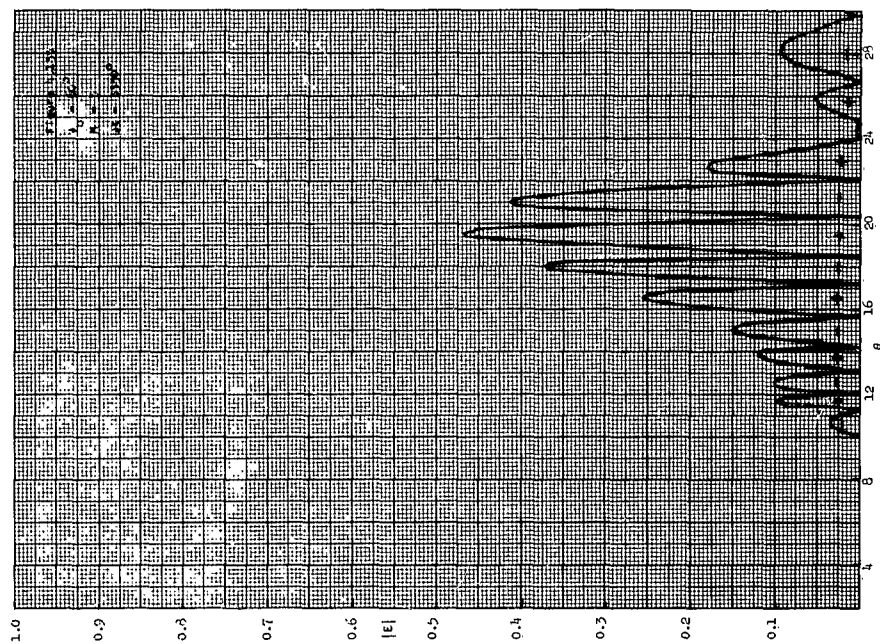
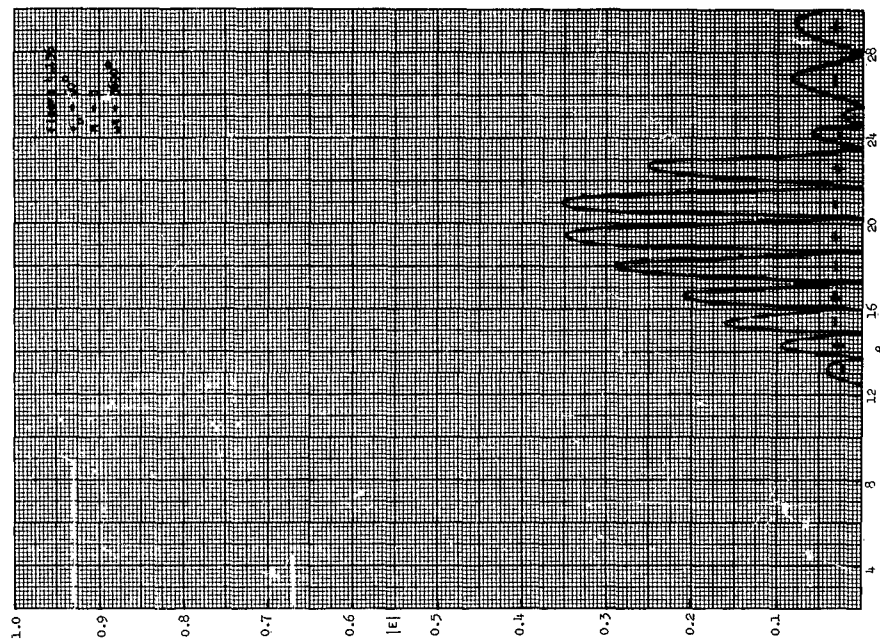


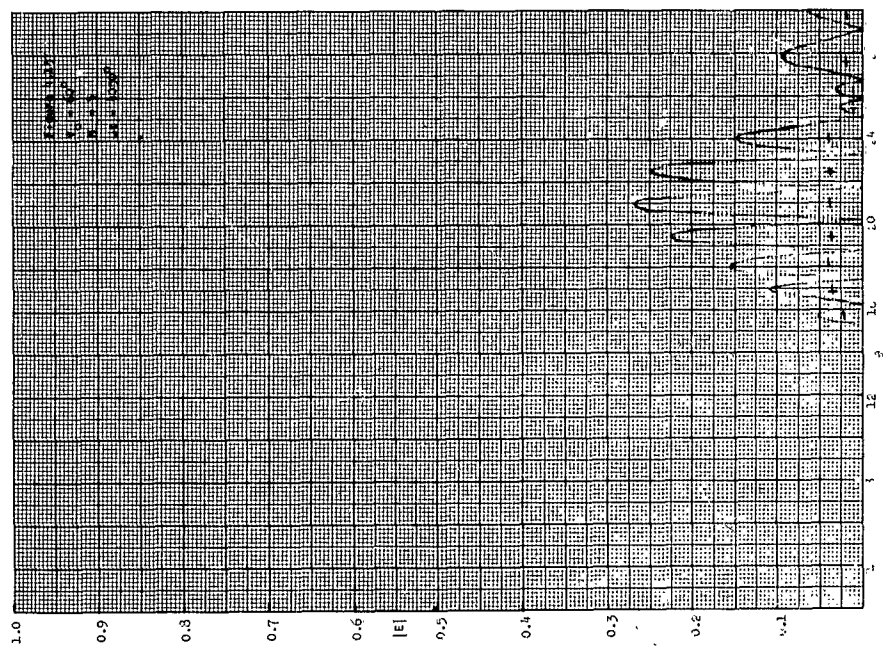
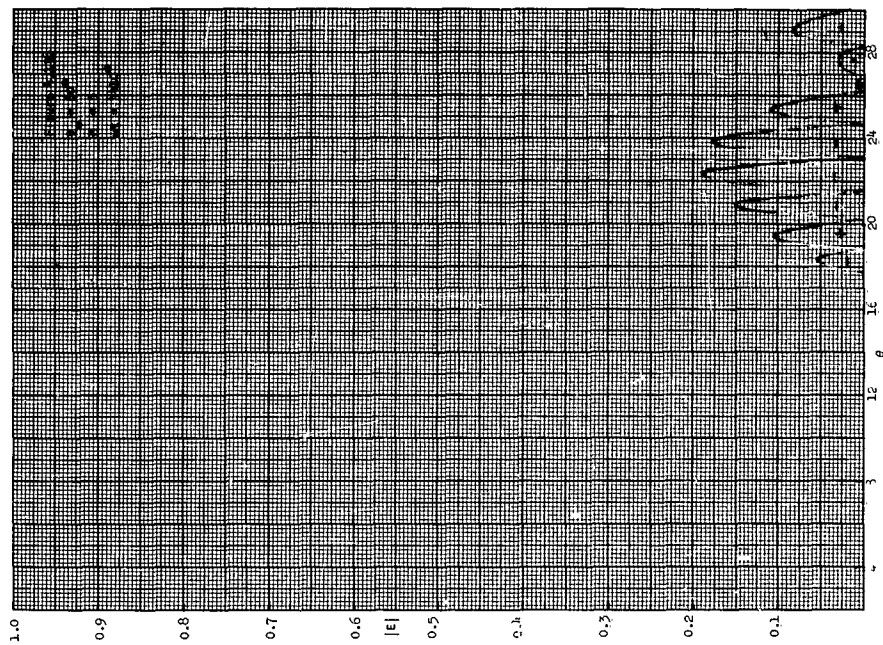












V. ANALYSIS OF RADIATION PATTERNS

A critical examination of the data compiled in this study shows some very interesting features which are a result of using very short pulses, and others which are caused by the instantaneous excitation aspect.

Because of the peculiar appearance of the radiation patterns, when viewed by anyone who is accustomed to seeing the conventional patterns, a set of instantaneous patterns were made for the case where the antenna is excited by long duration pulses. The time was chosen such that all transients had died out, using the solid curves on the pulse diagrams. The technique for plotting these patterns, was the same as before. Figures 5.1 through 5.4 show patterns for the 30° phase case with values of ωt separated by 90° . The four patterns show the variations through one full cycle of excitation. Comparison of these diagrams with the conventional pattern for the 30° phase case, Figure 3.9, show some radical differences. One should keep in mind that these patterns are changing with time at a rate governed by the source frequency, and that a field strength meter would not show these variations but only the peak (or rms) value with no indication of manner of variation with time.

5.1 Uniform Amplitude, Constant Phase

The time variation in the radiation patterns for the one cycle excitation pulse case are characterized by the initial appearance of a single main lobe, with no side lobes, but instead the main lobe gradually tapers to zero. As time progresses, the amplitude of this lobe decreases and splits into two peaks which move away from the on-axis position. These two peaks very rapidly attenuate to zero. Meanwhile a central lobe of opposite phase appears on the axis. It too splits into two and rapidly attenuates.

For the three cycle case we can see in more detail the formation of side lobes as the result of apparent splitting of the main lobe and progression of the side lobes away from the axis as time progresses. In Figure 4.1 there are no side lobes, in Figure 4.8 a single side lobe, as we are accustomed to seeing them, has appeared. In Figure

4.12 three side lobes are present. Intermediate Figures show intermediate steps and the opposite phasing situation. At the end of three cycles the patterns change in character because the transient decay begins at this time. Prior to this time the pattern was undergoing a transient build-up. The transient decay is characterized by side lobes which are moving away from the axis and decreasing in amplitude as time progresses. A main lobe is totally absent.

For the five cycle case, there are five side lobes present after an elapsed time equivalent to three cycles of excitation. During each half cycle an additional side lobe of appropriate polarity appears. The region of exponentially decaying signal strength which is not characterized by the side lobe structure but rather has the form of the side lobe envelope, is gradually being replaced by side lobes. The envelope of the side lobes remains constant throughout, discounting the minor errors which cannot be entirely eliminated due to the computing and plotting procedures used.

5.2 Uniform Amplitude, 30° Progressive Phase

The radiation patterns for the 30° phase case are entirely different in appearance from those of the zero phase case. Computations were carried out in the vicinity of the main beam, which is centered at $\theta = 9.54$. Symmetries about that angle do not occur, as they did in the in-phase case, although as pulse durations increase the patterns approach symmetry in the steady state. For short pulses we are dealing more with the transient than the steady-state situation and this is where the extreme lack of symmetry is very evident. In all pattern diagrams if the signal is zero for an extended interval a line is drawn along the zero axis. If computations were not made for particular ranges of θ the curve is broken off at some non-zero value of $|E|$. In this case, lack of a curve does not imply zero signal.

The diagrams for this and subsequent cases are characterized by rapid fluctuations in both amplitude and phase. For the one cycle case a lobe resembling the main lobe begins to appear in

Figure 4.38 although Figure 4.34 has nothing which could be recognized as a main lobe. Side lobes begin to show up to the left of the main lobe but to the right there appears only a wide lobe.

The three cycle pulse patterns begin to take on the appearance of the instantaneous pattern shown in Figure 5.2 but the side lobe structure differs considerably (compare with Figure 4.45). Figures 4.46 through 4.51 show the transient decay behavior. Several lobes appear with essentially the same magnitude which could cause difficulty in target identification if such short pulses were used.

For the five cycle case we can observe the build-up of the pattern by comparing Figures 4.34, 4.36, 4.40, 4.42, 4.52, 4.54, 4.56 in that order, and with 5.2. The main lobe reaches unity for this case, with side lobes down to the expected level, particularly on the left side. The side lobes on the right hand side have not completely developed but are sufficiently low level not to be of concern. During the transient decay, shown in Figures 4.57 through 4.64, the main lobe collapses and the side lobes grow. The interval of time during which the transient decay could cause trouble because of the high side lobes that are developed is equivalent to about three cycles. Since the total elapsed time from arrival of the initial signal at the target to the time that the transient decay brings the signal strength down to the normal level of the first side lobe (<0.2) is less than 10 cycles of excitation time, this amounts to a rather high percentage.

Although computations were not made for values of $\theta > 16^\circ$ and $\theta < 1^\circ$ in this case, the trends of the patterns obtained led to the conclusion that there were no peculiarities beyond these points which should be examined.

5.3 Uniform Amplitude, 45° Progressive Phase

In this case the main lobe has been moved to $\theta = 14.5^\circ$. Computations were made for the range $0 < \theta < 15^\circ$. For the one cycle pulse a broad, rather flat, distribution first appeared. This was broken up as time progressed, into a string of irregular lobes, but no well-defined main lobe was ever apparent. Any one of several lobes could have qualified.

For the three cycle case the number of side lobes increased, although their forms were irregular. A

well-defined broad main lobe appeared, (see Figure 4.78) but it did not take on the appearance of the steady-state main lobe until fairly late in the transient decay period (see Figure 4.84). During the transient decay the side lobes took on the more normal side lobe appearance, however they were quite broad and approached the main lobe in intensity (see Figure 4.85).

The five cycle pulse case developed a well defined although quite broad, main beam, with relatively low, broad side-lobes, in a time interval equivalent to three cycles (see Figure 4.86). By the end of the transient build-up interval ($\omega t = 1800^\circ$) the main lobe exceeded 0.8 relative amplitude, but was still quite broad. The side lobes at this time were still very irregular. During the transient decay which followed the main beam decreased slowly but side lobes grew very rapidly, approaching but never exceeding, the magnitude of the main lobe; as in the 30° phase case, the side lobes could cause difficulties.

5.4 Uniform Amplitude, 60° Progressive Phase

For this case the main lobe centered at about 19.6° and therefore values of θ were selected ranging from 10° to 30° . This range included several side lobes either side of the main lobe and was considered to be sufficient to cover the most important peculiarities that might appear.

As before, early development of the pattern showed spreading lobes of extremely poor shape. For the one cycle pulse these lobes were inadequate and unusable. The transient decay produced more, better-defined lobes than appeared during the build-up interval.

A broad main lobe of moderate amplitude developed during the transient build-up for the three-cycle case as shown in Figure 4.111. As time progressed this lobe narrowed somewhat but this occurred during the decay period and therefore its amplitude continued to decrease with time, while side-lobes were enhanced.

For the five-cycle case there was a longer transient build-up interval with consequent increase in main lobe height during this time, reaching its maximum as shown in Figure 4.128. Thereafter the transient decay began, with the attendant

growth of side lobes and decrease in the main lobes.

5.5 General Discussion

Throughout this discussion reference has been made to build-up intervals and decay intervals. Actually these intervals are rather difficult to define. There is no single instant when one ends and the other begins. One might say that the build-up time ends when the energy from the first element terminates. However, for short pulses, the energy from several elements might not have arrived at the target by this time. Path length differences could be several wave lengths, many more than a pulse length. The build-up and decay terminology is therefore rather arbitrary.

Some additional discussion about general features of the patterns is in order. Some of the peculiarities that are observed in the radiation patterns could be attributed to the fact that very short pulses are employed, and others to the instantaneous excitation feature. In many applications of phased arrays the excitation is fed in at one end and phasing is accomplished by adjusting the path length between adjacent elements, or by other phasing devices. In any case, a transient build-up of the pattern is experienced which is in part due to the time required for each successive element to be energized, and in part by the differences in path lengths from each element to the point in space where the field is being measured. In this study the first of these two delay times is eliminated. However, the clipped leading portion

of the sine wave results, which causes differences in addition to those produced by the instantaneous excitation feature.

In most array studies the case of very short pulses is not considered but instead the effects of having the entire array energized is of prime consideration. In this study, for a large range of the angle θ the effect is similar to that of having an array of much less than the total number of elements. Since the wave from element zero dies out before that of element k arrives (the wave from element $k - 1$ having arrived just before the wave from element zero terminated) then the field intensity at the target point up to that time is only that which would have resulted if only k elements has originally been present. This phenomena has the effect which is to be expected. Smaller arrays have broader main lobes and larger side lobes. Comparison of Figure 4.52 and 4.123 show the effects of shifting the main lobe away from boresight. In Figure 4.123 fewer elements formed the apparent array than for the case in Figure 4.52 and therefore the main lobe is not as high and at the same time it is broader at the base. This effect is increased as the main lobe is shifted further from boresight to produce scanning of the beam. Very short pulses, of the order of a few wave lengths, will result in a diminishing and broadening main lobe as the beam is scanned away from broadside. The same effect would be produced by increasing the array length, for a fixed pulse width. In other words the longer the array, the longer the excitation pulse must be to prevent rapid deterioration of the main beam.

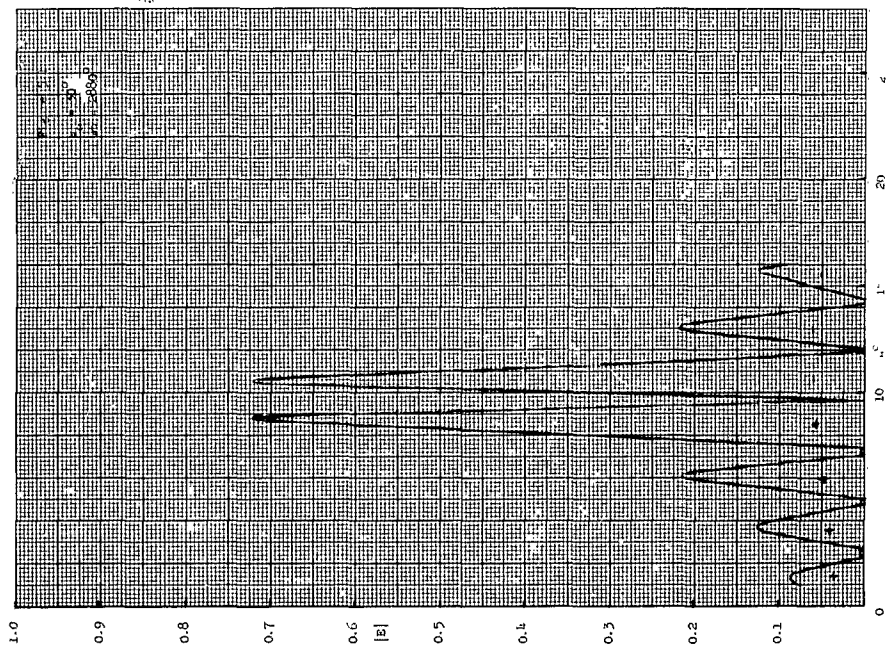
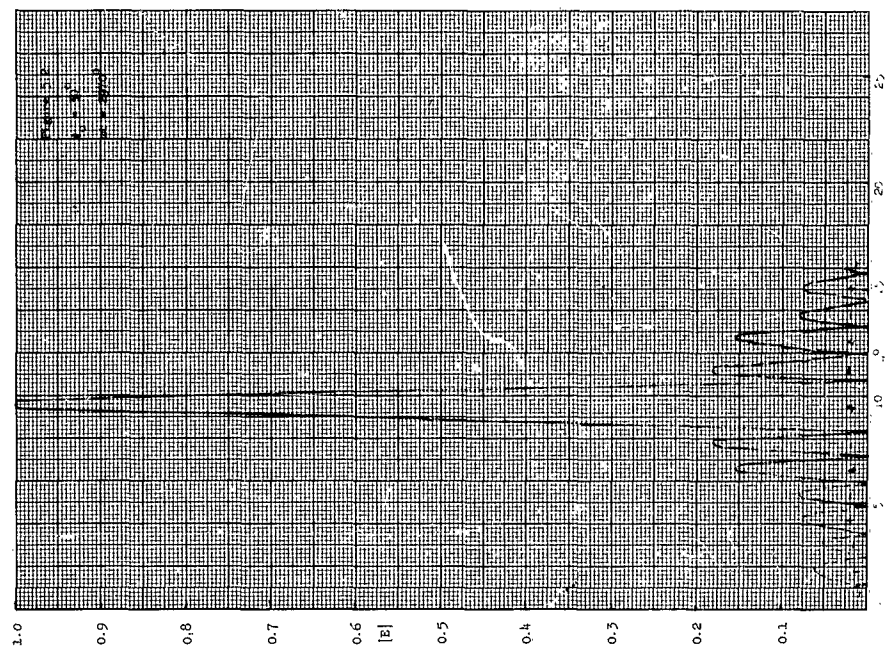
VI. SUMMARY AND CONCLUSIONS

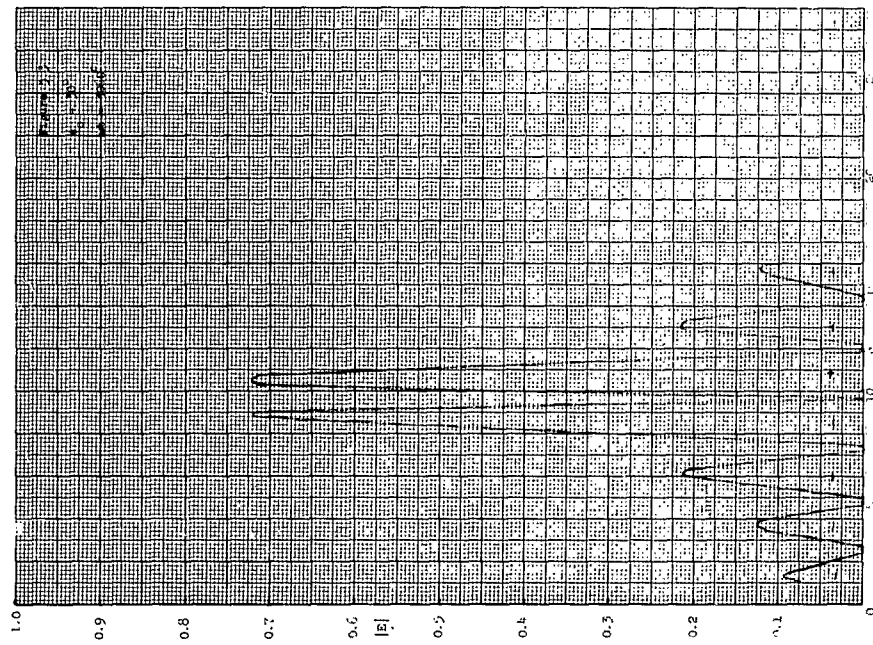
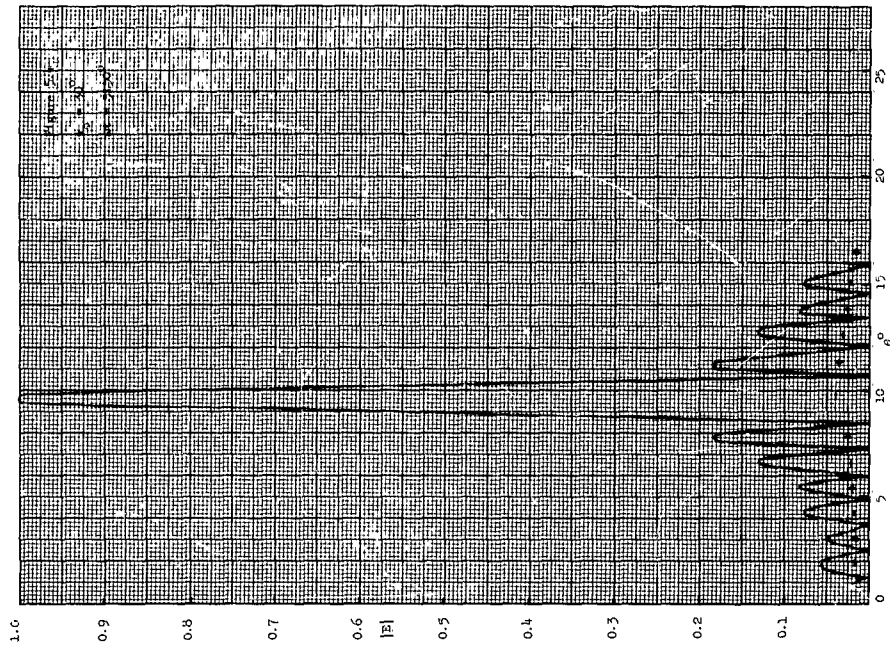
The results of this study have shown that when a large array is excited by very short pulses, with all elements of the array excited simultaneously, the main lobe increases in width and decreases in amplitude as it is scanned off boresight, and that the sidelobes increase in relative strength. The study has shown that during the transient build-up and decay, which together could constitute the entire duration of the pattern, the lobe structure could be very irregular, when viewed as a function of time. For rather large portions of the pattern duration the main lobe loses its identity, side lobes having attained strengths equal to it. There are limitations to the minimum pulse duration that can be applied if the main beam is to be swept by varying the phase angle, with the pulse being applied simultaneously to all elements. Sufficient time must be given for the main lobe to become established, the minimum time required being a function of the maximum angle of boresight to which the beam is to be swept, as well as the array length. For the cases studied, a respectable main lobe was obtained with a five cycle excitation pulse and the main lobe sweeping through 20 degrees off boresight. In this case, side lobes during the decay interval became undesirably large. Increasing the scan angle appreciably would require pulses of more than five cycles duration.

Other types of amplitude distributions could aid in suppression of side lobes, which is desirable, however they would not overcome the difficulties brought about by the short pulse duration, namely broadening and reduction in amplitude of the main lobe.

A study was made by Polk³ in which he examined transient behaviors of large arrays. He applied the excitation to the end of the array and obtained results which showed dependency of the transients upon array length, assuming that the excitation is propagated down the array at the velocity of light. Methods of excitation therefore are the main differences in the two studies; however, he did not encounter the difficulty of working with clipped sinusoids, which make a radical difference when signals from the several elements are combined at a point in space.

It is concluded that this method of excitation and lobe switching is feasible but for any given array the minimum pulse duration, depending upon the desired scan angle, must be determined. The basis for this determination would be the amount of degradation of the main beam that can be permitted. To some extent, side lobe-levels could be suppressed by using some non-uniform amplitude distribution.





VII. REFERENCES

1. S. Silver, "Microwave Antenna Theory and Design," Radiation Laboratory Series, Vol. 12, McGraw-Hill Book Company, 1949.
2. J. D. Kraus, "Antennas," McGraw-Hill Book Company, 1950.
3. C. Polk, "Transient Behavior of Aperture Antennas," Proc. IRE, Vol. 48, Number 7, p. 1281, July, 1960.

<p>Rome Air Development Center, Griffiss AF Base, N. Y.</p> <p>Rpt No. RADG-TDR-63-67. TRANSIT TIME EFFECTS IN PHASED ARRAYS. Task Rpt No. 4 Feb. 63, 115 p. incl. illus., 3 ref.</p> <p>Unclassified Report</p> <p>Generation and analysis of radiation patterns as a function of time for a 49-element linear array with half-wave element spacing the elements excited simultaneously with uniform amplitude and progressive phase. The analysis covers the range of excitation pulse durations</p>	<p>1. Dipole Antennas</p> <p>2. Antenna Radiation Patterns</p> <p>I. Project 4506, Task 450604</p> <p>II. Contract AF30(602)-2646</p> <p>III. Syracuse University, Syracuse, N. Y.</p> <p>IV. Gildersleeve, R. E.</p> <p>V. SURI EE957-6302T4</p> <p>VI. In ASTIA Collection</p>	<p>Rome Air Development Center, Griffiss AF Base, N. Y.</p> <p>Rpt No. RADG-TDR-63-67. TRANSIT TIME EFFECTS IN PHASED ARRAYS. Task Rpt No. 4 Feb. 63, 115 p. incl. illus., 3 ref.</p> <p>Unclassified Report</p> <p>Generation and analysis of radiation patterns as a function of time for a 49-element linear array with half-wave element spacing the elements excited simultaneously with uniform amplitude and progressive phase. The analysis covers the range of excitation pulse durations</p>	<p>1. Dipole Antennas</p> <p>2. Antenna Radiation Patterns</p> <p>I. Project 4506, Task 450604</p> <p>II. Contract AF30(602)-2646</p> <p>III. Syracuse University, Syracuse, N. Y.</p> <p>IV. Gildersleeve, R. E.</p> <p>V. SURI EE957-6302T4</p> <p>VI. In ASTIA Collection</p>
<p>Rome Air Development Center, Griffiss AF Base, N. Y.</p> <p>Rpt No. RADG-TDR-63-67. TRANSIT TIME EFFECTS IN PHASED ARRAYS. Task Rpt No. 4 Feb. 63, 115 p. incl. illus., 3 ref.</p> <p>Unclassified Report</p> <p>Generation and analysis of radiation patterns as a function of time for a 49-element linear array with half-wave element spacing the elements excited simultaneously with uniform amplitude and progressive phase. The analysis covers the range of excitation pulse durations</p>	<p>1. Dipole Antennas</p> <p>2. Antenna Radiation Patterns</p> <p>I. Project 4506, Task 450604</p> <p>II. Contract AF30(602)-2646</p> <p>III. Syracuse University, Syracuse, N. Y.</p> <p>IV. Gildersleeve, R. E.</p> <p>V. SURI EE957-6302T4</p> <p>VI. In ASTIA Collection</p>	<p>Rome Air Development Center, Griffiss AF Base, N. Y.</p> <p>Rpt No. RADG-TDR-63-67. TRANSIT TIME EFFECTS IN PHASED ARRAYS. Task Rpt No. 4 Feb. 63, 115 p. incl. illus., 3 ref.</p> <p>Unclassified Report</p> <p>Generation and analysis of radiation patterns as a function of time for a 49-element linear array with half-wave element spacing the elements excited simultaneously with uniform amplitude and progressive phase. The analysis covers the range of excitation pulse durations</p>	<p>1. Dipole Antennas</p> <p>2. Antenna Radiation Patterns</p> <p>I. Project 4506, Task 450604</p> <p>II. Contract AF30(602)-2646</p> <p>III. Syracuse University, Syracuse, N. Y.</p> <p>IV. Gildersleeve, R. E.</p> <p>V. SURI EE957-6302T4</p> <p>VI. In ASTIA Collection</p>

from one cycle to cw. Selected patterns are illustrated to show the time variations in the patterns at time intervals corresponding to one quarter of an excitation cycle, and at intervals of one full excitation cycle, for selected excitation pulse durations. The results are then extended to include longer excitation pulse duration. The formation of pulses at a distant target is illustrated for a selected range of scan angles off the main beam.



from one cycle to cw. Selected patterns are illustrated to show the time variations in the patterns at time intervals corresponding to one quarter of an excitation cycle, and at intervals of one full excitation cycle, for selected excitation pulse durations. The results are then extended to include longer excitation pulse duration. The formation of pulses at a distant target is illustrated for a selected range of scan angles off the main beam.






from one cycle to cw. Selected patterns are illustrated to show the time variations in the patterns at time intervals corresponding to one quarter of an excitation cycle, and at intervals of one full excitation cycle, for selected excitation pulse durations. The results are then extended to include longer excitation pulse duration. The formation of pulses at a distant target is illustrated for a selected range of scan angles off the main beam.



from one cycle to cw. Selected patterns are illustrated to show the time variations in the patterns at time intervals corresponding to one quarter of an excitation cycle, and at intervals of one full excitation cycle, for selected excitation pulse durations. The results are then extended to include longer excitation pulse duration. The formation of pulses at a distant target is illustrated for a selected range of scan angles off the main beam.



<p>Rome Air Development Center, Griffiss AF Base, N. Y.</p> <p>Rpt No. RADG-TDR-63-67. TRANSIT TIME EFFECTS IN PHASED ARRAYS. Task Rpt No. 4 Feb. 63, 115 p. incl. illus., 3 ref.</p> <p>Unclassified Report</p> <p>Generation and analysis of radiation patterns as a function of time for a 49-element linear array with half-wave element spacing the elements excited simultaneously with uniform amplitude and progressive phase. The analysis covers the range of excitation pulse durations</p> <p>○</p>	<p>1. Dipole Antennas</p> <p>2. Antenna Radiation Patterns</p> <p>I. Project 4506, Task 450604</p> <p>II. Contract AF30(602)-2646</p> <p>III. Syracuse University, Syracuse, N. Y.</p> <p>IV. Gildersleeve, R. E.</p> <p>V. SURI EE957-6302T4</p> <p>VI. In ASTIA Collection</p>	<p>Rome Air Development Center, Griffiss AF Base, N. Y.</p> <p>Rpt No. RADG-TDR-63-67. TRANSIT TIME EFFECTS IN PHASED ARRAYS. Task Rpt No. 4 Feb. 63, 115 p. incl. illus., 3 ref.</p> <p>Unclassified Report</p> <p>Generation and analysis of radiation patterns as a function of time for a 49-element linear array with half-wave element spacing the elements excited simultaneously with uniform amplitude and progressive phase. The analysis covers the range of excitation pulse durations</p> <p>○</p>	<p>1. Dipole Antennas</p> <p>2. Antenna Radiation Patterns</p> <p>I. Project 4506, Task 450604</p> <p>II. Contract AF30(602)-2646</p> <p>III. Syracuse University, Syracuse, N. Y.</p> <p>IV. Gildersleeve, R. E.</p> <p>V. SURI EE957-6302T4</p> <p>VI. In ASTIA Collection</p>	<p>1. Dipole Antennas</p> <p>2. Antenna Radiation Patterns</p> <p>I. Project 4506, Task 450604</p> <p>II. Contract AF30(602)-2646</p> <p>III. Syracuse University, Syracuse, N. Y.</p> <p>IV. Gildersleeve, R. E.</p> <p>V. SURI EE957-6302T4</p> <p>VI. In ASTIA Collection</p>	<p>Rome Air Development Center, Griffiss AF Base, N. Y.</p> <p>Rpt No. RADG-TDR-63-67. TRANSIT TIME EFFECTS IN PHASED ARRAYS. Task Rpt No. 4 Feb. 63, 115 p. incl. illus., 3 ref.</p> <p>Unclassified Report</p> <p>Generation and analysis of radiation patterns as a function of time for a 49-element linear array with half-wave element spacing the elements excited simultaneously with uniform amplitude and progressive phase. The analysis covers the range of excitation pulse durations</p> <p>○</p>	<p>1. Dipole Antennas</p> <p>2. Antenna Radiation Patterns</p> <p>I. Project 4506, Task 450604</p> <p>II. Contract AF30(602)-2646</p> <p>III. Syracuse University, Syracuse, N. Y.</p> <p>IV. Gildersleeve, R. E.</p> <p>V. SURI EE957-6302T4</p> <p>VI. In ASTIA Collection</p>	<p>Rome Air Development Center, Griffiss AF Base, N. Y.</p> <p>Rpt No. RADG-TDR-63-67. TRANSIT TIME EFFECTS IN PHASED ARRAYS. Task Rpt No. 4 Feb. 63, 115 p. incl. illus., 3 ref.</p> <p>Unclassified Report</p> <p>Generation and analysis of radiation patterns as a function of time for a 49-element linear array with half-wave element spacing the elements excited simultaneously with uniform amplitude and progressive phase. The analysis covers the range of excitation pulse durations</p> <p>○</p>	<p>1. Dipole Antennas</p> <p>2. Antenna Radiation Patterns</p> <p>I. Project 4506, Task 450604</p> <p>II. Contract AF30(602)-2646</p> <p>III. Syracuse University, Syracuse, N. Y.</p> <p>IV. Gildersleeve, R. E.</p> <p>V. SURI EE957-6302T4</p> <p>VI. In ASTIA Collection</p>	<p>Rome Air Development Center, Griffiss AF Base, N. Y.</p> <p>Rpt No. RADG-TDR-63-67. TRANSIT TIME EFFECTS IN PHASED ARRAYS. Task Rpt No. 4 Feb. 63, 115 p. incl. illus., 3 ref.</p> <p>Unclassified Report</p> <p>Generation and analysis of radiation patterns as a function of time for a 49-element linear array with half-wave element spacing the elements excited simultaneously with uniform amplitude and progressive phase. The analysis covers the range of excitation pulse durations</p> <p>○</p>	<p>1. Dipole Antennas</p> <p>2. Antenna Radiation Patterns</p> <p>I. Project 4506, Task 450604</p> <p>II. Contract AF30(602)-2646</p> <p>III. Syracuse University, Syracuse, N. Y.</p> <p>IV. Gildersleeve, R. E.</p> <p>V. SURI EE957-6302T4</p> <p>VI. In ASTIA Collection</p>
---	--	---	--	--	---	--	---	--	---	--

	<p>from one cycle to cw. Selected patterns are illustrated to show the time variations in the patterns at time intervals corresponding to one quarter of an excitation cycle, and at intervals of one full excitation cycle, for selected excitation pulse durations. The results are then extended to include longer excitation pulse duration. The formation of pulses at a distant target is illustrated for a selected range of scan angles off the main beam.</p> 		<p>from one cycle to cw. Selected patterns are illustrated to show the time variations in the patterns at time intervals corresponding to one quarter of an excitation cycle, and at intervals of one full excitation cycle, for selected excitation pulse durations. The results are then extended to include longer excitation pulse duration. The formation of pulses at a distant target is illustrated for a selected range of scan angles off the main beam.</p> 
	<p>from one cycle to cw. Selected patterns are illustrated to show the time variations in the patterns at time intervals corresponding to one quarter of an excitation cycle, and at intervals of one full excitation cycle, for selected excitation pulse durations. The results are then extended to include longer excitation pulse duration. The formation of pulses at a distant target is illustrated for a selected range of scan angles off the main beam.</p> 		<p>from one cycle to cw. Selected patterns are illustrated to show the time variations in the patterns at time intervals corresponding to one quarter of an excitation cycle, and at intervals of one full excitation cycle, for selected excitation pulse durations. The results are then extended to include longer excitation pulse duration. The formation of pulses at a distant target is illustrated for a selected range of scan angles off the main beam.</p> 